DEFINING THE INTERACTOME AND FUNCTIONAL REGULATION OF THE O-GLCNACASE ENZYME DURING OXIDATIVE STRESS

by
Jennifer A. Groves

A dissertation submitted to Johns Hopkins University in conformity with the requirements for the degree of Doctor of Philosophy

Baltimore, Maryland
October, 2017

Abstract

The essential post-translational modification O-linked β-N-acetylglucosamine (O-GlcNAc) regulates thousands of nuclear, cytoplasmic, and mitochondrial proteins. O-GlcNAc is dynamically added and removed from proteins by the O-GlcNAc transferase (OGT) and the O-GlcNAcase (OGA), respectively. Dysregulation of O-GlcNAc-cycling is implicated in the etiology of numerous diseases, including cancer, neurodegeneration, and metabolic dysfunction. Underpinning these observations, O-GlcNAc regulates nearly every major cellular process including transcription, translation, protein degradation, protein localization, and the cell cycle. Furthermore, many forms of cellular stress and injury, including oxidative stress, elicit an increase in O-GlcNAcylation on numerous proteins, which has been demonstrated to promote cell survival. However, the mechanisms by which OGT and OGA are regulated during oxidative stress to alter O-GlcNAcylation are not fully characterized. Here, we demonstrate that oxidative stress leads to elevated O-GlcNAc levels in U2OS cells but has little impact on the activity of OGT. In contrast, the expression and activity of OGA are enhanced. We hypothesized that this seeming paradox could be explained by proteins that bind to and control the local activity or substrate targeting of OGA, thereby resulting in the observed stress-induced elevations of O-GlcNAc. To identify potential protein partners and regulators, we utilized BioID proximity biotinylation in combination with Stable Isotopic Labeling of Amino Acids in Cell Culture (SILAC). This analysis revealed 90 OGA-interacting partners, many of which exhibited increased binding to OGA upon stress. The associations of OGA with fatty acid synthase (FAS), filamin-A, heat shock cognate 70 kDa protein, and OGT were confirmed by co-immunoprecipitation. The pool of OGA bound to FAS demonstrated a substantial (~85%)

reduction in specific activity, suggesting that FAS inhibits OGA. Consistent with this observation, FAS overexpression augmented stress-induced O-GlcNAcylation on a subset of proteins. Although the mechanism by which FAS sequesters OGA remains unknown, these data suggest that FAS fine-tunes the cell's response to stress and injury by remodeling cellular O-GlcNAcylation. Finally, our studies characterized the use of two commercially available and three non-commercially available antibodies for detecting and enriching full-length OGA from lysates of mouse and human origin in order to facilitate future studies probing the regulation of OGA in disease.

Dissertation Advisor: Natasha E. Zachara, Ph.D.

Dissertation Reader: Steven M. Claypool, Ph.D.

Preface

My goals for graduate school were to strengthen my knowledge of biological life science and medical research at a molecular level, learn a broad range of techniques and skills that would apply to numerous career paths, and to develop meaningful friendships and a long-lasting professional network. My success in each of these areas is a direct result of the help and support of a number of individuals.

First and foremost, I am incredibly grateful that Dr. Natasha E. Zachara gave me the opportunity to train in her laboratory. Natasha fostered my development into a confident and independent scientist, never wavered on her support of my non-academic career goals, and went above and beyond to help in times of personal need. I would also like to thank the members of my thesis committee, Dr.'s Ronald Schnaar, Robert Cole, Katherine Wilson, and Steven Claypool, for their insight, suggestions, and support of my professional goals. Furthermore, I would like to thank my formal and informal collaborators, Dr.'s Jennifer Van Eyk, Akhilesh Pandey, Alfredo Quiñones-Hinojosa, Partha Banerjee, Gerald Hart, Michael Wolfgang, and Sagar Shah, as well as Robert O'Meally, Caitlyn Bowman, and Chris Saeui, for their contributions to this work and my professional development. This work was supported by grants from the National Institutes of Health, including a pre-doctoral National Research Service Award from the National Institute on Aging.

I would also like to acknowledge all past and current members of the Zachara laboratory, especially Dr.'s Albert Lee, Kamau Fahie, Marissa Martinez, Devin Miller, Thiago Dias, and Russell Reeves, as well as Gokben Yildirir, Cathrine McKen, Roger Henry, Peter Natov, Srona Sengupa, and Austin Maduka. These individuals have become

part of my family, providing scientific and technical guidance as well as friendship and laughter during the hardships of graduate school. None of this work could have been successful without the efforts of the Biological Chemistry Department Graduate Program and Administrative Office, especially Darlene Sutton, Danelle Daniels, and Natalie Peters. Finally, I would like to thank my family for their support of my career that took me thousands of miles across the country, and for their faith that I will reach any goal I set my mind to.

Table of Contents

List of Tables

List of Figures

Abbreviations

4MU: 4-methylumbelliferyl, **Aβ**: amyloid β, **Ac-5SGlcNAc**: 2-acetamido-1,3,4,6-tetra-*O*-acetyl-2-deoxy-5-thio-α-D-glucopyranose, **AD**: Alzheimer's disease, **APP**: amyloid β precursor protein, **ATP**: adenosine trisphosphate, **Bcl-2**: B-cell lymphoma 2, **BEMAD**: beta elimination and Michael addition, **bRP**: basic reversed phase, **BSA**: bovine serum albumin, **BSA-X**: BSA/Triton X-100, **CaMK**: calcium/calmodulin-dependent kinase, **CD**: catalytic domain, **CKII**: casein kinase II, **EDTA**: ethylenediaminetetraacetic acid, ***EMeg32***: glucosamine-6-phosphate acetyltransferase, **eNOS**: endothelial nitric oxide synthase, **ER**: endoplasmic reticulum, **ESI**: electrospray ionization, **ETD**: electron transfer dissociation, **FAS**: fatty acid synthase, **FDR**: false discovery rate, **FLNA**: filamin-A, **fOGA**: full-length OGA, **Foxo**: forkhead box, **FRET**: Förster resonance energy transfer**,** **G6P-I**: glucose-6-phosphate isomerase, **GalNAz**: tetraacetylated N-azidoacetylgalactosamine, **GalT1**: UDP-galactose:GlcNAc β-1,4-galactosyltransferase, **GFAT**: glutamine:fructose-6-phosphate amidotransferase, **GlcNAc**: β-N-acetylglucosamine, **GlcNAz**: tetraacetylated N-azidoacetylglucosamine, **GPX1**: glutathione peroxidase 1, **GSK3β**: glycogen synthase kinase 3β, **H**: heavy, **H_2O_2**: hydrogen peroxide, **HAT**: histone acetyltransferase, **HBP**: hexosamine biosynthetic pathway, **HEK**: human embryonic kidney, **HK**: hexokinase, **HRP**: horseradish peroxidase, **HSC70:** heat shock cognate 70 kDa protein, **HSF1**: heat shock factor 1, **HSP**: heat shock protein, **I/R**: ischemia reperfusion, **Ig**: immunoglobulin, **IKKβ**: inhibitor of NFκB kinase, **IL**: interleukin, **IP**: immunoprecipitation, **IP_3**: inositol (3,4,5)-trisphosphate, **IRS-1**: insulin receptor substrate 1, **JHUSOM**: Johns Hopkins University School of Medicine, **K18**: keratin 18, **L**: light, **LC**: liquid chromatography, **LWAC**: Lectin Weak Affinity

Chromatography, **M**: medium, **m/z**: mass/charge, **MAPK**: mitogen-activated protein kinase, **MCS**: multiple cloning site, **MCT**: multiple comparison test, **MEF**: mouse embryonic fibroblast, ***Mgea5***: meningioma expressed antigen 5, **mPTP**: mitochondrial permeability transition pore, **MS**: mass spectrometry, **MS/MS**: tandem mass spectrometry, **MW**: molecular weight, **N**: biological replicate, **NaCl**: sodium chloride, **NIH**: National Institutes of Health, **NFκB**: nuclear factor κB, **O-GlcNAc**: O-linked β-N-acetylglucosamine, **O-GlcNAcylated**: O-GlcNAc-modified, **OGA**: O-GlcNAcase; β-N-acetylglucosaminidase, **OGA-A**: OGA-Abcam, **OGA-B**: OGA-Bethyl, **OGT**: O-GlcNAc transferase; UDP-β-N-acetylglucosamine:peptide N-acetylglucosaminyl-transferase, **PAGE**: polyacrylamide gel electrophoresis, **PANTHER**: Protein Analysis Through Evolutionary Relationships, **PBS**: phosphate-buffered saline, **PD**: Parkinson's disease, **PGC1α**: peroxisome proliferator-activated receptor gamma coactivator 1α, ***Pgm3***: N-acetylglucosamine-phosphate mutase, **PI3K**: phosphoinositide 3-kinase, **PSM**: peptide spectral match, **PTM**: post-translational modification, **PUGNAc**: O-(2-acetamido-2-deoxy-d-glucopyranosylidene)amino-N-phenylcarbamate, **RM-1ANOVA**: repeated measures one-way analysis of variance, **RM-2ANOVA**: repeated measures two-way analysis of variance, **ROS**: reactive oxygen species, **RP**: reversed phase, **RPT**: ratio-paired t-test, **SDS**: sodium dodecyl sulfate, **SEM**: standard error of the mean, **SILAC**: Stable Isotopic Labeling of Amino acids in Cell culture, **SOD2**: superoxide dismutase 2, **sWGA**: succinylated WGA, **Tab-1**: TAK-1-binding protein, **TAK-1**: transforming growth factor-β-activated kinase I, **TBS**: Tris-buffered saline, **TCL**: total cell lysate, **TEAB**: triethylammonium bicarbonate, **TMG**: Thiamet-G; 2-ethylamino-3aR, 6S, 7R, 7aR-tetrahydro-5R-hydroxymethyl-5H-pyrano[3, 2-d]thiazole-6, 7-diol, **TNF-α**: tumor

necrosis factor-α, **TPR**: tetratricopeptide repeat, ***Uap1***: UDP-GlcNAc pyrophosphorylase, **UDP**: uridine diphosphate, **V**: vehicle, **VDAC**: voltage dependent anion channel, **WB**: Western blot, **WGA**: wheat germ agglutinin, **WT**: wild type

Amino Acid Codes

Amino Acid	Three letter code	One letter code
Alanine	Ala	A
Arginine	Arg	R
Asparagine	Asn	N
Aspartate	Asp	D
Cysteine	Cys	C
Glutamate	Glu	E
Glutamine	Gln	Q
Glycine	Gly	G
Histidine	His	H
Isoleucine	Ile	I
Leucine	Leu	L
Lysine	Lys	K
Methionine	Met	M
Phenylalanine	Phe	F
Proline	Pro	P
Serine	Ser	S
Threonine	Thr	T
Tryptophan	Trp	W
Tyrosine	Tyr	Y
Valine	Val	V

Chapter 1

Dynamic O-GlcNAcylation and its roles in the cellular stress response and homeostasis

Jennifer A. Groves[1], Albert Lee[1], Gokben Yildirir, and Natasha E. Zachara

[1]authors contributed equally

Originally published in *Cell Stress Chaperones*. 2013 Sep;18 (5):535-58.

Format adapted for dissertation

Summary

O-linked β-N-acetylglucosamine (O-GlcNAc) is a ubiquitous and dynamic post-translational modification known to modify over 3,000 nuclear, cytoplasmic, and mitochondrial eukaryotic proteins. Addition of O-GlcNAc to proteins is catalyzed by the O-GlcNAc transferase and is removed by a neutral pH β-N-acetylglucosaminidase. O-GlcNAc is thought to regulate proteins in a manner analogous to protein phosphorylation, and the cycling of this carbohydrate modification regulates many cellular functions such as the cellular stress response. Diverse forms of cellular stress and tissue injury result in enhanced O-GlcNAc-modification, or O-GlcNAcylation, of numerous intracellular proteins. Stress-induced O-GlcNAcylation appears to promote cell/tissue survival by regulating a multitude of biological processes including: the phosphoinositide 3-kinase/Akt pathway, heat shock protein expression, calcium homeostasis, levels of reactive oxygen species, endoplasmic reticulum stress, protein stability, mitochondrial dynamics, and inflammation. Here, we will discuss the regulation of these processes by O-GlcNAc and the impact of such regulation on survival in models of ischemia reperfusion injury and trauma hemorrhage. We will also discuss the misregulation of O-GlcNAc in diseases commonly associated with the stress response, namely Alzheimer's and Parkinson's diseases. Finally, we will highlight recent advancements in the tools and technologies used to study the O-GlcNAc-modification.

Introduction

O-linked β-N-acetylglucosamine (O-GlcNAc) is a dynamic post-translational modification (PTM) of more than 3,000 nuclear, cytoplasmic, and mitochondrial proteins (Torres and Hart 1984; Wells et al. 2002b; Vosseller et al. 2006; Gurcel et al. 2008; Rexach et al. 2008; Carapito et al. 2009; Teo et al. 2010; Wang et al. 2010a; Wang et al. 2010b). While O-GlcNAc appears more common in metazoans, there is evidence for this PTM in simple eukaryotes such as *Aspergillus niger* (Machida and Jigami 1994) and in some prokaryotes (Shen et al. 2006). O-GlcNAc is cycled on and off serine and threonine residues by just two enzymes: the O-GlcNAc transferase (OGT) that catalyzes the addition of O-GlcNAc and the O-GlcNAcase (OGA) that removes O-GlcNAc (Figure 1-1). Highlighting the importance of O-GlcNAc in cellular homeostasis, deletion of OGT, OGA, and other key enzymes in the hexosamine biosynthetic pathway (HBP) is lethal in mammals (Mio et al. 1999; Boehmelt et al. 2000a; Boehmelt et al. 2000b; Shafi et al. 2000; Forsythe et al. 2006; Greig et al. 2007; Yang et al. 2012).

Intracellular proteins that are O-GlcNAc-modified (O-GlcNAcylated) fall into diverse functional groups. Examples of O-GlcNAcylated proteins include chromatin-associated proteins and histones, transcription factors, ribosomal proteins, proteasomal proteins, cytoskeletal proteins, and many different types of signaling proteins such as kinases and metabolic enzymes (Wells et al. 2002b; Vosseller et al. 2006; Gurcel et al. 2008; Rexach et al. 2008; Carapito et al. 2009; Teo et al. 2010; Wang et al. 2010a; Wang et al. 2010b). O-GlcNAc is thought to regulate these proteins in a manner analogous to protein phosphorylation. O-GlcNAc has been demonstrated to alter numerous protein functions that include: DNA binding and transactivation (Jackson and Tjian 1989; Comer

and Hart 1999; Gao et al. 2003; Sayat et al. 2008; Ozcan et al. 2010), protein-protein interactions (Guinez et al. 2006; Guinez et al. 2007; Guinez et al. 2010; Ise et al. 2010; Lim and Chang 2010), protein degradation (Han and Kudlow 1997; Cheng and Hart 2001; Zhang et al. 2003), protein and enzyme activity (Zhang et al. 2003; Kim et al. 2006b; Rengifo et al. 2007; Dias et al. 2009; Bimboese et al. 2011), and protein localization (Dudognon et al. 2004; Sayat et al. 2008) amongst many others (Hart et al. 2011).

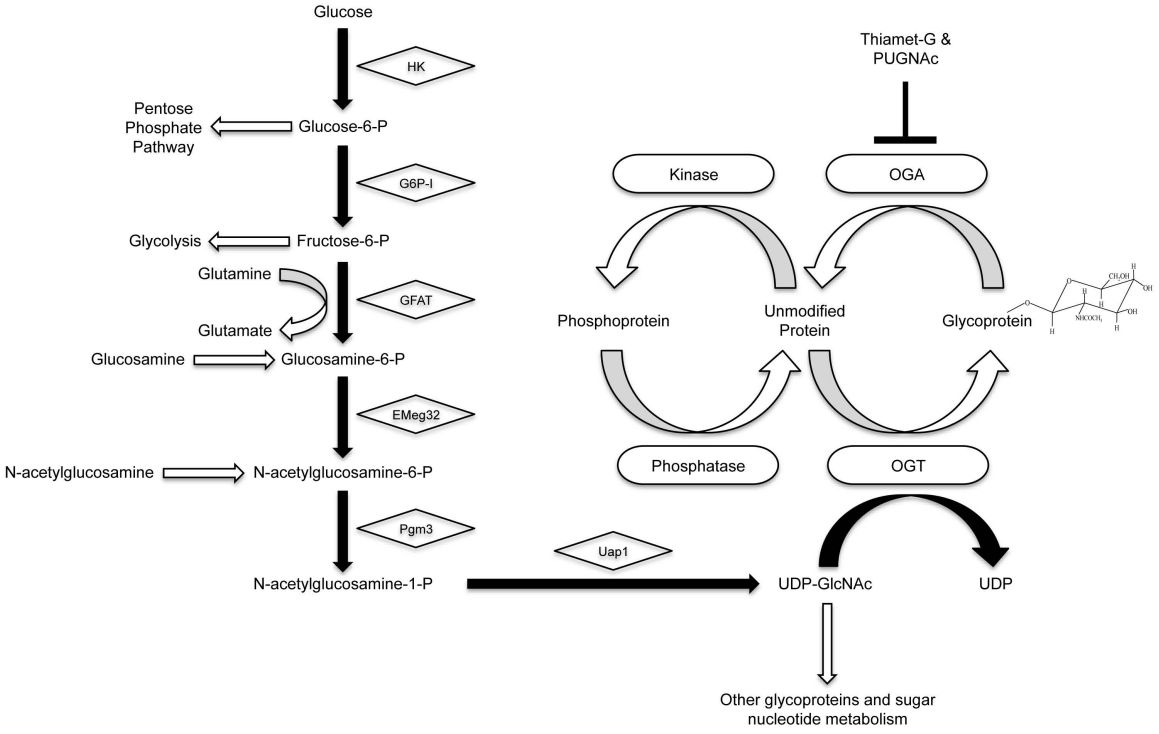

Figure 1-1: The hexosamine biosynthetic pathway provides the donor substrate for O-GlcNAcylation and other types of protein glycosylation. Upon entry into the cell, a small percentage of Glucose (2-5% in adipocytes) is directed into the hexosamine biosynthetic pathway and converted into UDP-GlcNAc via glutamine:fructose-6-phosphate amidotransferase (*Gfpt1*; GFAT), glucosamine-6-phosphate acetyltransferase (*EMeg32*), N-acetylglucosamine-phosphate mutase (*Pgm3*), and UDP-GlcNAc pyrophosphorylase (*Uap1*). OGT catalyzes the addition of the glycoside to yield O-GlcNAcylated nuclear, cytoplasmic, and mitochondrial proteins, whereas the enzyme O-GlcNAcase (OGA) catalyzes the removal of O-GlcNAc from proteins. O-GlcNAc-modified proteins are involved in many cellular processes including the cellular stress response. Abbreviations include: HK, hexokinase; G6P-I, glucose 6-phosphate isomerase.

Like phosphorylation, the levels of O-GlcNAc respond to both intracellular and extracellular stimuli including insulin, nutrient levels, and cellular stress (Kearse and Hart 1991; Walgren et al. 2003; Zachara et al. 2004b; Song et al. 2008; Whelan et al. 2008; Whelan et al. 2010; Hart et al. 2011), with the latter being the main focus of this review. In response to diverse forms of cellular stress, O-GlcNAc levels are elevated on numerous proteins (Zachara et al. 2004b). Augmenting O-GlcNAc levels promotes survival while suppressing O-GlcNAc levels sensitizes cells to death, suggesting that O-GlcNAc is a key regulator of the cellular stress response (Zachara et al. 2004b). While the exact mechanisms by which O-GlcNAc alters protein function leading to cell survival have not been defined, O-GlcNAc is known to regulate many signaling events and pathways, and this review will specifically focus on 1) the phosphoinositide 3-kinase (PI3K)/Akt pathway, 2) heat shock protein (HSP) expression, 3) calcium homeostasis, 4) reactive oxygen species (ROS) generation, 5) mitochondrial dynamics, 6) inflammation, and 7) the interplay with other PTMs. O-GlcNAc modulates these aspects of the cellular stress response to protect against ischemia reperfusion (I/R) injury, trauma hemorrhage, and neurodegeneration. We will also discuss the interplay between O-GlcNAc and other PTMs, future directions regarding novel technologies for detecting O-GlcNAc, and potential roles for O-GlcNAc in other disease mechanisms.

Biosynthesis of O-GlcNAc

Two enzymes modulate protein O-GlcNAcylation: uridine diphosphate (UDP)-β-N-acetylglucosamine (GlcNAc):peptide N-acetylglucosaminyl-transferase N-acetyl-β-D-glucosamine: peptide N-acetylglucosaminyl-transferase (O-GlcNAc transferase, OGT),

which catalyzes the addition of O-GlcNAc, and a neutral pH β-N-acetylglucosaminidase (O-GlcNAcase, OGA), which is responsible for the removal of O-GlcNAc (Figure 1-1). The levels of O-GlcNAc appear to be regulated by five main events: 1) expression and activity of OGT; 2) expression and activity of OGA; 3) the concentration of UDP-GlcNAc, the sugar nucleotide donor of OGT; 4) the availability of protein substrates; and 5) targeting of the enzymes to their substrates.

The hexosamine biosynthetic pathway

The synthesis of UDP-GlcNAc occurs via the HBP (Figure 1-1). Upon entering cells, glucose is rapidly converted to glucose-6-phosphate by hexokinase (HK), and subsequently to fructose-6-phosphate by glucose-6-phosphate isomerase (G6P-I). The first step of the HBP is rate limiting, and comprises of the conversion of fructose-6-phosphate to glucosamine-6-phosphate by glutamine:fructose-6-phosphate amidotransferase (*Gfpt1*; GFAT). Notably, glutamine is required for this step and can be used to alter cellular O-GlcNAc levels as well as the levels of other sugar metabolites (Marshall et al. 1991). Several subsequent reactions result in the production of UDP-GlcNAc, the sugar nucleotide donor substrate used by OGT and other glycosyltransferases. The HBP accounts for ~2-5% of glucose flux in 3T3-L1 adipocytes (Marshall et al. 1991) These and other observations have led some to suggest that O-GlcNAc regulates cellular function in a glucose-dependent manner. Although little is known about the regulation of GFAT, it appears to be inhibited by high concentrations of UDP-GlcNAc (Traxinger and Marshall 1991). Interestingly, free radicals promote GFAT activity suggesting one mechanism by which cellular stress and high glucose can lead to upregulation of UDP-GlcNAc pools (Du et al. 2000). Mutations in genes encoding enzymes that significantly lower O-GlcNAc

levels, such as glucosamine-6-phosphate acetyltransferase (*EMeg32*) and N-acetylglucosamine-phosphate mutase (*Pgm3*), are embryonic lethal highlighting the importance of O-GlcNAc and other forms of protein glycosylation that rely on UDP-GlcNAc (Boehmelt et al. 2000a; Boehmelt et al. 2000b; Greig et al. 2007).

O-GlcNAc transferase

Unlike many other glycosyltransferases, OGT is a soluble protein that is predominantly localized to the nucleus, mitochondria and cytoplasm of all tissues studied thus far (Haltiwanger et al. 1992; Kreppel et al. 1997; Lubas et al. 1997; Hanover et al. 2003; Love et al. 2003). Two functional domains characterize OGT: an N-terminal tetratricopeptide repeat (TPR) domain and a C-terminal catalytic domain belonging to the glycogen phosphorylase superfamily (Kreppel et al. 1997; Lubas et al. 1997; Wrabl and Grishin 2001). Recently the structure of OGT and the TPR domain have been solved (Jinek et al. 2004; Martinez-Fleites et al. 2008; Lazarus et al. 2011). The TPR domain forms an extended alpha-helix similar to importin-α (Jinek et al. 2004), and is important for mediating protein-protein interactions and enzyme activity (Kreppel and Hart 1999; Lubas and Hanover 2000). The catalytic domain contains two Rossman folds, separated by an intervening sequence. Notably, this linker is missing in the bacterial homologs of OGT that do not appear to modify protein substrates (Lazarus et al. 2011).

The gene for OGT maps to Xq13 on the mammalian X chromosome and encodes three well-characterized variants: short OGT, mitochondrial OGT, and nuclear/cytoplasmic OGT (Kreppel et al. 1997; Lubas et al. 1997; Hanover et al. 2003; Love et al. 2003). Mitochondrial OGT is an alternatively-spliced isoform, which uses intron 4 of nuclear/cytoplasmic OGT as an exon to generate a unique N-terminus (Love et

al. 2003). Intron 4 encodes an abbreviated TPR domain with an N-terminal mitochondrial targeting sequence (Love et al. 2003). Interestingly, overexpression of mitochondrial OGT appears to induce apoptosis (Shin et al. 2011). OGT is essential for embryonic stem cell viability and somatic cell function (Shafi et al. 2000; O'Donnell et al. 2004). Deletion of OGT in *Arabidopsis thaliana* (Jacobsen et al. 1996), *Drosophila melanogaster* (Gambetta et al. 2009; Sinclair et al. 2009), and mice is lethal (Shafi et al. 2000), and leads to dauer phenotypes in *Caenorhabditis elegans* (Hanover et al. 2005), suggesting that O-GlcNAc is essential for cellular homeostasis.

The mechanism of OGT substrate specificity is not fully understood; however, deletions in the TPR domain can affect the ability of OGT to O-GlcNAcylate protein and peptide substrates. It is generally thought that protein-protein interactions of OGT form a series of OGT complexes with different substrate specificities (Kreppel and Hart 1999). In support of this hypothesis, OGT has been found to associate with numerous proteins (Cheung et al. 2008) and is targeted to its substrates by p38 mitogen activated protein kinase (MAPK) under conditions of nutritional deprivation (Cheung and Hart 2008). Moreover, OGT can bind phosphatidylinositol (3,4,5)-trisphosphate (PIP_3), which targets OGT to the plasma membrane during insulin signaling (Yang et al. 2008). These observations may also explain why there is no consensus sequence or motif for the addition of O-GlcNAc, although a recent paper has developed a neural network for predicting O-GlcNAc-modification sites (Wang et al. 2011).

The activity of OGT appears to be regulated by substrate targeting (discussed above), the levels of UDP and UDP-GlcNAc, and potentially by other PTMs. OGT is both tyrosine phosphorylated (Kreppel et al. 1997; Kreppel and Hart 1999) and O-GlcNAc-

modified (Kreppel and Hart 1999; Lubas and Hanover 2000), although the consequence of these modifications has not been defined. Interestingly, OGT is phosphorylated and activated by active calcium/calmodulin-dependent kinase (CaMK)IV (Song et al. 2008). Recently, it has been demonstrated that OGT is S-nitrosylated in resting cells, and its denitrosylation following induction of the innate immune response results in increased catalytic activity (Ryu and Do 2011). While UDP-GlcNAc levels may alter OGT activity by providing more substrate, there is also evidence that UDP-GlcNAc alters the substrate specificity of OGT. Thus, OGT may glycosylate one group of proteins at low concentrations of UDP-GlcNAc, but at higher concentrations may target a completely different panel of proteins (Kreppel and Hart 1999).

Little is known about how stress affects the activity of OGT, but stress alters glucose uptake and the activity of the HBP (discussed above) presumably augmenting UDP-GlcNAc pools. During heat stress, the activity of OGT is upregulated 3-fold by currently unknown mechanisms (Zachara et al. 2004b) and OGT translocates to the nucleus (Kazemi et al. 2010). Suggesting yet another mechanism by which stress alters O-GlcNAc levels, stressors such as sodium chloride (NaCl), ethanol, and arsenite appear to alter the expression of OGT (Zachara et al. 2004b). During glucose deprivation, the expression of OGT is partially dependent on adenosine monophosphate-activated protein kinase (AMPK), and OGT is targeted to its substrates by p38 MAPK (Cheung and Hart 2008). This results in a dramatic increase in O-GlcNAcylation of the neuronal protein neurofilament H, suggesting a possible mechanism by which defective glucose metabolism in the brain may directly contribute to the loss of axonal structure and stability (Cheung and Hart 2008).

Several assays have been used to detect OGT activity. The most common involves the addition of a tritiated UDP-GlcNAc (^{3}H-UDP-GlcNAc) to a peptide substrate (Haltiwanger et al. 1997). Recently, an effective fluorescence-based substrate analogue displacement assay was developed to assess the activity of OGT (Gross et al. 2005). The spatiotemporal dynamics of O-GlcNAc have also been characterized using a series of genetically-based O-GlcNAc Förster resonance energy transfer (FRET) sensors targeted to specific subcellular compartments (Carrillo et al. 2006; Carrillo et al. 2011). For example, a study utilizing the O-GlcNAc FRET sensor found that during serum-stimulated signal transduction rapid increases in O-GlcNAcylation were observed at the plasma membrane and in the nucleus, with a concomitant decrease in O-GlcNAcylation in the cytoplasm (Carrillo et al. 2011).

O-GlcNAcase

OGA is approximately 103 kDa in size and catalyzes the removal of O-GlcNAc from proteins. OGA appears to be predominantly cytoplasmic, and like OGT is ubiquitously expressed (Dong and Hart 1994). The gene encoding OGA was identified as meningioma expressed antigen 5 (*Mgea5*) and characterized as a hyaluronidase (Heckel et al. 1998). However, further analysis indicated that the product of the *Mgea5* gene was active at neutral pH, localized to the cytoplasm, and would remove O-GlcNAc from peptides suggesting that it was the O-GlcNAcase biochemically characterized by Dong and Hart (Comtesse et al. 2001; Gao et al. 2001). OGA exists as two isoforms: the full-length isoform with a histone acetyltransferase (HAT)-like domain in its C-terminus and a short isoform lacking the C-terminal HAT domain.

OGA is serine phosphorylated and O-GlcNAcylated, although the functional significance of these modifications has yet to be elucidated (Gao et al. 2001; Wells et al. 2002a). Like OGT, OGA from bovine brain appears to exist in complexes with other proteins including HSP110, heat shock cognate 70 kDa protein (HSC70), amphiphysin, and dihydropyriminidase-related protein-2. Finally, OGA is cleaved by caspase-3 during apoptosis (Wells et al. 2002a). Notably, the cleavage products appear to remain associated with each other and the activity of OGA is unaffected (Butkinaree et al. 2008). Thus far, little is known about the regulation of OGA during the cellular stress response.

While little is known about the regulation of OGA, the activity of OGA can be conveniently assayed *in vitro* with a synthetic substrate p-nitrophenol-β-GlcNAc (Dong and Hart 1994). However, care must be taken to exclude the activities of lysosomal hexosaminidases A and B in total cell and tissue lysates. Recent studies have shown that fluorogenic substrates exhibit higher sensitivity and can be used to study both OGA isoforms. Both fluorescein di-GlcNAc (Kim et al. 2006a) and 4-methylumbelliferyl-2-N-acetyl-2-deoxy-β-D-glucopyranoside have been used successfully (Macauley et al. 2005), however the latter is 10-fold less sensitive than fluorescein di-GlcNAc (Kim et al. 2006a).

O-GlcNAc and the cellular stress response

In response to injury, cells have the ability to modify their metabolic, transcriptional, translational, and signaling pathways to promote survival, collectively this is known as the "cellular stress response" (Lindquist 1986; Nollen and Morimoto 2002). Recent data suggests that O-GlcNAc is one component of the cellular stress response that is relevant to a variety of models of injury in several cell and tissue types. O-GlcNAc levels

become elevated in response to numerous forms of cell stress and tissue injury including: heat stress (Sohn et al. 2004; Zachara et al. 2004b), oxidative stress (Zachara et al. 2004b; Jones et al. 2008), ethanolic stress (Zachara et al. 2004b; Ngoh et al. 2009b), genotoxic stress (doxorubicin, belocin, ultraviolet B irradiation) (Zachara et al. 2004b; Love et al. 2010; Zachara et al. 2011a), reductive stress (iodoacetamide) (Zachara et al. 2004b), endoplasmic reticulum (ER) stress (dithiothreitol, tunicamycin) (Zachara et al. 2004b; Ngoh et al. 2009b), hypoxia-reoxygenation (Ngoh et al. 2008; Ngoh et al. 2009a; Ngoh et al. 2011), osmotic stress (NaCl, sorbitol, sucrose) (Zachara et al. 2004b; Zou et al. 2007), adenosine triphosphate (ATP) depletion (sodium arsenite) (Zachara et al. 2004b), I/R injury (Pang et al. 2002; Liu et al. 2006; Nagy et al. 2006; Champattanachai et al. 2007; Fulop et al. 2007a; Fulop et al. 2007b; Liu et al. 2007; Champattanachai et al. 2008; Jones et al. 2008; Ngoh et al. 2008; Ngoh et al. 2009a; Ngoh et al. 2009b; Zou et al. 2009; Hwang et al. 2010; Laczy et al. 2010; Ngoh et al. 2011), and trauma hemorrhage (Yang et al. 2006a; Not et al. 2007; Zou et al. 2007; Zou et al. 2009; Not et al. 2010). This response occurs in primary and transformed cells, as well as in tissues *in vivo* and *ex vivo*. Suggesting that the addition of O-GlcNAc to proteins is part of a pro-survival signaling program, elevating O-GlcNAc levels prior (Zachara et al. 2004b; Chatham et al. 2008; Ngoh et al. 2008) or immediately following (Liu et al. 2007) cellular injury dramatically improves survival. Conversely, lowering O-GlcNAc levels sensitizes cells and tissues to injury (Zachara et al. 2004b; Ngoh et al. 2008; Ngoh et al. 2009a; Ngoh et al. 2011).

Modulating the levels of O-GlcNAc in a manner consistent with improved survival regulates a number of biological pathways. Some examples include: 1) increased protein solubility during heat stress (Lim and Chang 2006; Cheung and Hart 2008) or Alzheimer's

disease (AD) (Yuzwa et al. 2012); 2) reduced calcium overload (Liu et al. 2006; Liu et al. 2007); 3) decreased calpain activation (Liu et al. 2007); 4) altered p38 MAPK activation in response to I/R injury (Fulop et al. 2007b; Cheung and Hart 2008); 5) modulation of pro-inflammatory cytokine expression (Huang et al. 2007; Zou et al. 2009); 6) reduced mitochondrial permeability transition pore (mPTP) formation (Jones et al. 2008); 7) increased B-cell lymphoma 2 (Bcl-2) expression and translocation (Champattanachai et al. 2008); and 8) regulation of the expression of a subset of molecular chaperones (Sohn et al. 2004; Zachara et al. 2004b; Kazemi et al. 2010).

Numerous reports have suggested that O-GlcNAc regulates many processes in the heart and vasculature (Fulop et al. 2007a; Liu et al. 2007; Champattanachai et al. 2008; Chatham and Marchase 2010; Ngoh et al. 2011) in models of I/R injury. For example, O-GlcNAc appears to regulate many of the hallmarks of I/R injury such as calcium overload, oxidative damage, ER stress, and mitochondrial aberrations (Chatham and Marchase 2010). Elevating O-GlcNAc levels with glucosamine, O-(2-acetamido-2-deoxy-d-glucopyranosylidene)amino-N-phenylcarbamate (PUGNAc), or 2-ethylamino-3aR, 6S, 7R, 7aR-tetrahydro-5R-hydroxymethyl-5H-pyrano[3, 2-d]thiazole-6, 7-diol (Thiamet-G; TMG) leads to improved function and reduced tissue death in both *ex vivo* and *in vivo* models of I/R injury in the heart (Liu et al. 2006; Fulop et al. 2007b; Liu et al. 2007; Jones et al. 2008). Collectively, these data suggest that the stress-induced elevation of the O-GlcNAc-modification is a pro-survival response of cells and tissues (Champattanachai et al. 2007; Champattanachai et al. 2008; Hwang et al. 2010).

The PI3K/Akt pathway

The role of O-GlcNAc in the PI3K/Akt pathway has been extensively studied in the context of nutrient sensing, insulin resistance and type II diabetes, and readers are directed to pertinent reviews on this topic for more extensive details (Akimoto et al. 2005; Buse 2006; Slawson et al. 2010; Hart et al. 2011). In contrast to these data, the interplay between O-GlcNAc and Akt signaling has been observed to inhibit apoptosis in a number of models including murine pancreatic β-cells (Kang et al. 2008), mouse embryonic fibroblasts (Kazemi et al. 2010), and murine liver (Ku et al. 2010), as discussed below.

Recently, it was demonstrated that O-GlcNAcylation of keratin 18 (K18) is a regulator of Akt1 phosphorylation, which promotes downstream anti-apoptotic and cytoprotective signaling (Ku et al. 2010). Mouse mutants expressing human K18 S30/31/49A mutations, which cannot be glycosylated ($K18^{-}Gly^{-}$), were more susceptible to liver and pancreatic injury induced by treatment with either streptozotocin or combined OGA inhibition and Fas ligand administration (Ku et al. 2010). It is thought that the pro-survival mechanism is O-GlcNAcylation of K18, which leads to its interaction with Akt1 and keratin 8 ultimately promoting the phosphorylation of Akt1 at Thr308. Akt is activated by phosphorylation at Thr308 and then phosphorylates substrates such as forkhead box protein (Foxo) and glycogen synthase kinase 3β (GSK3β), thereby enhancing cell survival (Ku et al. 2010) (Figure 1-2). It is also important to note that Akt itself is dynamically modified by O-GlcNAc at Ser473 (Gandy et al. 2006; Kang et al. 2008). While hyper-O-GlcNAcylation of Akt has deleterious effects in hepatic cell and tissue models of euglycemia (Soesanto et al. 2008) and in pancreatic β-cells under hyperglycemic conditions (Kang et al. 2008), it is unclear if Akt is glycosylated in models of tissue injury.

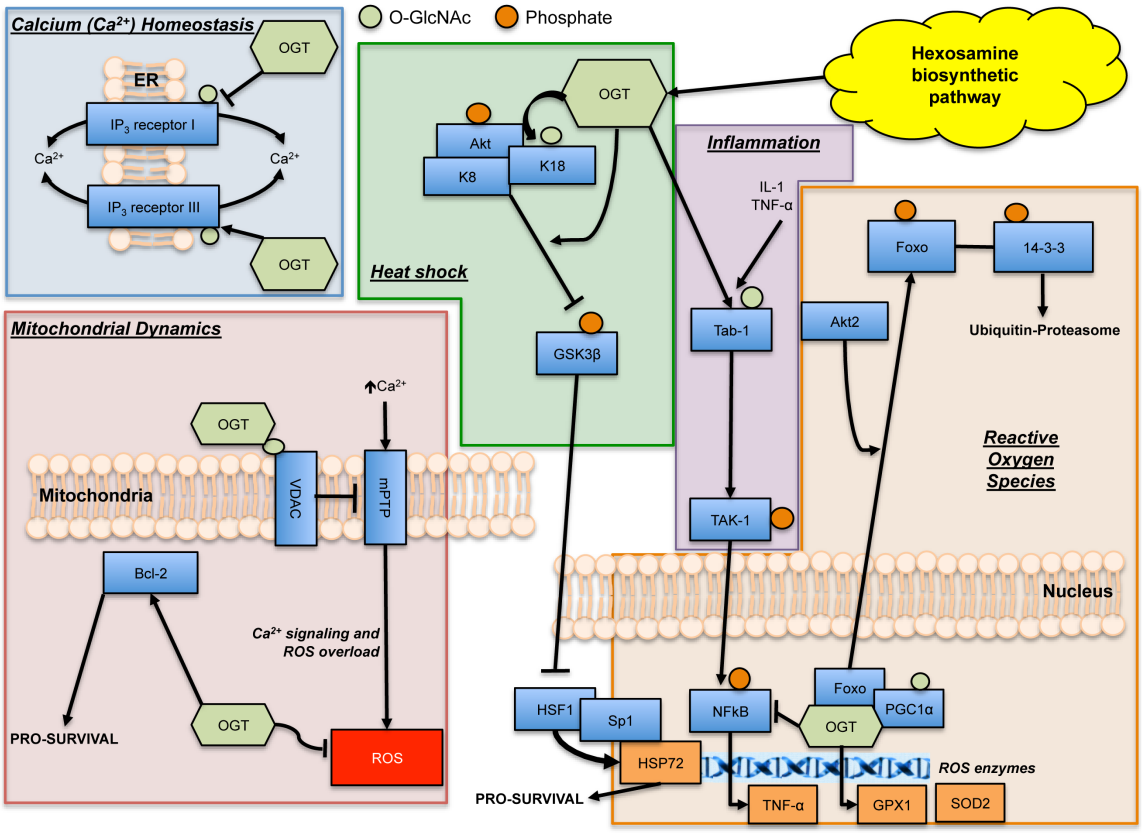

Figure 1-2: O-GlcNAc is involved in the cellular stress response. Glucose and glucosamine can enter cells via glucose transporters and are directed towards the hexosamine biosynthetic pathway (HBP) for conversion to UDP-GlcNAc. O-GlcNAcylation of key proteins is essential for maintaining cellular homeostasis and promoting survival during stress and injury. Key survival pathways modulated by O-GlcNAc include: 1) the PI3K/Akt pathway, 2) heat shock protein expression, 3) calcium (Ca^{2+}) homeostasis, 4) reactive oxygen species (ROS) regulation, 5) mitochondrial dynamics, 6) inflammation, and 7) PTM interplay. Note that proteins are shown as light blue squares, O-GlcNAc as green circles, and phosphates as orange circles. Arrows denote activation, whereas blunt ends denote inhibition.

Heat shock protein expression

One mechanism by which O-GlcNAc is thought to regulate cell survival is by modulating the expression of HSPs, the sentinels of the cellular stress response. Initial reports demonstrated that elevating O-GlcNAc levels augments the heat-induced expression of HSP72 and HSP40 (Sohn et al. 2004; Zachara et al. 2004b). Conversely, in cells in which O-GlcNAc levels had been lowered, by inhibition of the HBP or deletion of

OGT, the expression of HSPs was suppressed (Zachara et al. 2004b; Kazemi et al. 2010). Using a real-time polymerase chain reaction array of 84 chaperones, Kazemi and colleagues demonstrated that the expression of 18 molecular chaperones was inhibited when O-GlcNAc levels were lowered by deletion of OGT (Kazemi et al. 2010). These chaperones included HSP72, HSP40 J-domain containing proteins (*Dnaja1*, *Dnaja2*, *Dnaja3*, *Dnaja4*, *Dnajb1*, *Dnajb7*), the chaperone regulators Bag2 and Bag3, α-crystallin (*Cryab*, *Hspb8*), HSP25 (*Hspb1*), HSP110, HSP90α, and HSP60 (Kazemi et al. 2010). Interestingly, the expression of three proteins was upregulated (*Dnajb8*, *Dnajc5b*, *Dnajc5g*) (Kazemi et al. 2010).

The expression of HSPs is regulated by two key transcription factors: heat shock factor 1 (HSF1) and Sp1. Several studies have demonstrated that O-GlcNAc regulates both of these transcription factors, directly and indirectly, leading to the regulation of chaperone expression. One example by which O-GlcNAc is thought to regulate HSP expression is by promoting the phosphorylation and inactivation of the kinase GSK3β at Ser9 (Kazemi et al. 2010). In cells with reduced O-GlcNAcylation, increased inhibitory phosphorylation of HSF1 at Ser303 is observed (Kazemi et al. 2010). Conversely, elevating O-GlcNAc levels suppresses the phosphorylation of HSF1 at Ser303, promoting both its activation and downstream HSP expression (Kazemi et al. 2010). Recent reports suggest that GSK3β may suppress HSF1 activity by phosphorylating serine and threonine residues independent of Ser303 (Batista-Nascimento et al. 2011). Nonetheless, consistent with a model in which increased GSK3β activity suppresses HSF1 activation in the OGT null, inhibition of GSK3β rescues HSP72 expression in these cells (Kazemi et al. 2010). Further supporting this model, a reduction of Ser9 inhibitory phosphorylation of nuclear GSK3β was observed

in cells with lower O-GlcNAc levels (Kazemi et al. 2010). Notably, unlike the study by Gandy and colleagues (Gandy et al. 2006), the stress-induced phosphorylation of Akt was unaffected in this model, demonstrating that O-GlcNAc likely regulates numerous points upstream of GSK3β.

Glutamine has been demonstrated to protect cells and tissues from diverse forms of cellular stress and tissue injury (Wischmeyer et al. 2001). As glutamine is utilized by the HBP in the generation of UDP-GlcNAc (Figure 1-1), it has been postulated that glutamine may work in an O-GlcNAc dependent manner. In support of this hypothesis, *in vivo* treatment with glutamine has been shown to elevate O-GlcNAc levels (Singleton and Wischmeyer 2008; Hamiel et al. 2009). Moreover, the ability of glutamine to induce HSP70 is attenuated in cells in which O-GlcNAc levels have been lowered (Hamiel et al. 2009). In heat-stressed cells and a septic mouse model, glutamine treatment appears to promote the nuclear accumulation of HSF1 and Sp1 in an O-GlcNAc-dependent manner (Singleton and Wischmeyer 2008; Hamiel et al. 2009). Although the mechanisms underlying the above observations remain unclear, it may be explained in part by the observations of Lim and Chang who demonstrated that increased levels of O-GlcNAc are associated with a more soluble pool of Sp1 during thermal stress (Lim and Chang 2006). This may represent altered localization of Sp1, or that Sp1 exhibits increased thermal stability when it is O-GlcNAc-modified (Lim and Chang 2006) similar to Tau (Yuzwa et al. 2012). Together the data discussed above suggest that O-GlcNAc can regulate the expression of HSPs by regulating both HSF1 and Sp1.

Calcium homeostasis

Another mechanism by which O-GlcNAc may promote cell survival is by regulating calcium handling. Angiotensin II, an inositol (3,4,5)-trisphosphate (IP_3)-generating agonist, is a potent stimulator of cardiomyocyte hypertrophy that can elevate cytoplasmic calcium during vasoconstriction, increased blood pressure, and hemodynamic stress. A number of studies have demonstrated that angiotensin II treatment leads to an increase in basal calcium levels in adult and neonatal cardiomyocytes (Kem et al. 1991; Shao et al. 1998; Hunton et al. 2004), with sustained exposure affecting numerous cellular pathways (Meldrum et al. 1996; Liu et al. 2004b; Zhang et al. 2004) and eventually resulting in cell death (Kajstura et al. 1997; Goldenberg et al. 2001). Elevating UDP-GlcNAc and O-GlcNAc levels through treatment with glucosamine or the OGA inhibitor PUGNAc attenuates angiotensin II-induced capacitative calcium entry during I/R injury (Nagy et al. 2006). Further suggesting that regulation of calcium homeostasis in the heart is modulated by HBP flux and altered O-GlcNAc levels, O-GlcNAc appears to regulate a number of pathways downstream of calcium in models of ischemic injury. Consistent with decreased calcium influx, CaMKII phosphorylation is reduced, as are downstream events such as calpain proteolysis of structural proteins such as α-fodrin (Liu et al. 2007). Moreover, augmented O-GlcNAc signaling, via inhibition of OGA or overexpression of OGT, has been shown to attenuate oxidative stress and calcium overload in cardiomyocytes (Ngoh et al. 2011). Although the mechanism by which this occurs is unknown, it is accompanied by a reduction in ROS release and reduced formation of the mPTP (Ngoh et al. 2011).

While the mechanism by which O-GlcNAc regulates calcium handling in the ischemic heart has not been parsed out, recent studies have demonstrated that several IP_3 receptors are O-GlcNAc-modified suggesting a potential molecular mechanism by which O-GlcNAc can modulate calcium flux. The IP_3 type I receptor is the principle intracellular calcium release channel in many cell types including neurons, and it is regulated by calcium, ATP and O-GlcNAc. O-GlcNAcylation of the IP_3 type I receptor decreased its activity, while the removal of O-GlcNAc restored its function (Rengifo et al. 2007). Following this study, it was demonstrated that the IP_3 type III receptor is functionally regulated by O-GlcNAc, except that O-GlcNAcylation enhanced its activity while O-GlcNAc removal negated its function (Bimboese et al. 2011). Thus, O-GlcNAcylation of IP_3 type I and III receptors regulates their function(s) in controlling calcium flux and ultimately attenuating calcium-dependent apoptosis (Rengifo et al. 2007).

Reactive oxygen species

ROS participate in many intracellular signaling pathways that can ultimately lead to alterations in gene transcription, protein synthesis, and overall cellular function. Stressors such as I/R injury, which induces mitochondrial calcium overload (discussed previously) and ROS generation, favor the formation of the mPTP (discussed in the next section) and ultimately lead to cell death. Augmenting O-GlcNAc levels by adenoviral OGT overexpression or PUGNAc treatment has been shown to attenuate hypoxia and oxidative stress-induced ROS production. Conversely, suppression of O-GlcNAcylation by adenoviral OGA overexpression exacerbated ROS levels (Ngoh et al. 2011). One mechanism by which O-GlcNAc is thought to suppress ROS levels is by promoting the expression of antioxidant enzymes by stimulating the activity of Foxo1 and peroxisome

proliferator-activated receptor gamma coactivator 1α (PGC1α) (Housley et al. 2009). For example, it was demonstrated that induction of PGC1α in response to ROS leads to its O-GlcNAcylation and activation by OGT. Subsequently, the OGT-PGC1α complex is targeted to and hyper-O-GlcNAcylates Foxo1 (Figure 1-2) to promote increased transcription of ROS responsive enzymes, such as glutathione peroxidase 1 (GPX1) and superoxide dismutase 2 (SOD2), which protect against oxidative damage (St-Pierre et al. 2006; Housley et al. 2008; Housley et al. 2009). While the above studies were performed in hepatocytes, subsequent studies in a model of myocardial damage demonstrated that catalase mRNA levels were augmented above baseline following inhibition of OGA (PUGNAc), while overexpression of OGA reduced baseline catalase mRNA levels (Ngoh et al. 2011). Notably, in contrast to the studies discussed here, O-GlcNAc is thought to promote ROS generation in models of hyperglycemia and glucose toxicity (Goldberg et al. 2011), although the molecular basis for this paradox remains to be defined (Lima et al. 2012).

Mitochondrial dynamics

The mitochondrion is the powerhouse of the cell and is responsible for ATP production, maintenance of cellular byproducts, and overall regulation of cellular homeostasis. Altered mitochondrial dynamics leads to activation of the mitochondrial death pathway, which ultimately results in formation of the mPTP. Pore formation is activated by calcium surplus and ROS generation (previously discussed, Figure 1-2), and is responsible for non-specifically allowing small molecules (<1.5 kDa) to enter and exit the mitochondrial matrix (Crow et al. 2004). One postulated mechanism for the cytoprotective nature of O-GlcNAc is through the regulation of mitochondrial function

(Jones et al. 2008; Ngoh et al. 2008; Ngoh et al. 2010; Ngoh et al. 2011) by reducing calcium overload, dampening ROS production, and preventing mPTP formation (Jones et al. 2008; Ngoh et al. 2008; Ngoh et al. 2011). It has been suggested that O-GlcNAc may regulate the mPTP directly by modifying and modulating the voltage dependent anion channel (VDAC) (Jones et al. 2008; Ngoh et al. 2008) (Figure 1-2). For example, deletion of OGT led to reduced O-GlcNAcylation of VDAC, sensitizing cells to mitochondrial membrane potential collapse and mPTP formation (Jones et al. 2008; Ngoh et al. 2008). Notably, formation of the mPTP is also promoted by active GSK3β (Juhaszova et al. 2004; Miura and Miki 2009), which is inhibited in some models by stress-induced O-GlcNAcylation (Kazemi et al. 2010; Ku et al. 2010).

In addition to modulating VDAC, O-GlcNAc has been demonstrated to modulate Bcl-2 and the electron transport chain. Mitochondrial localization of Bcl-2 has been postulated to inhibit mPTP opening (Tsujimoto 2003; Tsujimoto et al. 2006), protect against a loss in mitochondrial membrane potential (Tsujimoto 2003; Murphy et al. 2005; Tsujimoto et al. 2006), prevent cytochrome c release (Tsujimoto 2003; Murphy et al. 2005; Tsujimoto et al. 2006), and attenuate mitochondria-mediated apoptosis (Tsujimoto 2003; Murphy et al. 2005; Tsujimoto et al. 2006). One study demonstrated that elevation of O-GlcNAc levels in hydrogen peroxide treated cells, an *ex vivo* model of I/R injury, led to increased mitochondrial Bcl-2 translocation (Champattanachai et al. 2008). There is some debate surrounding this finding, as PUGNAc did not appear to alter I/R-induced increases in mitochondrial Bcl-2 levels (Champattanachai et al. 2008). Finally, elevating levels of glucose in neonatal cardiomyocytes resulted in augmented O-GlcNAc levels and subsequently reduced function of mitochondrial electron transport complexes I, III, and IV

(Hu et al. 2005), however, its role in stress has not been studied yet. Interestingly, overexpressing OGA to reduce O-GlcNAc levels can reverse the effects of reduced mitochondrial function when glucose levels are elevated (Hu et al. 2005).

Inflammation

Trauma hemorrhage injury, like infection, induces an acute inflammatory response necessary for tissue repair. However, a hyper-inflammatory response can compromise healthy tissue, leading to cell and tissue death (Jarrar et al. 1999; Nathan 2002). The inflammatory response is driven by secreted tissue-derived cytokines, such as tumor necrosis factor-α (TNF-α) and interleukin (IL)-6, that are responsible for inflammation in the damaged area. Recent studies have shown that augmenting O-GlcNAc levels prior to and following trauma hemorrhage injury improves survival, and this protective phenotype is associated with reduced expression of TNF-α and IL-6 and improved recovery of multiple tissues and blood pressure (Yang et al. 2006a; Not et al. 2007; Chatham et al. 2008; Not et al. 2010).

O-GlcNAc has also been demonstrated to suppress acute inflammation in other models of injury presumably promoting cell survival (Not et al. 2007; Xing et al. 2008; Pathak et al. 2012). For example, in a rat model of arterial injury elevating O-GlcNAc levels by administration of glucosamine or PUGNAc attenuated inflammatory mediator expression, leukocyte infiltration, and neointima formation (Xing et al. 2008). Reduced inflammation was attributed to decreased TNF-α-induced phosphorylation of the nuclear factor κB (NFκB) p65 subunit and subsequent inhibition of NFκB transcriptional activation and signaling (Xing et al. 2008). Additionally, augmenting O-GlcNAc levels reduced the expression of a number of chemokines (cytokine-induced neutrophil chemoattractant-2β

and monocyte chemotactic protein-1) and adhesion molecules (vascular cell adhesion molecule-1 and P-selectin) (Xing et al. 2008).

Pro-inflammatory cytokines, such as TNF-α and IL-1, activate downstream signals in a manner mediated by transforming growth factor-β-activated kinase I (TAK-1), also known as mitogen-activated protein kinase kinase kinase 7 (Sakurai et al. 2000; Wang et al. 2001). A recent study showed that O-GlcNAcylation of TAK-1-binding protein (Tab-1) modulates TAK-1-mediated cytokine release when induced by IL-1 and osmotic stress (Pathak et al. 2012). Utilizing wild type (WT) and O-GlcNAc-deficient mutant Tab-1 (S395A) in *Tab-1*$^{-/-}$ mouse embryonic fibroblasts, this study demonstrated that the O-GlcNAc-modification of Tab-1 at Ser395 is essential for full TAK-1 autophosphorylation at Thr187 and activation upon stress, as well as the subsequent downstream activation of NFκB and production of IL-6 and TNF-α (Pathak et al. 2012).

Interplay between O-GlcNAc and other PTMs

One mechanism by which O-GlcNAc is thought to regulate proteins is by directly or indirectly regulating other post-translational modifications including phosphorylation, nitrosylation, and ubiquitination.

Phosphorylation

Phosphate (PO_4^{3-}) and GlcNAc ($C_8H_{15}NO_6$) moieties are both covalently and reversibly added in an O-linkage to serine and threonine residues in a manner known as phosphorylation and O-GlcNAcylation respectively. There is extensive crosstalk between these two modifications, and this dynamic interplay is implicated in regulating numerous signaling networks (Wang et al. 2007; Wang et al. 2008; Wang et al. 2010b; Hart et al.

2011). For a subset of proteins (Kelly et al. 1993; Cheng and Hart 2001; Comer and Hart 2001; Du et al. 2001), O-GlcNAc and phosphorylation appear to compete for the same serine or threonine residue, such as on the proto-oncogene c-Myc (Chou et al. 1995). Alternatively, for numerous proteins O-GlcNAc can sterically hinder nearby phosphorylation sites (Yang et al. 2006b; Housley et al. 2008; Dias et al. 2009; Wang et al. 2010b; Tarrant et al. 2012), for example in the CK2 protein where O-GlcNAcylation of Ser347 prevents its phosphorylation at nearby amino acid Thr344 (Tarrant et al. 2012). The idea that these modifications are reciprocal comes from data demonstrating that phosphorylation of subsets of proteins is suppressed when global O-GlcNAc levels are elevated (Griffith and Schmitz 1999; Lefebvre et al. 2001; Wang et al. 2008). One elegant study demonstrated that *in vitro* O-GlcNAcylation of the C-terminal domain of RNA polymerase II blocked its phosphorylation and vice versa (Comer and Hart 2001). Suggesting that this interplay also alters protein function *in vivo*, additional studies have demonstrated that tau is hyper-phosphorylated in a brain OGT knockout (O'Donnell et al. 2004). However, readers should be cautioned as the reciprocal relationship between O-GlcNAc and phosphorylation exists only for a subset of proteins, while for others there is no direct association and proteins can be both phosphorylated and O-GlcNAcylated simultaneously, such as insulin receptor substrate-1 (IRS-1) (Ball et al. 2006).

In addition to cross talk associated with site-occupancy, there is cross talk between the enzymes responsible for O-GlcNAcylation and phosphorylation. OGT and OGA are known to associate with and modify kinase and phosphatase enzymes (Khidekel et al. 2004; Wells et al. 2004; Cheung et al. 2008; Slawson et al. 2008; Dias et al. 2009; Wang et al. 2010b; Dias et al. 2012). For example, CaMKIV is inhibited by O-GlcNAc-

modification within its ATP-binding region, and de-O-GlcNAcylation and subsequent phosphorylation is required for CaMKIV activation (Dias et al. 2009). Several proteomic analyses have been performed to further delineate the interplay between O-GlcNAc and phosphorylation in cell cycle progression. One of these studies demonstrated that the kinase Aurora B, which regulates mitotic progression, forms a transient complex with OGT and OGA in the mitotic phase of the cell cycle and colocalizes with OGT to midbodies during telophase and cytokinesis (Slawson et al. 2008). Inhibition of Aurora B leads to diminished midbody localization of OGT and an increase in global O-GlcNAc levels (Slawson et al. 2008). This study also demonstrated that vimentin, a substrate for Aurora B and OGT during mitosis, exhibited alterations in its O-GlcNAcylation and phosphorylation patterns upon modulation of OGT or OGA activity (Slawson et al. 2008). A second study identified 141 previously unreported O-GlcNAc sites on proteins that are involved in spindle assembly and cytokinesis, many of which are the same site as or are in close proximity to sites of phosphorylation (Wang et al. 2010b). Finally, modulation of O-GlcNAc levels was found to alter the phosphorylation status of proteins localized to the mitotic spindle and midbody, for example upon OGT overexpression, cyclin dependent kinase 1 becomes hyper-phosphorylated thereby reducing its activity and subsequently decreasing the phosphorylation status of its target proteins (Wang et al. 2010b).

Endothelial nitric oxide synthase (eNOS) generates nitric oxide and stimulates vasodilation by inhibiting smooth muscle contraction and platelet aggregation, with these functions reported to be impaired in diabetes-associated erectile dysfunction. One study demonstrated that in rats treated with alloxan to induce diabetes, eNOS was hyper-O-GlcNAcylated and hypo-phosphorylated at Ser1177 (Musicki et al. 2005). Phosphorylation

of eNOS at this site is mediated by Akt phosphorylation, and this study demonstrated that the phosphorylation of both Akt and eNOS was decreased in the diabetic model, implicating that O-GlcNAcylation at Ser1177 is one potential mechanism for eNOS inactivation and thereby diminished vasodilation (Musicki et al. 2005).

Other PTM roles

There is emerging evidence for the interplay of O-GlcNAc with other post-translational modifications such as protein ubiquitination and nitrosylation, although it is important to note that the exact mechanisms by which these modifications interact are still being elucidated.

A growing body of evidence suggests that O-GlcNAc may be a regulator of protein degradation. This evidence includes data demonstrating that enhanced O-GlcNAcylation is associated with an extended half-life of proteins, such as with Sp1 (Han and Kudlow 1997) and the murine β-estrogen receptor (Jiang and Hart 1997; Cheng and Hart 2001). At least three mechanisms have been postulated to underlie these observations. Firstly, O-GlcNAc can block the phosphorylation of PEST (Pro-Glu-Ser-Thr) domains in the murine β-estrogen receptor thereby preventing its degradation (Cheng et al. 2000; Cheng and Hart 2001). Secondly, as discussed below, data suggests that O-GlcNAc may regulate ubiquitination. Thirdly, O-GlcNAc is implicated in regulating the proteasome directly, as highlighted by studies showing that numerous proteins in the proteasome are O-GlcNAc-modified and that enhanced O-GlcNAcylation may inhibit proteasome function (Sumegi et al. 2003; Zhang et al. 2003). One study demonstrated that both ubiquitination and O-GlcNAcylation increase upon heat-shock treatment and that these PTMs can occur on some proteins concomitantly (Guinez et al. 2008). O-GlcNAc-modified proteins were not

observed to be stabilized following proteasome inhibition, and ubiquitination could be enhanced or reduced by increasing or decreasing O-GlcNAc levels respectively (Guinez et al. 2008). It was speculated that an E1 ubiquitin-activating enzyme interacts with HSP70 only in its O-GlcNAcylated form (Guinez et al. 2008). An agonistic relationship between these two modifications is suggested such that O-GlcNAc may alter the activity of E1 enzymes to modulate stress-induced ubiquitination (Shimura et al. 2001; Shrikhande et al. 2010; Fujiki et al. 2011). It has also been shown that O-GlcNAcylation of a protein may facilitate its subsequent ubiquitination. For example, O-GlcNAcylation of histone H2B at Ser112 facilitates monoubiquitination at Lys120 to regulate transcription (Fujiki et al. 2011).

S-nitrosylation is a cysteine modification that is found and maintained on OGT in resting cells, and S-nitrosylated OGT has greatly reduced catalytic activity compared to the native form of the protein (Ryu and Do 2011). OGT becomes denitrosylated in macrophages treated with lipopolysacharides to trigger an innate immune response, which leads to increased catalytic activity and hyper-O-GlcNAcylation of proteins (Haberhausen et al. 1995). While other PTMs such as acetylation, methylation, sumoylation, and many others have pivotal roles in regulating protein function and signal transduction, the interplay of these modifications with O-GlcNAcylation has yet to be defined.

Molecular mechanisms of disease

There are many facets of the cellular stress response whose misregulation can contribute to neurodegenerative disease pathophysiology, and O-GlcNAc is implicated in the etiology of some of these diseases. Notably, the OGT gene is on the X chromosome at

position Xq13.1, the same locus associated with dystonia-parkinsonism syndrome (Haberhausen et al. 1995), and OGA maps to chromosome 10 near the locus associated with late-onset AD (10q24.1-q24.3) (Bertram et al. 2000).

Alzheimer's disease

AD is a form of dementia that is characterized by reduced brain function and cognitive deficits, where both genetic and environmental factors play a role in pathogenesis (Hardy and Allsop 1991). AD phenotypes are often the result of unfolded or aggregated proteins, aberrant signaling, and oxidative stress. While there are many mechanisms by which these events are regulated, the most well studied proteins involved in AD are amyloid β precursor protein (APP), amyloid β (Aβ), and tau (Hardy and Allsop 1991). Dysregulation of APP, Aβ plaque formation, tau phosphorylation, and tangle formation dominate the cascade of events leading to AD and ultimately to neuronal death (Dong et al. 2004).

AD transgenic mouse models are characterized by Aβ plaque formation and this leads to decreased cell proliferation and defective contextual memory (Kang et al. 2007). APP, the precursor protein to Aβ, is O-GlcNAc-modified although the importance of this modification remained elusive for many years (Jacobsen and Iverfeldt 2011). It was later demonstrated that inhibiting OGA with PUGNAc or reducing the expression of OGA (small interfering RNA) increased the amount of APP O-GlcNAcylation and non-amyloidogenic α-secretase processing (Jacobsen and Iverfeldt 2011). This has further downstream effects such as increasing levels of the neuroprotective soluble APPα cleavage fragment, which reduces Aβ secretion and suggests a protective role for O-GlcNAc (Kim et al. 2012). Finally, treatment with the OGA inhibitor 1,2-dideoxy-2′-propyl-α-d-

glucopyranoso-[2,1-d]-Δ2′-thiazoline (NButGT) in a mouse model of AD resulted in reduced γ-secretase activity and subsequent attenuation of Aβ plaque production and inflammation *in vivo*, further highlighting the important protective role of O-GlcNAc under conditions of stress and neurodegeneration (Rissman et al. 2007; Rissman et al. 2012).

Tau was demonstrated to be directly O-GlcNAc-modified (Arnold et al. 1996; Liu et al. 2004a) and it was later shown that O-GlcNAcylation negatively regulates site-specific phosphorylation of tau in the human brain (Liu et al. 2004a). Notably, increased phosphorylation of Tau has been implicated in the formation of the toxic tangles associated with neurodegeneration. Recent data have demonstrated that inhibition of OGA, which leads to an increase in O-GlcNAc levels, in a murine model of AD led to increased O-GlcNAcylation of tau, decreased tau aggregation, and diminished neuronal cell death. Together, these data highlight the protective role of O-GlcNAc and suggest that OGA could be a therapeutic target for slowing AD progression (Yuzwa et al. 2012). Interestingly, low glucose uptake and metabolism during aging has been postulated to lead to decreased O-GlcNAcylation of key proteins such as Tau, potentially exacerbating the AD phenotype during aging (Yuzwa et al. 2012).

Parkinson's disease

Parkinson's disease (PD) is a brain disorder characterized by the degeneration of midbrain dopaminergic neurons, which is often accompanied by the formation of Lewy bodies (abnormal protein aggregates) (Henchcliffe and Beal 2008). Together this leads to improper signaling and loss of muscle function. Genetic alterations in the nucleus have been linked to disrupted mitochondrial morphology and function that can then modulate

protein activity, trigger apoptosis, or lead to accumulation of misfolded or damaged proteins in PD pathogenesis (Henchcliffe and Beal 2008).

Aggregation of the α-synuclein protein or mutations in the α-synuclein gene (A53T) which lead to an impairment of mitochondrial dynamics, morphology, and movement have been linked to rare inherited forms of PD (Polymeropoulos et al. 1997; Spillantini et al. 1997; Xie and Chung 2012). One study identified a 22 kDa O-glycosylated form of α-synuclein in a protein complex with parkin (an E3 ubiquitin ligase) and UbcH7 (an E2 ubiquitin-conjugating enzyme). These studies suggested that the glycosylated form of α-synuclein was bound and ubiquitinated by parkin (Shimura et al. 2001). On the contrary, a subsequent study postulated that α-synuclein is modified by O-GlcNAc and that its nonglycosylated form interacts with parkin in embryonic hippocampal cells, although the specific type of glycosylation was never confirmed (Kim et al. 2003). Recently, the O-GlcNAc-modification status of α-synuclein was mapped to Thr72 (Wang et al. 2010a), which has been demonstrated to prevent its aggregation (Marotta et al. 2012). Further data (discussed previously) highlights the interplay between O-GlcNAcylation and ubiquitination to regulate protein stability and degradation, although a direct link between these phenomena and PD has yet to be elucidated.

Methods to study O-GlcNAcomics

In this section, we will discuss the current methodologies used to modulate O-GlcNAc levels, enrich O-GlcNAc-modified proteins, and identify sites of O-GlcNAcylation.

In vitro and *in vivo* modulation of O-GlcNAc levels

O-GlcNAc levels can be directly or indirectly altered *in vitro* and *in vivo* by modulating the activity or expression of OGT (Gross et al. 2005; Dorfmueller et al. 2011; Gloster et al. 2011), OGA (Beer et al. 1990; Dong and Hart 1994; Haltiwanger et al. 1998; Konrad et al. 2002; Liu et al. 2002; Dorfmueller et al. 2006; Knapp et al. 2007; Whitworth et al. 2007; Macauley et al. 2008; Yuzwa et al. 2008; Laczy et al. 2010), or other key enzymes in the HBP (Marshall et al. 1991; Traxinger and Marshall 1991; Patti et al. 1999; Ross et al. 2000; Buse et al. 2002; McClain 2002). Techniques such as overexpression of OGT (Zachara et al. 2004b), OGA (Slawson et al. 2005), and GFAT (Chen et al. 1997; James et al. 2000; Marshall et al. 2004) by both transient transfection and viral transduction have been successful, as has reducing the expression of these enzymes using RNA interference (Zachara et al. 2004b; Ngoh et al. 2009a; Hsieh et al. 2012). OGT has also been overexpressed using a tetracycline-inducible OGT stably expressed in HeLa human cervical cancer cells, although for effective overexpression a histone deacetylase inhibitor was included with the tetracycline for appropriate regulation of OGT (Marshall et al. 2003).

Murine models and the $OGT^{F/Y,mER\text{-}Cre\text{-}2A\text{-}GFP}$ cell line

Several mouse models and cell lines exist in which the levels of O-GlcNAc can be modulated. Notably, in murine models, deletion of *Ogt* (Shafi et al. 2000; O'Donnell et al. 2004), *EMeg32* (Boehmelt et al. 2000b), or *Pgm3* (Greig et al. 2007) leads to embryonic lethality, whereas deletion of *Mgea5* (OGA) leads to perinatal lethality (Yang et al. 2012). A number of hypomorphic alleles of *Pgm3* have been characterized, leading to cells and mice with different concentrations of UDP-GlcNAc (Greig et al. 2007). Unlike deletion of *EMeg32*, deletion of *Ogt* is lethal in isolated embryonic fibroblasts (O'Donnell et al. 2004).

To overcome this challenge, researchers have immortalized cells in which the first two exons of *Ogt* are flanked by loxP recombination sites (O'Donnell et al. 2004; Kazemi et al. 2010). These cells ($OGT^{F/Y}$) have been stably transfected with a Cre recombinase estrogen receptor chimera (Cre-ERT2-GFP) that is induced by 4-hydroxytamoxifen ($OGT^{F/Y,mER\text{-}Cre\text{-}2A\text{-}GFP}$) (Kazemi et al. 2010). Addition of 4-hydroxytamoxifen activates Cre recombinase, resulting in recombination of the LoxP sites and deletion of OGT.

Modulating O-GlcNAc levels using inhibitors of OGT, OGA, and the HBP

A large number of inhibitors have been developed for blocking the activity of OGA in both cell culture and animal models (Beer et al. 1990; Dong and Hart 1994; Haltiwanger et al. 1998; Konrad et al. 2002; Liu et al. 2002; Dorfmueller et al. 2006; Knapp et al. 2007; Whitworth et al. 2007; Macauley et al. 2008; Yuzwa et al. 2008), and here we will focus on those that are commercially available. PUGNAc was the first OGA inhibitor isolated and inhibits OGA at a K_i of 52 nM *in vitro* (Dong and Hart 1994; Haltiwanger et al. 1998). PUGNAc is suitable for use in cells (10-100 μM, 4-18 h) and in animals (50 mg/kg, 4-12 h) (Jones et al. 2008), however prolonged use (>36 h) can lead to cell cycle defects (Slawson et al. 2005). While widely used, recent evidence demonstrates that PUGNAc can also inhibit other lysosomal glycosidases including hexosaminidases A and B (Macauley et al. 2005; Ficko-Blean et al. 2008), suggesting that PUGNAc may have effects on other cellular pathways aside from O-GlcNAcylation. Streptozotocin has also been widely used, but only inhibits OGA at very high concentrations (Roos et al. 1998; Gao et al. 2000; Okuyama and Yachi 2001; Liu et al. 2002; Toleman et al. 2006). It is important to note that streptozotocin is also a DNA-alkylating agent and can release nitric oxide, making it difficult to determine whether the observed effects are due to OGA inhibition or

streptozotocin toxicity (Kwon et al. 1994). Alloxan has been suggested to inhibit OGA (Lee et al. 2006), but has been reported to also inhibit OGT and as such should be used with extreme caution (Konrad et al. 2002; Macauley et al. 2005). More recently, TMG has been introduced, and unlike PUGNAc, TMG is effective in crossing the blood brain barrier and does not appear to inhibit hexosaminidase A or B (Yuzwa et al. 2008).

Several OGT inhibitors have also been isolated that work well *in vitro* (Gross et al. 2005), and thus far these have been useful in isolated neonatal cardiomyocytes (5 μM) (Ngoh et al. 2008) and breast cancer cells (200 μM) (Caldwell et al. 2010). A more recent study has focused on synthesizing novel OGT inhibitors with structural analogues to UDP-GlcNAc/UDP (Dorfmueller et al. 2011). While the synthesized compounds inhibit OGT in the micromolar range, it should be noted that they are inactive when used on living cells (Dorfmueller et al. 2011). Another recent study developed a synthetic carbohydrate precursor, 2-acetamido-1,3,4,6-tetra-O-acetyl-2-deoxy-5-thio-α-d-glucopyranose (Ac-5SGlcNAc), which can be successfully converted by the cell to produce UDP-5SGlcNAc in cell culture and *in vitro* models (Gloster et al. 2011). UDP-5SGlcNAc is not an efficient substrate for OGT, but excludes binding of UDP-GlcNAc therefore inhibiting OGT function (Gloster et al. 2011). It is important to note that these inhibitors are not yet commercially available.

There are numerous commercially available chemicals for suppressing flux through the HBP (Marshall et al. 1991; Traxinger and Marshall 1991; Patti et al. 1999; Ross et al. 2000; Buse et al. 2002; McClain 2002; Ngoh et al. 2010), which reduced UDP-GlcNAc levels and thus the O-GlcNAc-modification. Treatment with exogenous glucose, glutamine, or glucosamine leads to increased O-GlcNAc levels by increasing flux through

the HBP (Traxinger and Marshall 1991), although it is important to note that these compounds enter numerous pathways in the cell and observed effects may not be due to changes in O-GlcNAcylation. Azaserine and 6-diazo-5-oxo-L-norleucine (DON) are GFAT inhibitors, and treatment with these compounds decreases flux through the HBP thereby reducing O-GlcNAc levels (Marshall et al. 1991). Despite their common usage, both of these GFAT inhibitors do not act specifically on the HBP and may have effects on other enzymes and cellular pathways, especially those involved in glutamine metabolism.

Isolation, purification, and detection of O-GlcNAc and O-GlcNAc-modified proteins

Our understanding of the role of O-GlcNAc has been hampered due to the lack of specific and sensitive tools. Many challenges arise as the most commonly used analytical protein techniques, including gel electrophoresis, liquid chromatography (LC), and mass spectrometry (MS), often fail to detect O-GlcNAc. This is due to a number of factors such as 1) the addition of a monosaccharide of O-GlcNAc does not generally affect the migration of the glycoprotein during 1- or 2-dimensional gel electrophoresis; 2) the O-GlcNAc-modification is rapidly hydrolyzed by hexosaminidases during protein isolation unless appropriate inhibitors are included; 3) the β-O-glycosidic linkage is chemically labile and is rapidly released under conditions of mild acid or base; 4) due to its lability, O-GlcNAc is usually lost at the ion source of electrospray ionization (ESI) or during ionization by matrix-assisted laser desorption ionization mass spectrometry; and 5) ionization of peptides modified by O-GlcNAc is suppressed during mass spectrometry and as such need to be enriched. Here, we will review the most robust techniques for the

detection and purification of O-GlcNAc-modified proteins, as well as techniques for defining sites of O-GlcNAcylation.

Detecting O-GlcNAc-modified proteins by ^{3}H-galactose labeling

The gold standard for the detection of O-GlcNAc-modified proteins has been UDP-galactose:GlcNAc β-1,4-galactosyltransferase (GalT1) labeling, which transfers ^{3}H-galactose from UDP-^{3}H-galactose to any terminal GlcNAc residue (Torres and Hart 1984; Roquemore et al. 1994). One advantage of this technique is the generation of a radiolabeled sugar (^{3}H-galactose-R) that can be followed in subsequent analyses. As GalT1 will transfer galactose to any terminal GlcNAc reside, it is important to treat samples with peptide N-glycosidase F to enzymatically remove N-glycans prior to ^{3}H-galactose labeling. Recently this technique has also been adapted to incorporate an unnatural tetraacetylated N-azidoacetylgalactosamine (GalNAz) onto proteins (see section Click-iT).

Immunopurification with antibodies and lectins

In contrast to protein phosphorylation where a range of pan- and site-specific phospho-antibodies are commercially available, only a few such tools exist for the O-GlcNAc-modification. These antibodies fall into two classes: those that can be considered pan-specific and others that are site-specific (Zachara et al. 2011c). The two most commonly used pan-specific antibodies for detecting O-GlcNAc-modified proteins are CTD110.6 (Comer and Hart 2001), a mouse immunoglobulin (Ig)M antibody raised against the C-terminus of RNA polymerase II, and RL2 (Snow et al. 1987), a mouse IgG antibody raised against O-GlcNAc-modified components of the nuclear pore complex. Recently, a number of monoclonal IgG antibodies have been introduced for detecting O-GlcNAc-modified proteins including 1F5.D6(14), 18B10.C7(3) and 9D1.E3(10) (Teo et

al. 2010). These antibodies were raised against a three-component immunogen-containing epitope regions from the casein kinase II (CKII) α-subunit 15, a mouse major histocompatibility complex class II restricted helper T-cell epitope, and a Toll-like receptor 2 agonist (Teo et al. 2010). Like RL2, these antibodies are mouse IgGs and appear to only recognize O-GlcNAc in certain 3-dimensional environments. In addition to the antibodies discussed previously, anti-streptococcal monoclonal mouse IgG antibodies have been commonly used for detecting proteins containing GlcNAc residues. These antibodies were raised against streptococcal group A carbohydrates, which is composed of a polyrhamnose backbone with GlcNAc side chains (Turner et al. 1990).

There has only been a small cohort of studies that have incorporated a top-down shotgun proteomics approach for identifying O-GlcNAc-modified proteins using the antibodies previously discussed. These studies have been hampered because none of the discussed antibodies appear to bind O-GlcNAc-modified peptides. As such, proteins that interact with O-GlcNAc-modified proteins are also identified, and in most cases O-GlcNAc-modified peptides are suppressed in the MS making O-GlcNAc-modification sites difficult to map. Nonetheless, a number of studies have been performed highlighting proteins that are potentially O-GlcNAc-modified in response to cellular stress and tissue injury (Jones et al. 2008; Teo et al. 2010; Zachara et al. 2011c), and the O-GlcNAcylation status of a number of proteins has been confirmed by independent techniques (Table 1-1). One recent study used 1F5.D6(14), 18B10.C7(3) and 9D1.E3(10) to immunoprecipitate O-GlcNAc-modified proteins followed by large-scale shotgun proteomics to identify more than 200 differentially expressed glycoproteins from human embryonic kidney (HEK)293 cells and rat livers responding to trauma hemorrhage and resuscitation (Teo et al. 2010).

Another recent study relied on Stable Isotopic Labeling of Amino acids in Cell culture (SILAC) (Ong et al. 2002; Ong et al. 2003) in combination with CTD110.6 immunoprecipitation (Zachara et al. 2011a). Here, Cos-7 African green monkey kidney cells were isotopically labeled in SILAC media ($^{13}C_6$ L-arginine and $^{13}C_6{}^{15}N_4$ L-arginine) and treated with heat shock or an inhibitor of OGA, PUGNAc. Labeled proteins were combined in equal ratios, and O-GlcNAc-modified proteins were immunoprecipitated using CTD110.6 immobilized to agarose and subsequently identified by LC in conjunction with tandem mass spectrometry (MS/MS) (Zachara et al. 2011a). Numerous proteins with diverse functions were identified, including nuclear factor 90, RuvB-like 1 (Tip49α), RuvB-like 2 (Tip49β), and several COPII vesicle transport proteins. Many of these proteins bind double-stranded DNA-dependent protein kinase or double-stranded DNA breaks, suggesting a role for O-GlcNAc in regulating DNA damage signaling or repair (Zachara et al. 2011a).

Lectin affinity chromatography

Wheat germ agglutinin (WGA) is a commonly used plant lectin for enriching and detecting O-GlcNAc-modified proteins (Zachara et al. 2004a; Vosseller et al. 2006; Zachara et al. 2011b). WGA has weak affinity for single GlcNAc residues, but its affinity is dramatically increased for GlcNAc-residues that are clustered (Finlay et al. 1987; Lee and Lee 2000; Lundquist and Toone 2002). The drawback of WGA as a tool for O-GlcNAc enrichment and detection is its additional recognition of sialic acid (NeuAcα(2-3)) residues (Monsigny et al. 1980). Treating samples initially with peptide N-glycosidase F to remove N-glycans, and by performing nuclear and cytoplasmic protein extractions (Zachara et al. 2011b) can resolve these shortcomings. Succinylation of WGA (sWGA) increases its

specificity for GlcNAc as it ablates its reactivity to sialic acid (Monsigny et al. 1980). However, succinylation reduces the affinity of sWGA for O-GlcNAc and thereby decreases its utility for immunoprecipitation.

Lectin Weak Affinity Chromatography (LWAC) utilizes the affinity of WGA in an extended column format (>3 meters in length) with a small diameter (~1 cm) to enrich O-GlcNAc-modified peptides (Vosseller et al. 2006). This chromatography technique employs low flow rates and an isocratic elution buffer containing low concentrations of GlcNAc (Vosseller et al. 2006). LWAC has been adapted successfully for shotgun characterization of O-GlcNAc-modified proteomes from postsynaptic density preparations (Vosseller et al. 2006), *A. thaliana* (Xu et al. 2012), and mouse embryonic stem cells (Myers et al. 2011).

Table 1-1: A summary of O-GlcNAc-modified proteins, their biological significance, and the methods by which they were detected. This table highlights the wide range of techniques and tools for the enrichment and detection of O-GlcNAc-modified proteins, including but not limited to O-GlcNAc antibodies, click-iT methods, immunoprecipitation, and proteomics tools. Abbreviations include: BEMAD, beta elimination and Michael addition; ETD, electron transfer dissociation; GalT1, β-1,4-galactosyltransferase; LC, liquid chromatography; MS, mass spectrometry; MS/MS, tandem mass spectrometry.

O-GlcNAc-modified protein	Biological Function, Implication, Significance	Cell Type/ Model	Detection	Secondary Confirmation	Reference
Casein kinase II (CKII) α subunit	O-GlcNAc antagonizes Thr344 phosphorylation, promotes proteasomal degradation, and alters substrate specificity	HEK293T cells	Western blotting (CTD110.6, 1F5.D6(14), 18B10.C7(3), 9D1.E3(10))	Ion trap ETD MS/MS, GalT1, LC-MS/MS	(Tarrant et al. 2012)
Protein Arginine Methyltransferase 4 (PRMT4/Carm1)	O-GlcNAcylated Carm1 does not exhibit mitotic phosphorylation or proper mitotic cellular localization	Neuro2a cells	Western blotting (CTD110.6)	Immunoprecipitation, Yeast-2-hybrid	(Cheung and Hart 2008; Sakabe et al. 2010),
Forkhead Box O1 (Foxo1)	O-GlcNAc regulates activation in response to glucose, resulting in increased expression of gluconeogenic genes and genes encoding enzymes that detoxify ROS	Fao rat hepatoma cells	Western blotting (CTD110.6)	OGT assay, Immunoprecipitation, Ion trap ETD MS/MS	(Housley et al. 2008; Kuo et al. 2008; Housley et al. 2009)
Inhibitor of NFκB kinase (IKKβ)	Catalytic activity of IKKβ is enhanced through O-GlcNAcylation and loss of p53	$p53^{-/-}$, $p65^{-/-}$, and $p53^{-/-}p65^{-/-}$ MEFs	Western blotting (CTD110.6)	Immunoprecipitation	(Kawauchi et al. 2009)
NFκB	Increased O-GlcNAc levels is associated with reduced activation of NFκB and reduced expression of proinflammatory cytokines	HeLa cells	Azide-tag, nano-HPLC/tandem MS	Immunoprecipitation, Western blotting	(Nandi et al. 2006; Golks et al. 2007)
p53	Modification of p53 with O-GlcNAc regulates p53 stability by blocking ubiquitin-dependent proteolysis	MCF-7 and H1299 cells	Western blotting (CTD110.6)	2-dimesional gel electrophoresis, BEMAD, quadrupole time-of-flight MS	(Yang et al. 2006b)

O-GlcNAc-modified protein	Biological Function, Implication, Significance	Cell Type/ Model	Detection	Secondary Confirmation	Reference
IP_3 Receptor Type I	Regulation (up or down/ in or out) of Ca^{2+} flux through the ER and Ca^{2+} signaling	SH-SY5Y and DT40 B cells, Mouse and Rat Cerebella	Western blotting (CTD110.6 & RL2)	Immunoprecipitation	(Rengifo et al. 2007)
IP_3 Receptor Type III	Regulation (up or down/ in or out) of calcium flux through the ER and Ca^{2+} signaling	$AR4^{-}2J$ cells	Western blotting (RL2)	Immunoprecipitation	(Bimboese et al. 2011)
Tab-1	O-GlcNAcylation of Tab-1 is required for full TAK-1 activation upon stimulation by IL-1/osmotic stress, and downstream activation of NFκB, and production of IL-6 and TNF-α	Tab-$1^{-/-}$ MEFs	Western blotting (CTD110.6), LC-ETD-MS/MS	Immunoprecipitation (O-GlcNAc specific Tab-1 Ser395 antibody), *In vitro* O-GlcNAc assay, GalT1 labeling	(Pathak et al. 2012)
Insulin receptor substrate 1 (IRS-1)	O-GlcNAc contributes to insulin resistance by inhibiting phosphorylation at the PI3K p85 binding motif in IRS-1	HEK293T cells	BEMAD, Ion trap MS/MS/MS	Western blotting (CTD110.6)	(Ball et al. 2006; Whelan et al. 2010),
HSP70 & HSP90	No function currently associated with glycosylation of these proteins	HeLa cells	Azide-tag, nano-HPLC/tandem MS	Immunoprecipitation, Western blotting	(Wells et al. 2002b; Walgren et al. 2003; Nandi et al. 2006)
K18	Glycosylation of K18 increases upon heat stress. In models of liver damage, O-GlcNAcylated K18 promotes the phosphorylation and activation of Akt	Transgenic $K18^{-}Gly^{-}$ mice, BHK21 cells	Western blotting (CTD110.6)	Immunostaining, Immunofluorescence, GalT1 activity assays	(Ku et al. 2010)
HSF1	O-GlcNAcylation of HSF1 promotes its nuclear translocation and activation leading to HSP expression	C57Bl/6 mice	Western blotting (CTD110.6)	Immunoprecipitation	(Singleton and Wischmeyer 2008)

O-GlcNAc-modified protein	Biological Function, Implication, Significance	Cell Type/ Model	Detection	Secondary Confirmation	Reference
Calcium/Calmodulin-dependent Kinase IV (CaMKIV)	O-GlcNAcylation of the CaMKIV active site blocks its phosphorylation at Thr200 and ATP binding, inhibiting its kinase activity	HEK293A cells	Western blotting (CTD110.6)	Immunoprecipitation, GalT1 labeling, BEMAD, Ion trap MS/MS	(Dias et al. 2009)
Peroxisome proliferator-activated receptor gamma coactivator 1α (PGC1α)	Co-localizes with OGT and targets the enzyme to FoxOs, leading to increased transcriptional of metabolic enzymes	HEK293T cells	Ion trap ETD-MS/MS	Western blotting (CTD110.6), sWGA, GalT1 labeling, Immunoprecipitation, OGT activity assay	(Housley et al. 2009)
Voltage Dependent Anion Channel (VDAC)	O-GlcNAc–modified VDAC is associated with reduced calcium-induced swelling of the mitochondria	Mouse hearts, isolated cardiac myocytes	Immunoprecipitation (CTD110.6)		(Jones et al. 2008; Ngoh et al. 2008)

Click-iT and other chemically based strategies to detect O-GlcNAc-modified proteins

Click chemistry is a chemoenzymatic strategy for quickly and reliably synthesizing compounds of interest. By this method, target substrates are labeled with a probe of interest that can be derivatized to detect or enrich proteins and peptides. This technique has been adapted for the detection and enrichment of O-GlcNAc-modified proteins and peptides. Sugars containing either ketones or azido groups are incorporated into O-GlcNAc-modified proteins using one of two techniques: 1) a mutant GalT1 (Y289L) with an enlarged active site is used to add UDP-GalNAz to terminal GlcNAc residues similar to the GalT1 labeling discussed above (Khidekel et al. 2003); and 2) in cells by metabolic labeling with a peracetylated azido-GlcNAc substrate (Vocadlo et al. 2003; Sprung et al. 2005), as many of the enzymes in the HBP will tolerate unnatural sugars. However, the kinetics of O-linked tetraacetylated N-azidoacetylglucosamine (GlcNAz) removal from proteins by OGA is significantly reduced. These unnatural sugars can be derivatized further to incorporate a biotin tag, which facilitates the detection and enrichment of O-GlcNAc-modified proteins and peptides (Wang et al. 2010a). Alternatively, this method has been used to incorporate polyethylene glycol moieties (Rexach et al. 2010), which results in a molecular weight shift (~2 kDa) for each GlcNAc residue found on a protein and thus makes it possible to estimate the stoichiometry of modification. Additionally, this method has been used to incorporate fluorescent tags, allowing researchers to quantitatively measure and image intracellular O-GlcNAc-modified proteins *in vivo* (Clark et al. 2008). Although these established methods provided great advancements for the detection of O-GlcNAc-modified proteins, the weak nature of metabolic labeling with peracetylated

GlcNAz has led to the development of better technologies. Subsequent studies have shown that GalNAz can be converted to UDP-GalNAz and epimerized to UDP-GlcNAz by mammalian biosynthetic enzymes, which can be used as a substrate by OGT (Boyce et al. 2011). Proof-of-principle experiments highlighting this metabolic labeling demonstrated that numerous proteins are O-GlcNAc-modified, laying a solid framework for future studies to visualize and characterize dynamic O-GlcNAc-mediated signaling events (Boyce et al. 2011).

Mass spectrometry

MS-based methods have become widely and successfully employed for studying proteins and proteomes as well as PTMs such as phosphorylation and methylation using collision-induced dissociation in MS/MS. However, detection and site mapping of O-GlcNAc-modified peptides by mass spectrometric techniques is challenging. This is largely due to the labile nature of the β-linkage in the gas phase, which is lost prior to fragmentation of the peptide backbone and often prevents correct peptide identification, localization of the O-GlcNAc site, and consequently relative quantification. More importantly, distinguishing O-GlcNAc peptides from a complex mixture is problematic because ion intensities of O-GlcNAc peptides are often suppressed when compared to unmodified peptides. Despite these pitfalls, the generation of diagnostic fragment ions of O-GlcNAc-modified peptides, for example [M+H]1+ of m/z 204.1 for GlcNAc oxonium ions (Carr et al. 1993; Huddleston et al. 1993), can be used to distinguish O-GlcNAc-modified peptides from complex mixtures. By optimizing fragmentation energy to release O-GlcNAc (m/z 204.1), O-GlcNAc-modified peptides can be detected by ESI-MS, which

has been employed in mapping O-GlcNAcylation sites in human cytomegalovirus tegument basic phosphoprotein to Ser921 and Ser952 (Greis et al. 1994).

In contrast to collision-induced dissociation, electron capture dissociation and electron transfer dissociation (ETD) are alternative fragmentation methods used to preserve more labile modifications such as phosphorylation, methylation, acetylation, glycosylation, nitrosylation, and sulfation, and allow for direct mapping of peptide/protein modifications (Syka et al. 2004; Mikesh et al. 2006; Udeshi et al. 2007; Wu et al. 2007; Udeshi et al. 2008; Sobott et al. 2009; Wang et al. 2010a). ETD fragmentation cleaves along the peptide backbone between the Cα-N producing c and z ions while still maintaining peptide side chains and modifications (Syka et al. 2004; Sobott et al. 2009). ETD-MS has been utilized to identify dynamically O-GlcNAcylated proteins and their modification sites in excitatory neurons in the brain (Khidekel et al. 2007), the cell adhesion protein paxillin (Kwak et al. 2010), transcription activation of Foxo1 in response to glucose (Housley et al. 2008), examination of the extensive crosstalk between phosphorylation and O-GlcNAcylation during cytokinesis (Wang et al. 2010b), and many other processes (Chou et al. 1995). Although the emergence of ETD-MS has proven to be a successful technique, again enrichment of O-GlcNAcylated peptides is ideal for effective sequencing and identification of these peptides by MS.

Future directions

Phosphorylation and other PTMs have historically been the exclusive focus of studies on cellular signal transduction events. As discussed in this review, O-GlcNAc is emerging as a PTM that should also be considered as an equally important contributor and

regulator of signaling pathways, especially those involved in regulating the cells response to stress and injury. Previously, it has proven difficult to detect O-GlcNAc and O-GlcNAc-modified proteins. The work of numerous groups has resulted in the development of alternative approaches that solve many of the caveats associated with studying this labile protein modification. The application of these techniques will answer many of the remaining questions: Which proteins are O-GlcNAc-modified in response to stress?; Are the proteins modified in a stress- and/or tissue-specific manner?; How does the O-GlcNAc-modification alter the function of these proteins at a molecular level?; How are OGT and OGA regulated during stress and injury?; and importantly, how is the O-GlcNAc-mediated stress response misregulated in disease?

Acknowledgements

We apologize to our colleagues whose work was not cited in this review due to theme or space restrictions. Natasha E. Zachara, Ph.D., is funded by grants from the American Heart Association (SD0930162N) and the National Institutes of Health (NIH) National Heart, Lung, and Blood Institute (R21HL108003 and P01HL107153). Albert Lee, Ph.D., receives funding as a GCF fellow from the NIH National Heart, Lung and Blood Institute PEG Program (P01HL107153).

Disclosures

There are no conflicts of interest, financial or otherwise, declared by the authors of this paper.

References

1. Akimoto Y, Hart GW, Hirano H, Kawakami H (2005) O-GlcNAc modification of nucleocytoplasmic proteins and diabetes. Med Mol Morphol 38 (2):84-91.
2. Arnold CS, Johnson GV, Cole RN, Dong DL, Lee M, Hart GW (1996) The microtubule-associated protein tau is extensively modified with O-linked N-acetylglucosamine. J Biol Chem 271 (46):28741-28744.
3. Ball LE, Berkaw MN, Buse MG (2006) Identification of the major site of O-linked beta-N-acetylglucosamine modification in the C terminus of insulin receptor substrate-1. Mol Cell Proteomics 5 (2):313-323.
4. Batista-Nascimento L, Neef DW, Liu PC, Rodrigues-Pousada C, Thiele DJ (2011) Deciphering human heat shock transcription factor 1 regulation via post-translational modification in yeast. PLoS One 6 (1):e15976.
5. Beer D, Maloisel J-L, Rast DM, Vasella A (1990) Synthesis of 2-Acetamido-2-deoxy-D-gluconhydroximolactone-and Chitobionhydroximolactone-Derived N-Phenylcarbamates, Potential Inhibitors of beta-N-Acetylglucosaminidase. Helv Chim Acta 73 (7):1918-1922.
6. Bertram L, Blacker D, Mullin K, Keeney D, Jones J, Basu S, Yhu S, McInnis MG, Go RC, Vekrellis K, Selkoe DJ, Saunders AJ, Tanzi RE (2000) Evidence for genetic linkage of Alzheimer's disease to chromosome 10q. Science 290 (5500):2302-2303.
7. Bimboese P, Gibson CJ, Schmidt S, Xiang W, Ehrlich BE (2011) Isoform-specific regulation of the inositol 1,4,5-trisphosphate receptor by O-linked glycosylation. J Biol Chem 286 (18):15688-15697.

8. Boehmelt G, Fialka I, Brothers G, McGinley MD, Patterson SD, Mo R, Hui CC, Chung S, Huber LA, Mak TW, Iscove NN (2000a) Cloning and characterization of the murine glucosamine-6-phosphate acetyltransferase EMeg32. Differential expression and intracellular membrane association. J Biol Chem 275 (17):12821-12832.

9. Boehmelt G, Wakeham A, Elia A, Sasaki T, Plyte S, Potter J, Yang Y, Tsang E, Ruland J, Iscove NN, Dennis JW, Mak TW (2000b) Decreased UDP-GlcNAc levels abrogate proliferation control in EMeg32-deficient cells. EMBO J 19 (19):5092-5104.

10. Boyce M, Carrico IS, Ganguli AS, Yu SH, Hangauer MJ, Hubbard SC, Kohler JJ, Bertozzi CR (2011) Metabolic cross-talk allows labeling of O-linked beta-N-acetylglucosamine-modified proteins via the N-acetylgalactosamine salvage pathway. Proc Natl Acad Sci U S A 108 (8):3141-3146.

11. Buse MG (2006) Hexosamines, insulin resistance, and the complications of diabetes: current status. Am J Physiol Endocrinol Metab 290 (1):E1-E8.

12. Buse MG, Robinson KA, Marshall BA, Hresko RC, Mueckler MM (2002) Enhanced O-GlcNAc protein modification is associated with insulin resistance in GLUT1-overexpressing muscles. Am J Physiol Endocrinol Metab 283 (2):E241-250.

13. Butkinaree C, Cheung WD, Park S, Park K, Barber M, Hart GW (2008) Characterization of beta-N-acetylglucosaminidase cleavage by caspase-3 during apoptosis. J Biol Chem 283 (35):23557-23566.

14. Caldwell SA, Jackson SR, Shahriari KS, Lynch TP, Sethi G, Walker S, Vosseller K, Reginato MJ (2010) Nutrient sensor O-GlcNAc transferase regulates breast cancer

tumorigenesis through targeting of the oncogenic transcription factor FoxM1. Oncogene 29 (19):2831-2842.

15. Carapito C, Klemm C, Aebersold R, Domon B (2009) Systematic LC-MS analysis of labile post-translational modifications in complex mixtures. J Proteome Res 8 (5):2608-2614.

16. Carr SA, Huddleston MJ, Bean MF (1993) Selective identification and differentiation of N- and O-linked oligosaccharides in glycoproteins by liquid chromatography-mass spectrometry. Protein Sci 2 (2):183-196.

17. Carrillo LD, Froemming JA, Mahal LK (2011) Targeted in Vivo O-GlcNAc Sensors Reveal Discrete Compartment-specific Dynamics during Signal Transduction. J Biol Chem 286 (8):6650-6658.

18. Carrillo LD, Krishnamoorthy L, Mahal LK (2006) A cellular FRET-based sensor for beta-O-GlcNAc, a dynamic carbohydrate modification involved in signaling. J Am Chem Soc 128 (46):14768-14769.

19. Champattanachai V, Marchase RB, Chatham JC (2007) Glucosamine protects neonatal cardiomyocytes from ischemia-reperfusion injury via increased protein-associated O-GlcNAc. Am J Physiol Cell Physiol 292 (1):C178-187.

20. Champattanachai V, Marchase RB, Chatham JC (2008) Glucosamine protects neonatal cardiomyocytes from ischemia-reperfusion injury via increased protein O-GlcNAc and increased mitochondrial Bcl-2. Am J Physiol Cell Physiol 294 (6):C1509-C1520.

21. Chatham JC, Marchase RB (2010) The role of protein O-linked beta-N-acetylglucosamine in mediating cardiac stress responses. Biochim Biophys Acta 1800 (2):57-66.

22. Chatham JC, Not LG, Fulop N, Marchase RB (2008) Hexosamine biosynthesis and protein O-glycosylation: the first line of defense against stress, ischemia, and trauma. Shock 29 (4):431-440.

23. Chen H, Ing BL, Robinson KA, Feagin AC, Buse MG, Quon MJ (1997) Effects of overexpression of glutamine:fructose-6-phosphate amidotransferase (GFAT) and glucosamine treatment on translocation of GLUT4 in rat adipose cells. Mol Cell Endocrinol 135 (1):67-77.

24. Cheng X, Cole RN, Zaia J, Hart GW (2000) Alternative O-glycosylation/O-phosphorylation of the murine estrogen receptor beta. Biochemistry 39 (38):11609-11620.

25. Cheng X, Hart GW (2001) Alternative O-glycosylation/O-phosphorylation of serine-16 in murine estrogen receptor beta: post-translational regulation of turnover and transactivation activity. J Biol Chem 276 (13):10570-10575.

26. Cheung WD, Hart GW (2008) AMP-activated protein kinase and p38 MAPK activate O-GlcNAcylation of neuronal proteins during glucose deprivation. J Biol Chem 283 (19):13009-13020.

27. Cheung WD, Sakabe K, Housley MP, Dias WB, Hart GW (2008) O-linked beta-N-acetylglucosaminyltransferase substrate specificity is regulated by myosin phosphatase targeting and other interacting proteins. J Biol Chem 283 (49):33935-33941.

28. Chou T-Y, Hart GW, Dang CV (1995) c-Myc is Glycosylated at Threonine 58, a Known Phosphorylation Site and a Mutational Hot Spot in Lymphomas. J Biol Chem 270(32):18961-18965.

29. Clark PM, Dweck JF, Mason DE, Hart CR, Buck SB, Peters EC, Agnew BJ, Hsieh-Wilson LC (2008) Direct in-gel fluorescence detection and cellular imaging of O-GlcNAc-modified proteins. J Am Chem Soc 130 (35):11576-11577.

30. Comer FI, Hart GW (1999) O-GlcNAc and the control of gene expression. Biochim Biophys Acta 1473 (1):161-171.

31. Comer FI, Hart GW (2001) Reciprocity between O-GlcNAc and O-phosphate on the carboxyl terminal domain of RNA polymerase II. Biochemistry 40 (26):7845-7852.

32. Comtesse N, Maldener E, Meese E (2001) Identification of a nuclear variant of MGEA5, a cytoplasmic hyaluronidase and a beta-N-acetylglucosaminidase. Biochem Biophys Res Commun 283 (3):634-640.

33. Crow MT, Mani K, Nam YJ, Kitsis RN (2004) The mitochondrial death pathway and cardiac myocyte apoptosis. Circulation research 95 (10):957-970.

34. Dias WB, Cheung WD, Hart GW (2012) O-GlcNAcylation of kinases. Biochem Biophys Res Commun 422 (2):224-228.

35. Dias WB, Cheung WD, Wang Z, Hart GW (2009) Regulation of calcium/calmodulin-dependent kinase IV by O-GlcNAc modification. J Biol Chem 284 (32):21327-21337.

36. Dong DL, Hart GW (1994) Purification and characterization of an O-GlcNAc selective N-acetyl-beta-D-glucosaminidase from rat spleen cytosol. J Biol Chem 269 (30):19321-19330.

37. Dong H, Goico B, Martin M, Csernansky CA, Bertchume A, Csernansky JG (2004) Modulation of hippocampal cell proliferation, memory, and amyloid plaque deposition in APPsw (Tg2576) mutant mice by isolation stress. Neuroscience 127 (3):601-609.

38. Dorfmueller HC, Borodkin VS, Blair DE, Pathak S, Navratilova I, van Aalten DM (2011) Substrate and product analogues as human O-GlcNAc transferase inhibitors. Amino Acids 40 (3):781-792.

39. Dorfmueller HC, Borodkin VS, Schimpl M, Shepherd SM, Shpiro NA, van Aalten DM (2006) GlcNAcstatin: a picomolar, selective O-GlcNAcase inhibitor that modulates intracellular O-glcNAcylation levels. J Am Chem Soc 128 (51):16484-16485.

40. Du XL, Edelstein D, Dimmeler S, Ju Q, Sui C, Brownlee M (2001) Hyperglycemia inhibits endothelial nitric oxide synthase activity by posttranslational modification at the Akt site. J Clin Invest 108 (9):1341-1348.

41. Du XL, Edelstein D, Rossetti L, Fantus IG, Goldberg H, Ziyadeh F, Wu J, Brownlee M (2000) Hyperglycemia-induced mitochondrial superoxide overproduction activates the hexosamine pathway and induces plasminogen activator inhibitor-1 expression by increasing Sp1 glycosylation. Proc Natl Acad Sci U S A 97 (22):12222-12226.

42. Dudognon P, Maeder-Garavaglia C, Carpentier JL, Paccaud JP (2004) Regulation of a COPII component by cytosolic O-glycosylation during mitosis. FEBS Lett 561 (1-3):44-50.

43. Ficko-Blean E, Stubbs KA, Nemirovsky O, Vocadlo DJ, Boraston AB (2008) Structural and mechanistic insight into the basis of mucopolysaccharidosis IIIB. Proceedings of the National Academy of Sciences of the United States of America 105 (18):6560-6565.

44. Finlay DR, Newmeyer DD, Price TM, Forbes DJ (1987) Inhibition of *in vitro* nuclear transport by a lectin that binds to nuclear pores. J Cell Biol 104 (2):189-200.

45. Forsythe ME, Love DC, Lazarus BD, Kim EJ, Prinz WA, Ashwell G, Krause MW, Hanover JA (2006) Caenorhabditis elegans ortholog of a diabetes susceptibility locus: oga-1 (O-GlcNAcase) knockout impacts O-GlcNAc cycling, metabolism, and dauer. Proc Natl Acad Sci U S A 103 (32):11952-11957.

46. Fujiki R, Hashiba W, Sekine H, Yokoyama A, Chikanishi T, Ito S, Imai Y, Kim J, He HH, Igarashi K, Kanno J, Ohtake F, Kitagawa H, Roeder RG, Brown M, Kato S (2011) GlcNAcylation of histone H2B facilitates its monoubiquitination. Nature 480 (7378):557-560.

47. Fulop N, Marchase RB, Chatham JC (2007a) Role of protein O-linked N-acetyl-glucosamine in mediating cell function and survival in the cardiovascular system. Cardiovasc Res 73 (2):288-297.

48. Fulop N, Zhang Z, Marchase RB, Chatham JC (2007b) Glucosamine cardioprotection in perfused rat hearts associated with increased O-linked N-acetylglucosamine protein modification and altered p38 activation. Am J Physiol Heart Circ Physiol 292 (5):H2227-2236.

49. Gambetta MC, Oktaba K, Muller J (2009) Essential role of the glycosyltransferase sxc/Ogt in polycomb repression. Science 325 (5936):93-96.

50. Gandy JC, Rountree AE, Bijur GN (2006) Akt1 is dynamically modified with O-GlcNAc following treatments with PUGNAc and insulin-like growth factor-1. FEBS Lett 580 (13):3051-3058.

51. Gao Y, Miyazaki J, Hart GW (2003) The transcription factor PDX-1 is post-translationally modified by O-linked N-acetylglucosamine and this modification is correlated with its DNA binding activity and insulin secretion in min6 beta-cells. Arch Biochem Biophys 415 (2):155-163.

52. Gao Y, Parker GJ, Hart GW (2000) Streptozotocin-induced beta-cell death is independent of its inhibition of O-GlcNAcase in pancreatic Min6 cells. Arch Biochem Biophys 383 (2):296-302.

53. Gao Y, Wells L, Comer FI, Parker GJ, Hart GW (2001) Dynamic O-glycosylation of nuclear and cytosolic proteins - Cloning and characterization of a neutral, cytosolic beta-N-acetylglucosam inidase from human brain. J Biol Chem 276 (13):9838-9845.

54. Gloster TM, Zandberg WF, Heinonen JE, Shen DL, Deng L, Vocadlo DJ (2011) Hijacking a biosynthetic pathway yields a glycosyltransferase inhibitor within cells. Nat Chem Biol 7 (3):174-181.

55. Goldberg H, Whiteside C, Fantus IG (2011) O-linked beta-N-acetylglucosamine supports p38 MAPK activation by high glucose in glomerular mesangial cells. Am J Physiol Endocrinol Metab 301 (4):E713-726.

56. Goldenberg I, Grossman E, Jacobson KA, Shneyvays V, Shainberg A (2001) Angiotensin II-induced apoptosis in rat cardiomyocyte culture: a possible role of AT1 and AT2 receptors. J Hypertens 19 (9):1681-1689.

57. Golks A, Tran TT, Goetschy JF, Guerini D (2007) Requirement for O-linked N-acetylglucosaminyltransferase in lymphocytes activation. EMBO J 26 (20):4368-4379.

58. Greig KT, Antonchuk J, Metcalf D, Morgan PO, Krebs DL, Zhang JG, Hacking DF, Bode L, Robb L, Kranz C, de Graaf C, Bahlo M, Nicola NA, Nutt SL, Freeze HH, Alexander WS, Hilton DJ, Kile BT (2007) Agm1/Pgm3-mediated sugar nucleotide synthesis is essential for hematopoiesis and development. Mol Cell Biol 27 (16):5849-5859.

59. Greis KD, Gibson W, Hart GW (1994) Site-specific glycosylation of the human cytomegalovirus tegument basic phosphoprotein (UL32) at serine 921 and serine 952. J Virol 68 (12):8339-8349.

60. Griffith LS, Schmitz B (1999) O-linked N-acetylglucosamine levels in cerebellar neurons respond reciprocally to pertubations of phosphorylation. Eur J Biochem 262 (3):824-831.

61. Gross BJ, Kraybill BC, Walker S (2005) Discovery of O-GlcNAc transferase inhibitors. J Am Chem Soc 127 (42):14588-14589.

62. Guinez C, Losfeld ME, Cacan R, Michalski JC, Lefebvre T (2006) Modulation of HSP70 GlcNAc-directed lectin activity by glucose availability and utilization. Glycobiology 16 (1):22-28.

63. Guinez C, Mir AM, Dehennaut V, Cacan R, Harduin-Lepers A, Michalski JC, Lefebvre T (2008) Protein ubiquitination is modulated by O-GlcNAc glycosylation. FASEB J 22 (8):2901-2911.

64. Guinez C, Mir AM, Leroy Y, Cacan R, Michalski JC, Lefebvre T (2007) Hsp70-GlcNAc-binding activity is released by stress, proteasome inhibition, and protein misfolding. Biochemical and biophysical research communications 361 (2):414-420.

65. Guinez C, Mir AM, Martin N, Leprince D, Michalski JC, Vergoten G, Lefebvre T (2010) Arginine 469 is a pivotal residue for the Hsc70-GlcNAc-binding property. Biochemical and biophysical research communications 400 (4):537-542.

66. Gurcel C, Vercoutter-Edouart AS, Fonbonne C, Mortuaire M, Salvador A, Michalski JC, Lemoine J (2008) Identification of new O-GlcNAc modified proteins using a click-chemistry-based tagging. Anal Bioanal Chem 390 (8):2089-2097.

67. Haberhausen G, Schmitt I, Kohler A, Peters U, Rider S, Chelly J, Terwilliger JD, Monaco AP, Muller U (1995) Assignment of the dystonia-parkinsonism syndrome locus, DYT3, to a small region within a 1.8-Mb YAC contig of Xq13.1. Am J Hum Genet 57 (3):644-650.

68. Haltiwanger RS, Blomberg MA, Hart GW (1992) Glycosylation of nuclear and cytoplasmic proteins. Purification and characterization of a uridine diphospho-N-acetylglucosamine:polypeptide beta-N-acetylglucosaminyltransferase. J Biol Chem 267 (13):9005-9013.

69. Haltiwanger RS, Busby S, Grove K, Li S, Mason D, Medina L, Moloney D, Philipsberg G, Scartozzi R (1997) O-glycosylation of nuclear and cytoplasmic proteins: Regulation analogous to phosphorylation? BiochemBiophysResCommun 231:237-242.

70. Haltiwanger RS, Grove K, Philipsberg GA (1998) Modulation of O-linked N-acetylglucosamine levels on nuclear and cytoplasmic proteins *in vivo* using the

peptide O-GlcNAc-beta-N-acetylglucosaminidase inhibitor O-(2-acetamido-2-deoxy-D-glucopyranosylidene)amino-N-phenylcarbamate. J Biol Chem 273 (6):3611-3617.

71. Hamiel CR, Pinto S, Hau A, Wischmeyer PE (2009) Glutamine enhances heat shock protein 70 expression via increased hexosamine biosynthetic pathway activity. Am J Physiol Cell Physiol 297 (6):C1509-1519.

72. Han I, Kudlow JE (1997) Reduced O glycosylation of Sp1 is associated with increased proteasome susceptibility. Mol Cell Biol 17 (5):2550-2558.

73. Hanover JA, Forsythe ME, Hennessey PT, Brodigan TM, Love DC, Ashwell G, Krause M (2005) A Caenorhabditis elegans model of insulin resistance: altered macronutrient storage and dauer formation in an OGT-1 knockout. Proc Natl Acad Sci U S A 102 (32):11266-11271.

74. Hanover JA, Yu S, Lubas WB, Shin SH, Ragano-Caracciola M, Kochran J, Love DC (2003) Mitochondrial and nucleocytoplasmic isoforms of O-linked GlcNAc transferase encoded by a single mammalian gene. Archives of biochemistry and biophysics 409 (2):287-297.

75. Hardy J, Allsop D (1991) Amyloid deposition as the central event in the aetiology of Alzheimer's disease. Trends Pharmacol Sci 12 (10):383-388.

76. Hart GW, Slawson C, Ramirez-Correa G, Lagerlof O (2011) Cross Talk Between O-GlcNAcylation and Phosphorylation: Roles in Signaling, Transcription, and Chronic Disease. Annu Rev Biochem 80:825-858.

77. Heckel D, Comtesse N, Brass N, Blin N, Zang KD, Meese E (1998) Novel immunogenic antigen homologous to hyaluronidase in meningioma. Hum Mol Genet 7 (12):1859-1872.

78. Henchcliffe C, Beal MF (2008) Mitochondrial biology and oxidative stress in Parkinson disease pathogenesis. Nat Clin Pract Neurol 4 (11):600-609.

79. Housley MP, Rodgers JT, Udeshi ND, Kelly TJ, Shabanowitz J, Hunt DF, Puigserver P, Hart GW (2008) O-GlcNAc regulates FoxO activation in response to glucose. J Biol Chem 283 (24):16283-16292.

80. Housley MP, Udeshi ND, Rodgers JT, Shabanowitz J, Puigserver P, Hunt DF, Hart GW (2009) A PGC-1alpha-O-GlcNAc transferase complex regulates FoxO transcription factor activity in response to glucose. J Biol Chem 284 (8):5148-5157.

81. Hsieh TJ, Lin T, Hsieh PC, Liao MC, Shin SJ (2012) Suppression of Glutamine:fructose-6-phosphate amidotransferase-1 inhibits adipogenesis in 3T3-L1 adipocytes. J Cell Physiol 227 (1):108-115.

82. Hu Y, Belke D, Suarez J, Swanson E, Clark R, Hoshijima M, Dillmann WH (2005) Adenovirus-mediated overexpression of O-GlcNAcase improves contractile function in the diabetic heart. Circ Res 96 (9):1006-1013.

83. Huang JB, Clark AJ, Petty HR (2007) The hexosamine biosynthesis pathway negatively regulates IL-2 production by Jurkat T cells. Cell Immunol 245 (1):1-6.

84. Huddleston MJ, Bean MF, Carr SA (1993) Collisional fragmentation of glycopeptides by electrospray ionization LC/MS and LC/MS/MS: methods for selective detection of glycopeptides in protein digests. Anal Chem 65 (7):877-884.

85. Hunton DL, Zou L, Pang Y, Marchase RB (2004) Adult rat cardiomyocytes exhibit capacitative calcium entry. Am J Physiol Heart Circ Physiol 286 (3):H1124-1132.

86. Hwang SY, Shin JH, Hwang JS, Kim SY, Shin JA, Oh ES, Oh S, Kim JB, Lee JK, Han IO (2010) Glucosamine exerts a neuroprotective effect via suppression of inflammation in rat brain ischemia/reperfusion injury. Glia 58 (15):1881-1892.

87. Ise H, Kobayashi S, Goto M, Sato T, Kawakubo M, Takahashi M, Ikeda U, Akaike T (2010) Vimentin and desmin possess GlcNAc-binding lectin-like properties on cell surfaces. Glycobiology 20 (7):843-864.

88. Jackson SP, Tjian R (1989) Purification and analysis of RNA polymerase II transcription factors by using wheat germ agglutinin affinity chromatography. Proc Natl Acad Sci U S A 86 (6):1781-1785.

89. Jacobsen KT, Iverfeldt K (2011) O-GlcNAcylation increases non-amyloidogenic processing of the amyloid-beta precursor protein (APP). Biochem Biophys Res Commun 404 (3):882-886.

90. Jacobsen SE, Binkowski KA, Olszewski NE (1996) SPINDLY, a tetratricopeptide repeat protein involved in gibberellin signal transduction Arabidopsis. Proc Natl Acad Sci U S A 93 (17):9292-9296.

91. James LR, Fantus IG, Goldberg H, Ly H, Scholey JW (2000) Overexpression of GFAT activates PAI-1 promoter in mesangial cells. Am J Physiol Renal Physiol 279 (4):F718-727.

92. Jarrar D, Chaudry IH, Wang P (1999) Organ dysfunction following hemorrhage and sepsis: mechanisms and therapeutic approaches. Int J Mol Med 4 (6):575-583.

93. Jiang M-S, Hart GW (1997) A Subpopulation of Estrogen Receptors Are Modified by O-Linked N-Acetylglucosamine. JBiolChem 272:2421-2498.

94. Jinek M, Rehwinkel J, Lazarus BD, Izaurralde E, Hanover JA, Conti E (2004) The superhelical TPR-repeat domain of O-linked GlcNAc transferase exhibits structural similarities to importin alpha. Nat Struct Mol Biol 11 (10):1001-1007.

95. Jones SP, Zachara NE, Ngoh GA, Hill BG, Teshima Y, Bhatnagar A, Hart GW, Marban E (2008) Cardioprotection by N-acetylglucosamine linkage to cellular proteins. Circulation 117 (9):1172-1182.

96. Juhaszova M, Zorov DB, Kim SH, Pepe S, Fu Q, Fishbein KW, Ziman BD, Wang S, Ytrehus K, Antos CL, Olson EN, Sollott SJ (2004) Glycogen synthase kinase-3beta mediates convergence of protection signaling to inhibit the mitochondrial permeability transition pore. J Clin Invest 113 (11):1535-1549.

97. Kajstura J, Cigola E, Malhotra A, Li P, Cheng W, Meggs LG, Anversa P (1997) Angiotensin II induces apoptosis of adult ventricular myocytes *in vitro*. J Mol Cell Cardiol 29 (3):859-870.

98. Kang ES, Han D, Park J, Kwak TK, Oh MA, Lee SA, Choi S, Park ZY, Kim Y, Lee JW (2008) O-GlcNAc modulation at Akt1 Ser473 correlates with apoptosis of murine pancreatic beta cells. Exp Cell Res 314 (11-12):2238-2248.

99. Kang JE, Cirrito JR, Dong H, Csernansky JG, Holtzman DM (2007) Acute stress increases interstitial fluid amyloid-beta via corticotropin-releasing factor and neuronal activity. Proc Natl Acad Sci U S A 104 (25):10673-10678.

100. Kawauchi K, Araki K, Tobiume K, Tanaka N (2009) Loss of p53 enhances catalytic activity of IKKbeta through O-linked beta-N-acetyl glucosamine modification. Proc Natl Acad Sci U S A 106 (9):3431-3436.

101. Kazemi Z, Chang H, Haserodt S, McKen C, Zachara NE (2010) O-linked beta-N-acetylglucosamine (O-GlcNAc) regulates stress-induced heat shock protein expression in a GSK-3beta-dependent manner. J Biol Chem 285 (50):39096-39107.

102. Kearse KP, Hart GW (1991) Lymphocyte activation induces rapid changes in nuclear and cytoplasmic glycoproteins. Proc Natl Acad Sci U S A 88 (5):1701-1705.

103. Kelly WG, Dahmus ME, Hart GW (1993) RNA polymerase II is a glycoprotein. Modification of the COOH-terminal domain by O-GlcNAc. J Biol Chem 268 (14):10416-10424.

104. Kem DC, Johnson EI, Capponi AM, Chardonnens D, Lang U, Blondel B, Koshida H, Vallotton MB (1991) Effect of angiotensin II on cytosolic free calcium in neonatal rat cardiomyocytes. Am J Physiol 261 (1 Pt 1):C77-85.

105. Khidekel N, Arndt S, Lamarre-Vincent N, Lippert A, Poulin-Kerstien KG, Ramakrishnan B, Qasba PK, Hsieh-Wilson LC (2003) A chemoenzymatic approach toward the rapid and sensitive detection of O-GlcNAc posttranslational modifications. J Am Chem Soc 125 (52):16162-16163.

106. Khidekel N, Ficarro SB, Clark PM, Bryan MC, Swaney DL, Rexach JE, Sun YE, Coon JJ, Peters EC, Hsieh-Wilson LC (2007) Probing the dynamics of O-GlcNAc glycosylation in the brain using quantitative proteomics. Nat Chem Biol 3 (6):339-348.

107. Khidekel N, Ficarro SB, Peters EC, Hsieh-Wilson LC (2004) Exploring the O-GlcNAc proteome: direct identification of O-GlcNAc-modified proteins from the brain. Proc Natl Acad Sci U S A 101 (36):13132-13137.

108. Kim C, Nam DW, Park SY, Song H, Hong HS, Boo JH, Jung ES, Kim Y, Baek JY, Kim KS, Cho JW, Mook-Jung I (2012) O-linked beta-N-acetylglucosaminidase inhibitor attenuates beta-amyloid plaque and rescues memory impairment. Neurobiol Aging 34 (1):275–285.

109. Kim EJ, Kang DO, Love DC, Hanover JA (2006a) Enzymatic characterization of O-GlcNAcase isoforms using a fluorogenic GlcNAc substrate. Carbohydr Res 341 (8):971-982.

110. Kim SJ, Sung JY, Um JW, Hattori N, Mizuno Y, Tanaka K, Paik SR, Kim J, Chung KC (2003) Parkin cleaves intracellular alpha-synuclein inclusions via the activation of calpain. J Biol Chem 278 (43):41890-41899.

111. Kim YH, Song M, Oh YS, Heo K, Choi JW, Park JM, Kim SH, Lim S, Kwon HM, Ryu SH, Suh PG (2006b) Inhibition of phospholipase C-beta1-mediated signaling by O-GlcNAc modification. J Cell Physiol 207 (3):689-696.

112. Knapp S, Abdo M, Ajayi K, Huhn RA, Emge TJ, Kim EJ, Hanover JA (2007) Tautomeric modification of GlcNAc-thiazoline. Org Lett 9 (12):2321-2324.

113. Konrad RJ, Zhang F, Hale JE, Knierman MD, Becker GW, Kudlow JE (2002) Alloxan is an inhibitor of the enzyme O-linked N-acetylglucosamine transferase. Biochem Biophys Res Commun 293 (1):207-212.

114. Kreppel LK, Blomberg MA, Hart GW (1997) Dynamic glycosylation of nuclear and cytosolic proteins. Cloning and characterization of a unique O-GlcNAc transferase with multiple tetratricopeptide repeats. J Biol Chem 272 (14):9308-9315.

115. Kreppel LK, Hart GW (1999) Regulation of a cytosolic and nuclear O-GlcNAc transferase. Role of the tetratricopeptide repeats. J Biol Chem 274 (45):32015-32022.

116. Ku NO, Toivola DM, Strnad P, Omary MB (2010) Cytoskeletal keratin glycosylation protects epithelial tissue from injury. Nat Cell Biol 12 (9):876-885.

117. Kuo M, Zilberfarb V, Gangneux N, Christeff N, Issad T (2008) O-GlcNAc modification of FoxO1 increases its transcriptional activity: a role in the glucotoxicity phenomenon? Biochimie 90 (5):679-685.

118. Kwak TK, Kim H, Jung O, Lee SA, Kang M, Kim HJ, Park JM, Kim SH, Lee JW (2010) Glucosamine treatment-mediated O-GlcNAc modification of paxillin depends on adhesion state of rat insulinoma INS-1 cells. J Biol Chem 285 (46):36021-36031.

119. Kwon NS, Lee SH, Choi CS, Kho T, Lee HS (1994) Nitric oxide generation from streptozotocin. FASEB journal : official publication of the Federation of American Societies for Experimental Biology 8 (8):529-533.

120. Laczy B, Marsh SA, Brocks CA, Wittmann I, Chatham JC (2010) Inhibition of O-GlcNAcase in perfused rat hearts by NAG-thiazolines at the time of reperfusion is cardioprotective in an O-GlcNAc dependent manner. Am J Physiol Heart Circ Physiol 299 (5):H1715-H1727.

121. Lazarus MB, Nam Y, Jiang J, Sliz P, Walker S (2011) Structure of human O-GlcNAc transferase and its complex with a peptide substrate. Nature 469 (7331):564-567.

122. Lee RT, Lee YC (2000) Affinity enhancement by multivalent lectin-carbohydrate interaction. Glycoconjugate journal 17 (7-9):543-551.

123. Lee TN, Alborn WE, Knierman MD, Konrad RJ (2006) Alloxan is an inhibitor of O-GlcNAc-selective N-acetyl-beta-D-glucosaminidase. Biochem Biophys Res Commun 350 (4):1038-1043.

124. Lefebvre T, Cieniewski C, Lemoine J, Guerardel Y, Leroy Y, Zanetta JP, Michalski JC (2001) Identification of N-acetyl-d-glucosamine-specific lectins from rat liver cytosolic and nuclear compartments as heat-shock proteins. Biochem J 360 (Pt 1):179-188.

125. Lim K, Chang HI (2010) O-GlcNAc inhibits interaction between Sp1 and sterol regulatory element binding protein 2. Biochemical and biophysical research communications 393 (2):314-318.

126. Lim KH, Chang HI (2006) O-linked N-acetylglucosamine suppresses thermal aggregation of Sp1. FEBS Lett 580 (19):4645-4652.

127. Lima VV, Spitler K, Choi H, Webb RC, Tostes RC (2012) O-GlcNAcylation and oxidation of proteins: is signalling in the cardiovascular system becoming sweeter? Clin Sci (Lond) 123 (8):473-486.

128. Lindquist S (1986) The heat-shock response. Annu Rev Biochem 55:1151-1191.

129. Liu F, Iqbal K, Grundke-Iqbal I, Hart GW, Gong CX (2004a) O-GlcNAcylation regulates phosphorylation of tau: a mechanism involved in Alzheimer's disease. Proc Natl Acad Sci U S A 101 (29):10804-10809.

130. Liu HR, Gao F, Tao L, Yan WL, Gao E, Christopher TA, Lopez BL, Hu A, Ma XL (2004b) Antiapoptotic mechanisms of benidipine in the ischemic/reperfused heart. Br J Pharmacol 142 (4):627-634.

131. Liu J, Marchase RB, Chatham JC (2007) Increased O-GlcNAc levels during reperfusion lead to improved functional recovery and reduced calpain proteolysis. Am J Physiol Heart Circ Physiol 293 (3):H1391-1399.

132. Liu J, Pang Y, Chang T, Bounelis P, Chatham JC, Marchase RB (2006) Increased hexosamine biosynthesis and protein O-GlcNAc levels associated with myocardial protection against calcium paradox and ischemia. J Mol Cell Cardiol 40 (2):303-312.

133. Liu K, Paterson AJ, Konrad RJ, Parlow AF, Jimi S, Roh M, Chin E, Jr., Kudlow JE (2002) Streptozotocin, an O-GlcNAcase inhibitor, blunts insulin and growth hormone secretion. Mol Cell Endocrinol 194 (1-2):135-146.

134. Love DC, Ghosh S, Mondoux MA, Fukushige T, Wang P, Wilson MA, Iser WB, Wolkow CA, Krause MW, Hanover JA (2010) Dynamic O-GlcNAc cycling at promoters of Caenorhabditis elegans genes regulating longevity, stress, and immunity. Proc Natl Acad Sci U S A 107 (16):7413-7418.

135. Love DC, Kochan J, Cathey RL, Shin SH, Hanover JA (2003) Mitochondrial and nucleocytoplasmic targeting of O-linked GlcNAc transferase. Journal of cell science 116 (Pt 4):647-654.

136. Lubas WA, Frank DW, Krause M, Hanover JA (1997) O-Linked GlcNAc transferase is a conserved nucleocytoplasmic protein containing tetratricopeptide repeats. J Biol Chem 272 (14):9316-9324.

137. Lubas WA, Hanover JA (2000) Functional expression of O-linked GlcNAc transferase. Domain structure and substrate specificity. J Biol Chem 275 (15):10983-10988.

138. Lundquist JJ, Toone EJ (2002) The cluster glycoside effect. Chemical reviews 102 (2):555-578.

139. Macauley MS, Bubb AK, Martinez-Fleites C, Davies GJ, Vocadlo DJ (2008) Elevation of Global O-GlcNAc Levels in 3T3-L1 Adipocytes by Selective Inhibition of O-GlcNAcase Does Not Induce Insulin Resistance. J Biol Chem 283 (50):34687-34695.

140. Macauley MS, Whitworth GE, Debowski AW, Chin D, Vocadlo DJ (2005) O-GlcNAcase uses substrate-assisted catalysis: kinetic analysis and development of highly selective mechanism-inspired inhibitors. J Biol Chem 280 (27):25313-25322.

141. Machida M, Jigami Y (1994) Glycosylated DNA-binding proteins from filamentous fungus, Aspergillus oryzae: Modification with N-acetylglucosamine monosaccharide through an O-glycosidic linkage. BiosciBiotechnolBiochem 58:344-348.

142. Marotta NP, Cherwien CA, Abeywardana T, Pratt MR (2012) O-GlcNAc modification prevents peptide-dependent acceleration of alpha-synuclein aggregation. ChemBioChem 13 (18):2665-2670.

143. Marshall S, Bacote V, Traxinger RR (1991) Discovery of a metabolic pathway mediating glucose-induced desensitization of the glucose transport system. Role of hexosamine biosynthesis in the induction of insulin resistance. J Biol Chem 266 (8):4706-4712.

144. Marshall S, Duong T, Wu T, Hering MA, Yada J, Higgins S, Orbus RJ, Yan ZH, Rumberger JM (2003) Enhanced expression of uridine diphosphate-N-acetylglucosaminyl transferase (OGT) in a stable, tetracycline-inducible HeLa cell line using histone deacetylase inhibitors: kinetics of cytosolic OGT accumulation and nuclear translocation. Anal Biochem 319 (2):304-313.

145. Marshall S, Nadeau O, Yamasaki K (2004) Dynamic actions of glucose and glucosamine on hexosamine biosynthesis in isolated adipocytes: differential effects on glucosamine 6-phosphate, UDP-N-acetylglucosamine, and ATP levels. J Biol Chem 279 (34):35313-35319.

146. Martinez-Fleites C, Macauley MS, He Y, Shen DL, Vocadlo DJ, Davies GJ (2008) Structure of an O-GlcNAc transferase homolog provides insight into intracellular glycosylation. Nat Struct Mol Biol 15 (7):764-765.

147. McClain DA (2002) Hexosamines as mediators of nutrient sensing and regulation in diabetes. J Diabetes Complications 16 (1):72-80.

148. Meldrum DR, Cleveland JC, Jr., Mitchell MB, Sheridan BC, Gamboni-Robertson F, Harken AH, Banerjee A (1996) Protein kinase C mediates Ca2(+)-induced cardioadaptation to ischemia-reperfusion injury. Am J Physiol 271 (3 Pt 2):R718-726.

149. Mikesh LM, Ueberheide B, Chi A, Coon JJ, Syka JE, Shabanowitz J, Hunt DF (2006) The utility of ETD mass spectrometry in proteomic analysis. Biochim Biophys Acta 1764 (12):1811-1822.

150. Mio T, Yamada-Okabe T, Arisawa M, Yamada-Okabe H (1999) Saccharomyces cerevisiae GNA1, an essential gene encoding a novel acetyltransferase involved in UDP-N-acetylglucosamine synthesis. J Biol Chem 274 (1):424-429.

151. Miura T, Miki T (2009) GSK-3beta, a therapeutic target for cardiomyocyte protection. Circ J 73 (7):1184-1192.

152. Monsigny M, Roche AC, Sene C, Maget-Dana R, Delmotte F (1980) Sugar-lectin interactions: how does wheat-germ agglutinin bind sialoglycoconjugates? European journal of biochemistry / FEBS 104 (1):147-153.

153. Murphy E, Imahashi K, Steenbergen C (2005) Bcl-2 regulation of mitochondrial energetics. Trends Cardiovasc Med 15 (8):283-290.

154. Musicki B, Kramer MF, Becker RE, Burnett AL (2005) Inactivation of phosphorylated endothelial nitric oxide synthase (Ser-1177) by O-GlcNAc in diabetes-associated erectile dysfunction. Proc Natl Acad Sci U S A 102 (33):11870-11875.

155. Myers SA, Panning B, Burlingame AL (2011) Polycomb repressive complex 2 is necessary for the normal site-specific O-GlcNAc distribution in mouse embryonic stem cells. Proc Natl Acad Sci U S A 108 (23):9490-9495.

156. Nagy T, Champattanachai V, Marchase RB, Chatham JC (2006) Glucosamine inhibits angiotensin II-induced cytoplasmic Ca2+ elevation in neonatal cardiomyocytes via protein-associated O-linked N-acetylglucosamine. Am J Physiol Cell Physiol 290 (1):C57-65.

157. Nandi A, Sprung R, Barma DK, Zhao Y, Kim SC, Falck JR (2006) Global identification of O-GlcNAc-modified proteins. Anal Chem 78 (2):452-458.

158. Nathan C (2002) Points of control in inflammation. Nature 420 (6917):846-852.

159. Ngoh GA, Facundo HT, Hamid T, Dillmann W, Zachara NE, Jones SP (2009a) Unique hexosaminidase reduces metabolic survival signal and sensitizes cardiac myocytes to hypoxia/reoxygenation injury. Circ Res 104 (1):41-49.

160. Ngoh GA, Facundo HT, Zafir A, Jones SP (2010) O-GlcNAc signaling in the cardiovascular system. Circ Res 107 (2):171-185.

161. Ngoh GA, Hamid T, Prabhu SD, Jones SP (2009b) O-GlcNAc signaling attenuates ER stress-induced cardiomyocyte death. Am J Physiol Heart Circ Physiol 297 (5):H1711-1719.

162. Ngoh GA, Watson LJ, Facundo HT, Dillmann W, Jones SP (2008) Non-canonical glycosyltransferase modulates post-hypoxic cardiac myocyte death and mitochondrial permeability transition. J Mol Cell Cardiol 45 (2):313-325.

163. Ngoh GA, Watson LJ, Facundo HT, Jones SP (2011) Augmented O-GlcNAc signaling attenuates oxidative stress and calcium overload in cardiomyocytes. Amino Acids 40 (3):895-911.

164. Nollen EA, Morimoto RI (2002) Chaperoning signaling pathways: molecular chaperones as stress-sensing 'heat shock' proteins. J Cell Sci 115 (Pt 14):2809-2816.

165. Not LG, Brocks CA, Vamhidy L, Marchase RB, Chatham JC (2010) Increased O-linked beta-N-acetylglucosamine levels on proteins improves survival, reduces inflammation and organ damage 24 hours after trauma-hemorrhage in rats. Crit Care Med 38 (2):562-571.

166. Not LG, Marchase RB, Fulop N, Brocks CA, Chatham JC (2007) Glucosamine Administration Improves Survival Rate after Severe Hemorrhagic Shock Combined with Trauma in Rats. Shock 28 (3):345-352.

167. O'Donnell N, Zachara NE, Hart GW, Marth JD (2004) Ogt-dependent X-chromosome-linked protein glycosylation is a requisite modification in somatic cell function and embryo viability. Mol Cell Biol 24 (4):1680-1690.

168. Okuyama R, Yachi M (2001) Cytosolic O-GlcNAc accumulation is not involved in beta-cell death in HIT-T15 or Min6. Biochem Biophys Res Commun 287 (2):366-371.

169. Ong SE, Blagoev B, Kratchmarova I, Kristensen DB, Steen H, Pandey A, Mann M (2002) Stable isotope labeling by amino acids in cell culture, SILAC, as a simple and accurate approach to expression proteomics. Mol Cell Proteomics 1 (5):376-386.

170. Ong SE, Kratchmarova I, Mann M (2003) Properties of 13C-substituted arginine in stable isotope labeling by amino acids in cell culture (SILAC). J Proteome Res 2 (2):173-181.

171. Ozcan S, Andrali SS, Cantrell JE (2010) Modulation of transcription factor function by O-GlcNAc modification. Biochim Biophys Acta 1799 (5-6):353-364.

172. Pang Y, Hunton DL, Bounelis P, Marchase RB (2002) Hyperglycemia inhibits capacitative calcium entry and hypertrophy in neonatal cardiomyocytes. Diabetes 51 (12):3461-3467.

173. Pathak S, Borodkin VS, Albarbarawi O, Campbell DG, Ibrahim A, van Aalten DM (2012) O-GlcNAcylation of TAB1 modulates TAK1-mediated cytokine release. EMBO J 31 (6):1394-1404.

174. Patti ME, Virkamaki A, Landaker EJ, Kahn CR, Yki-Jarvinen H (1999) Activation of the hexosamine pathway by glucosamine *in vivo* induces insulin resistance of early postreceptor insulin signaling events in skeletal muscle. Diabetes 48 (8):1562-1571.

175. Polymeropoulos MH, Lavedan C, Leroy E, Ide SE, Dehejia A, Dutra A, Pike B, Root H, Rubenstein J, Boyer R, Stenroos ES, Chandrasekharappa S, Athanassiadou A, Papapetropoulos T, Johnson WG, Lazzarini AM, Duvoisin RC, Di Iorio G, Golbe LI, Nussbaum RL (1997) Mutation in the alpha-synuclein gene identified in families with Parkinson's disease. Science 276 (5321):2045-2047.

176. Rengifo J, Gibson CJ, Winkler E, Collin T, Ehrlich BE (2007) Regulation of the inositol 1,4,5-trisphosphate receptor type I by O-GlcNAc glycosylation. J Neurosci 27 (50):13813-13821.

177. Rexach JE, Clark PM, Hsieh-Wilson LC (2008) Chemical approaches to understanding O-GlcNAc glycosylation in the brain. Nat Chem Biol 4 (2):97-106.

178. Rexach JE, Rogers CJ, Yu SH, Tao J, Sun YE, Hsieh-Wilson LC (2010) Quantification of O-glycosylation stoichiometry and dynamics using resolvable mass tags. Nat Chem Biol 6 (9):645-651.

179. Rissman RA, Lee KF, Vale W, Sawchenko PE (2007) Corticotropin-releasing factor receptors differentially regulate stress-induced tau phosphorylation. J neurosci 27 (24):6552-6562.

180. Rissman RA, Staup MA, Lee AR, Justice NJ, Rice KC, Vale W, Sawchenko PE (2012) Corticotropin-releasing factor receptor-dependent effects of repeated stress on tau phosphorylation, solubility, and aggregation. Proc Natl Acad Sci U S A 109 (16):6277-6282.

181. Roos MD, Xie W, Su K, Clark JA, Yang X, Chin E, Paterson AJ, Kudlow JE (1998) Streptozotocin, an analog of N-acetylglucosamine, blocks the removal of O-GlcNAc from intracellular proteins. Proc Assoc Am Physicians 110 (5):422-432.

182. Roquemore EP, Chou TY, Hart GW (1994) Detection of O-linked N-acetylglucosamine (O-GlcNAc) on cytoplasmic and nuclear proteins. Methods Enzymol 230:443-460.

183. Ross SA, Chen X, Hope HR, Sun S, McMahon EG, Broschat K, Gulve EA (2000) Development and comparison of two 3T3-L1 adipocyte models of insulin resistance: increased glucose flux vs glucosamine treatment. Biochem Biophys Res Commun 273 (3):1033-1041.

184. Ryu IH, Do SI (2011) Denitrosylation of S-nitrosylated OGT is triggered in LPS-stimulated innate immune response. Biochem Biophys Res Commun 408 (1):52-57.

185. Sakabe K, Wang Z, Hart GW (2010) Beta-N-acetylglucosamine (O-GlcNAc) is part of the histone code. Proc Natl Acad Sci U S A 107 (46):19915-19920.

186. Sakurai H, Miyoshi H, Mizukami J, Sugita T (2000) Phosphorylation-dependent activation of TAK1 mitogen-activated protein kinase kinase kinase by TAB1. FEBS Lett 474 (2-3):141-145.

187. Sayat R, Leber B, Grubac V, Wiltshire L, Persad S (2008) O-GlcNAc-glycosylation of beta-catenin regulates its nuclear localization and transcriptional activity. Exp Cell Res 314 (15):2774-2787.

188. Shafi R, Lyer SPN, Ellies LG, O'Donnell N, Marek KW, Chui D, Hart GW, Marth JD (2000) The O-GlcNAc transferase gene resides on the X chromosome and is

essential for embryonic stem cell viability and mouse ontogeny. Proc Natl Acad Sci USA 97 (11):5735-5739.

189. Shao Q, Saward L, Zahradka P, Dhalla NS (1998) Ca2+ mobilization in adult rat cardiomyocytes by angiotensin type 1 and 2 receptors. Biochem Pharmacol 55 (9):1413-1418.

190. Shen A, Kamp HD, Grundling A, Higgins DE (2006) A bifunctional O-GlcNAc transferase governs flagellar motility through anti-repression. Genes Dev 20 (23):3283-3295.

191. Shimura H, Schlossmacher MG, Hattori N, Frosch MP, Trockenbacher A, Schneider R, Mizuno Y, Kosik KS, Selkoe DJ (2001) Ubiquitination of a new form of alpha-synuclein by parkin from human brain: implications for Parkinson's disease. Science 293 (5528):263-269.

192. Shin SH, Love DC, Hanover JA (2011) Elevated O-GlcNAc-dependent signaling through inducible mOGT expression selectively triggers apoptosis. Amino Acids 40 (3):885-893.

193. Shrikhande GV, Scali ST, da Silva CG, Damrauer SM, Csizmadia E, Putheti P, Matthey M, Arjoon R, Patel R, Siracuse JJ, Maccariello ER, Andersen ND, Monahan T, Peterson C, Essayagh S, Studer P, Guedes RP, Kocher O, Usheva A, Veves A, Kaczmarek E, Ferran C (2010) O-glycosylation regulates ubiquitination and degradation of the anti-inflammatory protein A20 to accelerate atherosclerosis in diabetic ApoE-null mice. PLoS One 5 (12):e14240.

194. Sinclair DA, Syrzycka M, Macauley MS, Rastgardani T, Komljenovic I, Vocadlo DJ, Brock HW, Honda BM (2009) Drosophila O-GlcNAc transferase (OGT) is

encoded by the Polycomb group (PcG) gene, super sex combs (sxc). Proc Natl Acad Sci U S A 106 (32):13427-13432.

195. Singleton KD, Wischmeyer PE (2008) Glutamine induces heat shock protein expression via O-glycosylation and phosphorylation of HSF-1 and Sp1. JPEN J Parenter Enteral Nutr 32 (4):371-376.

196. Slawson C, Copeland RJ, Hart GW (2010) O-GlcNAc signaling: a metabolic link between diabetes and cancer? Trends Biochem Sci 35 (10):547-555.

197. Slawson C, Lakshmanan T, Knapp S, Hart GW (2008) A mitotic GlcNAcylation/phosphorylation signaling complex alters the posttranslational state of the cytoskeletal protein vimentin. Mol Biol Cell 19 (10):4130-4140.

198. Slawson C, Zachara NE, Vosseller K, Cheung WD, Lane MD, Hart GW (2005) Perturbations in O-linked beta-N-acetylglucosamine protein modification cause severe defects in mitotic progression and cytokinesis. J Biol Chem 280 (38):32944-32956.

199. Snow CM, Senior A, Gerace L (1987) Monoclonal antibodies identify a group of nuclear pore complex glycoproteins. J Cell Biol 104 (5):1143-1156.

200. Sobott F, Watt SJ, Smith J, Edelmann MJ, Kramer HB, Kessler BM (2009) Comparison of CID versus ETD based MS/MS fragmentation for the analysis of protein ubiquitination. J Am Soc Mass Spectrom 20 (9):1652-1659.

201. Soesanto YA, Luo B, Jones D, Taylor R, Gabrielsen JS, Parker G, McClain DA (2008) Regulation of Akt signaling by O-GlcNAc in euglycemia. Am J Physiol Endocrinol Metab 295 (4):E974-E980.

202. Sohn KC, Lee KY, Park JE, Do SI (2004) OGT functions as a catalytic chaperone under heat stress response: a unique defense role of OGT in hyperthermia. Biochem Biophys Res Commun 322 (3):1045-1051.

203. Song M, Kim HS, Park JM, Kim SH, Kim IH, Ryu SH, Suh PG (2008) o-GlcNAc transferase is activated by CaMKIV-dependent phosphorylation under potassium chloride-induced depolarization in NG-108-15 cells. Cell Signal 20 (1):94-104.

204. Spillantini MG, Schmidt ML, Lee VM, Trojanowski JQ, Jakes R, Goedert M (1997) Alpha-synuclein in Lewy bodies. Nature 388 (6645):839-840.

205. Sprung R, Nandi A, Chen Y, Kim SC, Barma D, Falck JR, Zhao Y (2005) Tagging-via-substrate strategy for probing O-GlcNAc modified proteins. J Proteome Res 4 (3):950-957.

206. St-Pierre J, Drori S, Uldry M, Silvaggi JM, Rhee J, Jager S, Handschin C, Zheng K, Lin J, Yang W, Simon DK, Bachoo R, Spiegelman BM (2006) Suppression of reactive oxygen species and neurodegeneration by the PGC-1 transcriptional coactivators. Cell 127 (2):397-408.

207. Sumegi M, Hunyadi-Gulyas E, Medzihradszky KF, Udvardy A (2003) 26S proteasome subunits are O-linked N-acetylglucosamine-modified in Drosophila melanogaster. Biochemical and biophysical research communications 312 (4):1284-1289.

208. Syka JE, Coon JJ, Schroeder MJ, Shabanowitz J, Hunt DF (2004) Peptide and protein sequence analysis by electron transfer dissociation mass spectrometry. Proc Natl Acad Sci U S A 101 (26):9528-9533.

209. Tarrant MK, Rho HS, Xie Z, Jiang YL, Gross C, Culhane JC, Yan G, Qian J, Ichikawa Y, Matsuoka T, Zachara N, Etzkorn FA, Hart GW, Jeong JS, Blackshaw S, Zhu H, Cole PA (2012) Regulation of CK2 by phosphorylation and O-GlcNAcylation revealed by semisynthesis. Nat Chem Biol 8 (3):262-269.

210. Teo CF, Ingale S, Wolfert MA, Elsayed GA, Not LG, Chatham JC, Wells L, Boons GJ (2010) Glycopeptide-specific monoclonal antibodies suggest new roles for O-GlcNAc. Nat Chem Biol 6 (5):338-343.

211. Toleman C, Paterson AJ, Shin R, Kudlow JE (2006) Streptozotocin inhibits O-GlcNAcase via the production of a transition state analog. Biochem Biophys Res Commun 340 (2):526-534.

212. Torres CR, Hart GW (1984) Topography and polypeptide distribution of terminal N-acetylglucosamine residues on the surfaces of intact lymphocytes. Evidence for O-linked GlcNAc. J Biol Chem 259 (5):3308-3317.

213. Traxinger RR, Marshall S (1991) Coordinated Regulation of Glutamine:Fructose-6-Phosphate Amidotransferase Activity by Insulin, Glucose, and Glutamine. Role of Hexosamine Biosynthesis in Enzyme Regulation. J Biol Chem 266(16):10148-10154.

214. Tsujimoto Y (2003) Cell death regulation by the Bcl-2 protein family in the mitochondria. J Cell Physiol 195 (2):158-167.

215. Tsujimoto Y, Nakagawa T, Shimizu S (2006) Mitochondrial membrane permeability transition and cell death. Biochim Biophys Acta 1757 (9-10):1297-1300.

216. Turner JR, Tartakoff AM, Greenspan NS (1990) Cytologic assessment of nuclear and cytoplasmic O-linked N-acetylglucosamine distribution by using anti-streptococcal monoclonal antibodies. Proc Natl Acad Sci U S A 87 (15):5608-5612.

217. Udeshi ND, Compton PD, Shabanowitz J, Hunt DF, Rose KL (2008) Methods for analyzing peptides and proteins on a chromatographic timescale by electron-transfer dissociation mass spectrometry. Nat protoc 3 (11):1709-1717.

218. Udeshi ND, Shabanowitz J, Hunt DF, Rose KL (2007) Analysis of proteins and peptides on a chromatographic timescale by electron-transfer dissociation MS. FEBS J 274 (24):6269-6276.

219. Vocadlo DJ, Hang HC, Kim EJ, Hanover JA, Bertozzi CR (2003) A chemical approach for identifying O-GlcNAc-modified proteins in cells. Proc Natl Acad Sci U S A 100 (16):9116-9121.

220. Vosseller K, Trinidad JC, Chalkley RJ, Specht CG, Thalhammer A, Lynn AJ, Snedecor JO, Guan S, Medzihradszky KF, Maltby DA, Schoepfer R, Burlingame AL (2006) O-Linked N-Acetylglucosamine Proteomics of Postsynaptic Density Preparations Using Lectin Weak Affinity Chromatography and Mass Spectrometry. Mol Cell Proteomics 5 (5):923-934.

221. Walgren JL, Vincent TS, Schey KL, Buse MG (2003) High glucose and insulin promote O-GlcNAc modification of proteins, including alpha-tubulin. Am J Physiol Endocrinol Metab 284 (2):E424-434.

222. Wang C, Deng L, Hong M, Akkaraju GR, Inoue J, Chen ZJ (2001) TAK1 is a ubiquitin-dependent kinase of MKK and IKK. Nature 412 (6844):346-351.

223. Wang J, Torii M, Liu H, Hart GW, Hu ZZ (2011) dbOGAP - an integrated bioinformatics resource for protein O-GlcNAcylation. BMC Bioinformatics 12:91.

224. Wang Z, Gucek M, Hart GW (2008) Cross-talk between GlcNAcylation and phosphorylation: site-specific phosphorylation dynamics in response to globally elevated O-GlcNAc. Proc Natl Acad Sci U S A 105 (37):13793-13798.

225. Wang Z, Pandey A, Hart GW (2007) Dynamic interplay between O-linked N-acetylglucosaminylation and glycogen synthase kinase-3-dependent phosphorylation. Mol Cell Proteomics 6 (8):1365-1379.

226. Wang Z, Udeshi ND, O'Malley M, Shabanowitz J, Hunt DF, Hart GW (2010a) Enrichment and site mapping of O-linked N-acetylglucosamine by a combination of chemical/enzymatic tagging, photochemical cleavage, and electron transfer dissociation mass spectrometry. Mol Cell Proteomics 9 (1):153-160.

227. Wang Z, Udeshi ND, Slawson C, Compton PD, Sakabe K, Cheung WD, Shabanowitz J, Hunt DF, Hart GW (2010b) Extensive crosstalk between O-GlcNAcylation and phosphorylation regulates cytokinesis. Sci Signal 3 (104):ra2.

228. Wells L, Gao Y, Mahoney JA, Vosseller K, Chen C, Rosen A, Hart GW (2002a) Dynamic O-glycosylation of nuclear and cytosolic proteins: further characterization of the nucleocytoplasmic beta-N-acetylglucosaminidase, O-GlcNAcase. J Biol Chem 277 (3):1755-1761.

229. Wells L, Kreppel LK, Comer FI, Wadzinski BE, Hart GW (2004) O-GlcNAc transferase is in a functional complex with protein phosphatase 1 catalytic subunits. J Biol Chem 279 (37):38466-38470.

230. Wells L, Vosseller K, Cole RN, Cronshaw JM, Matunis MJ, Hart GW (2002b) Mapping sites of O-GlcNAc modification using affinity tags for serine and threonine post-translational modifications. Mol Cell Proteomics 1 (10):791-804.

231. Whelan SA, Dias WB, Thiruneelakantapillai L, Lane MD, Hart GW (2010) Regulation of insulin receptor substrate 1 (IRS-1)/AKT kinase-mediated insulin signaling by O-Linked beta-N-acetylglucosamine in 3T3-L1 adipocytes. J Biol Chem 285 (8):5204-5211.

232. Whelan SA, Lane MD, Hart GW (2008) Regulation of the O-linked beta-N-acetylglucosamine transferase by insulin signaling. J Biol Chem 283 (31):21411-21417.

233. Whitworth GE, Macauley MS, Stubbs KA, Dennis RJ, Taylor EJ, Davies GJ, Greig IR, Vocadlo DJ (2007) Analysis of PUGNAc and NAG-thiazoline as transition state analogues for human O-GlcNAcase: mechanistic and structural insights into inhibitor selectivity and transition state poise. J Am Chem Soc 129 (3):635-644.

234. Wischmeyer PE, Kahana M, Wolfson R, Ren H, Musch MM, Chang EB (2001) Glutamine reduces cytokine release, organ damage, and mortality in a rat model of endotoxemia. Shock 16 (5):398-402.

235. Wrabl JO, Grishin NV (2001) Homology between O-linked GlcNAc transferases and proteins of the glycogen phosphorylase superfamily. J Mol Biol 314 (3):365-374.

236. Wu SL, Huhmer AF, Hao Z, Karger BL (2007) On-line LC-MS approach combining collision-induced dissociation (CID), electron-transfer dissociation (ETD), and CID of an isolated charge-reduced species for the trace-level characterization of proteins with post-translational modifications. J Proteome Res 6 (11):4230-4244.

237. Xie W, Chung KK (2012) Alpha-synuclein impairs normal dynamics of mitochondria in cell and animal models of Parkinson's disease. J Neurochem 122 (3):404-414.

238. Xing D, Feng W, Not LG, Miller AP, Zhang Y, Chen YF, Majid-Hassan E, Chatham JC, Oparil S (2008) Increased protein O-GlcNAc modification inhibits inflammatory and neointimal responses to acute endoluminal arterial injury. Am J Physiol Heart Circ Physiol 295 (1):H335-H342.

239. Xu SL, Chalkley RJ, Wang ZY, Burlingame AL (2012) Identification of O-linked beta-D-N-acetylglucosamine-modified proteins from Arabidopsis. Methods Mol Biol 876:33-45.

240. Yang S, Zou LY, Bounelis P, Chaudry I, Chatham JC, Marchase RB (2006a) Glucosamine administration during resuscitation improves organ function after trauma hemorrhage. Shock 25 (6):600-607.

241. Yang WH, Kim JE, Nam HW, Ju JW, Kim HS, Kim YS, Cho JW (2006b) Modification of p53 with O-linked N-acetylglucosamine regulates p53 activity and stability. Nat Cell Biol 8 (10):1074-1083.

242. Yang X, Ongusaha PP, Miles PD, Havstad JC, Zhang F, So WV, Kudlow JE, Michell RH, Olefsky JM, Field SJ, Evans RM (2008) Phosphoinositide signalling links O-GlcNAc transferase to insulin resistance. Nature 451 (7181):964-969.

243. Yang YR, Song M, Lee H, Jeon Y, Choi EJ, Jang HJ, Moon HY, Byun HY, Kim EK, Kim DH, Lee MN, Koh A, Ghim J, Choi JH, Lee-Kwon W, Kim KT, Ryu SH, Suh PG (2012) O-GlcNAcase is essential for embryonic development and maintenance of genomic stability. Aging cell 11 (3):439-448.

244. Yuzwa SA, Macauley MS, Heinonen JE, Shan X, Dennis RJ, He Y, Whitworth GE, Stubbs KA, McEachern EJ, Davies GJ, Vocadlo DJ (2008) A potent mechanism-inspired O-GlcNAcase inhibitor that blocks phosphorylation of tau *in vivo*. Nat Chem Biol 4 (8):483-490.

245. Yuzwa SA, Shan X, Macauley MS, Clark T, Skorobogatko Y, Vosseller K, Vocadlo DJ (2012) Increasing O-GlcNAc slows neurodegeneration and stabilizes tau against aggregation. Nat Chem Biol 8 (4):393-399.

246. Zachara NE, Cheung WD, Hart GW (2004a) Nucleocytoplasmic glycosylation, O-GlcNAc: identification and site mapping. Methods Mol Biol 284:175-194.

247. Zachara NE, Molina H, Wong KY, Pandey A, Hart GW (2011a) The dynamic stress-induced "O-GlcNAc-ome" highlights functions for O-GlcNAc in regulating DNA damage/repair and other cellular pathways. Amino Acids 40 (3):793-808.

248. Zachara NE, O'Donnell N, Cheung WD, Mercer JJ, Marth JD, Hart GW (2004b) Dynamic O-GlcNAc modification of nucleocytoplasmic proteins in response to stress. A survival response of mammalian cells. J Biol Chem 279 (29):30133-30142.

249. Zachara NE, Vosseller K, Hart GW (2011b) Detection and analysis of proteins modified by O-linked N-acetylglucosamine. Curr Protoc Mol Biol Chapter 17:Unit 17 16.

250. Zachara NE, Vosseller K, Hart GW (2011c) Detection and analysis of proteins modified by O-linked N-acetylglucosamine. Curr Protoc Mol Biol Chapter 12:Unit 8.

251. Zhang F, Su K, Yang X, Bowe DB, Paterson AJ, Kudlow JE (2003) O-GlcNAc modification is an endogenous inhibitor of the proteasome. Cell 115 (6):715-725.

252. Zhang T, Miyamoto S, Brown JH (2004) Cardiomyocyte calcium and calcium/calmodulin-dependent protein kinase II: friends or foes? Recent Prog Horm Res 59:141-168.

253. Zou L, Yang S, Champattanachai V, Hu S, Chaudry IH, Marchase RB, Chatham JC (2009) Glucosamine improves cardiac function following trauma-hemorrhage by increased protein O-GlcNAcylation and attenuation of NF-{kappa}B signaling. Am J PHysiol Heart Circ Physiol 296 (2):H515-H523.

254. Zou L, Yang S, Hu S, Chaudry IH, Marchase RB, Chatham JC (2007) The protective effects of PUGNAc on cardiac function after trauma-hemorrhage are mediated via increased protein O-GlcNAc levels. Shock 27 (4):402-408.

Chapter 2

Characterization of tools to detect and enrich human and mouse O-GlcNAcase

Jennifer A. Groves and Natasha E. Zachara

Originally published in *Glycobiology*. 2017 June 8. doi: 10.1093/glycob/cwx051.

Format adapted for dissertation

Summary

O-linked β-N-acetylglucosamine (O-GlcNAc) is an essential regulatory post-translational modification of thousands of nuclear, cytoplasmic, and mitochondrial proteins. O-GlcNAc is dynamically added and removed from proteins by the O-GlcNAc transferase and the O-GlcNAcase (OGA), respectively. Dysregulation of O-GlcNAc-cycling is implicated in the etiology of numerous diseases including tumorigenesis, metabolic dysfunction, and neurodegeneration. To facilitate studies focused on the role of O-GlcNAc and OGA in disease, we sought to identify commercially available antibodies that enable the enrichment of full-length OGA from lysates of mouse and human origin. Here, we report that antibodies from Abcam and Bethyl Laboratories can be used to immunoprecipitate OGA to near-saturation from human and mouse cell lysates. However, Western blotting analysis indicates that both antibodies, as well as three non-commercially available antibodies (OGA-345, OGA-346, OGA-352), detect full-length OGA and numerous cross-reacting proteins. These non-specific signals migrate similarly to full-length OGA and are detected robustly, suggesting that the use of appropriate controls is essential to avoid the misidentification of OGA.

Introduction

O-linked β-N-acetylglucosamine (O-GlcNAc) is a regulatory post-translational modification (PTM) of nuclear, cytoplasmic, and mitochondrial proteins that plays key roles in cellular physiology and disease progression such as metabolic dysfunction, tumorigenesis, and neurodegeneration (Hart et al. 2011; Groves et al. 2013; Bond and Hanover 2015; Martinez et al. 2017). Underpinning these observations are thousands of O-GlcNAc-modified proteins that regulate a broad range of cellular processes including epigenetics, transcription, translation, the cell cycle, and survival signaling (Hart et al. 2011; Groves et al. 2013; Bond and Hanover 2015; Martinez et al. 2017). The dynamic cycling of O-GlcNAc on proteins is regulated by the concerted actions of enzymes encoded by just two genes: the O-GlcNAc transferase (OGT) (Haltiwanger et al. 1992; Kreppel et al. 1997; Lubas et al. 1997) and the O-GlcNAcase (OGA) (Dong and Hart 1994; Gao et al. 2001; Wells et al. 2002), which add and remove O-GlcNAc, respectively. Highlighting their importance, OGT and OGA are essential for the viability of mice (Shafi et al. 2000; O'Donnell et al. 2004; Yang et al. 2012; Keembiyehetty et al. 2015).

OGA is a neutral pH N-acetylglucosaminidase (Comtesse et al. 2001; Gao et al. 2001; Wells et al. 2002) encoded by the meningioma expressed antigen 5 (*Mgea5*) gene. To date, five splice variants of OGA have been reported (Heckel et al. 1998; Comtesse et al. 2001; Gao et al. 2001; Schultz and Pils 2002; Wells et al. 2002; Toleman et al. 2004; Li et al. 2010; Keembiyehetty et al. 2011). Full-length OGA (fOGA; 916 amino acids; Figure 2-1A), the most abundant isoform, contains an N-terminal 350 amino acid catalytic domain and a C-terminal histone acetyltransferase (HAT)-like domain that are separated by a linker region (Comtesse et al. 2001; Schultz and Pils 2002; Rao et al. 2013). The 677 amino acid

variant of OGA contains the same N-terminus as fOGA, but lacks the HAT-like domain and has an alternative C-terminal sequence (Comtesse et al. 2001; Schultz and Pils 2002; Kim et al. 2006; Li et al. 2010; Keembiyehetty et al. 2011). Additional isoforms include short OGA (Li et al. 2010), which contains only the catalytic domain, and two splice variants of rat origin that lack amino acids 250-345/398 (Toleman et al. 2004).

Since the discovery of O-GlcNAc in 1984, the development of tools to probe O-GlcNAc-signaling has been critical for understanding its role in regulating cellular physiology. While a cohort of antibodies has been developed for detecting and enriching O-GlcNAc and OGT, specific antibodies for probing OGA in a broad range of sample types/sources have lagged behind. The majority of OGA antibodies generated to date were raised against sequences from human OGA. Despite ~97% sequence identity between the human and mouse homologs of OGA, existing antibodies preferentially recognize human OGA and do not efficiently enrich mouse OGA. Thus, the goal of this study was to identify commercially available antibodies that enrich OGA to saturation from both human and mouse sources. These studies focused on antibodies from Abcam and Bethyl Laboratories, herein referred to as OGA-A and OGA-B, respectively. OGA-A was raised against a synthetic N-terminal peptide derived from human OGA (proprietary; Figure 2-1A), and is reported to react with both human and mouse OGA for Western blotting and immunoprecipitation applications. OGA-B, which was raised against amino acids 500-550 (Figure 2-1A), is reported to react with only human OGA and is recommended for immunoprecipitation and Western blot detection of enriched OGA. This study also utilized non-commercially available antibodies (OGA-345, OGA-346, OGA-352) (Butkinaree et al. 2008), and the antigens used to generate these antibodies are outlined in Figure 2-1A.

Our studies demonstrate that all of the antibodies tested recognize fOGA by Western blot and that both commercially available antibodies enrich fOGA from human and mouse lysates. However, the presence of cross-reacting bands with a similar migration pattern to fOGA, especially in mouse cell lysates, suggests that careful antibody selection and data analysis are essential.

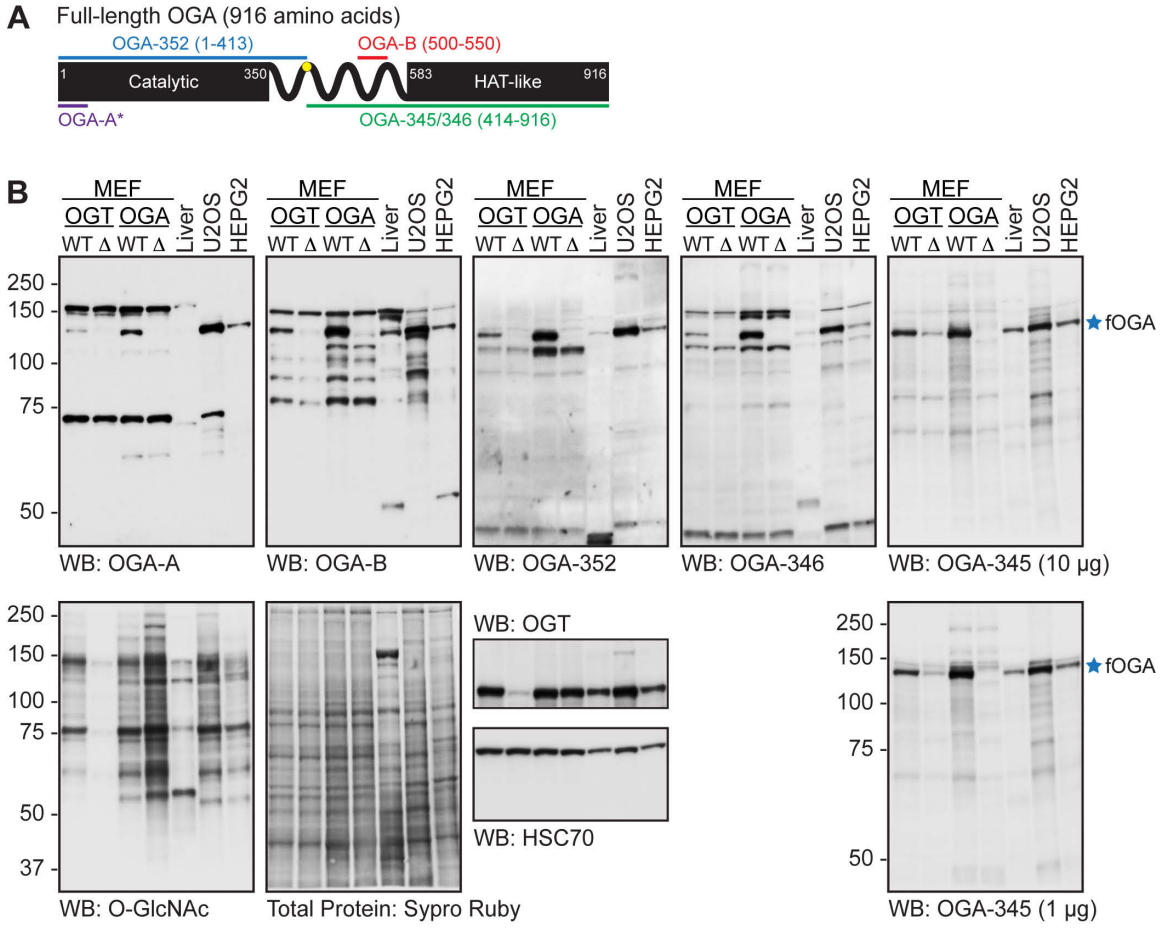

Figure 2-1: Detection of OGA with commercial and non-commercial antibodies. (A) Antigens in human OGA used to generate the antibodies used in this study. The N-terminal catalytic domain and C-terminal histone acetyltransferase (HAT)-like domain of full-length OGA are indicated. The yellow circle defines the Caspase-3 cleavage site (Asp413). The asterisk (*) denotes that the antibody from Abcam (OGA-A) was raised against a proprietary peptide within the first 50 amino acids of the N-terminus of OGA. OGA-B represents the antibody purchased from Bethyl Laboratories. (B) Equal amounts of protein (15 µg) from OGT wild type (WT) and null (Δ) mouse embryonic fibroblasts (MEFs), OGA WT and null MEFs, mouse liver tissue, U2OS human osteosarcoma cells, and HEPG2 human hepatocellular carcinoma cells were separated by SDS-PAGE. Western blots (WB) were performed for OGA (OGA-A, OGA-B, OGA-352, OGA-345, OGA-346), O-GlcNAc, and OGT (positive control). OGA-345 was used at high (0.33 µg/mL) and low (0.033 µg/mL) concentrations. Protein load was assessed by Western blotting for HSC70 and by Sypro Ruby total protein staining. The blue star indicates full-length OGA (fOGA).

Results and discussion

Detection of OGA by Western blotting

To verify the specificity of OGA antibodies for Western blotting, we utilized lysates (15 μg) of human and mouse origin that included: U2OS human osteosarcoma cells, HEPG2 human hepatocellular carcinoma cells, mouse liver tissue, OGA wild type (WT) and null mouse embryonic fibroblasts (MEFs) (Keembiyehetty et al. 2015; Olivier-Van Stichelen et al. 2017), and OGT WT and null MEFs (Kazemi et al. 2010). Notably, OGA expression is tightly regulated by O-GlcNAc levels (Slawson et al. 2005; Kazemi et al. 2010; Ghosh et al. 2014; Zhang et al. 2014), and we have previously demonstrated that OGA protein levels are significantly reduced in OGT null cells (Kazemi et al. 2010). As such, lysates from OGT null MEFs are a negative control for the detection of both OGT and OGA. OGA was detected by Western blot using the following antibodies: OGA-A, OGA-B, OGA-352, OGA-345, and OGA-346 (Figure 2-1B). Western blots were also performed using antibodies raised against O-GlcNAc, OGT, and heat shock cognate 70 kDa protein (HSC70; loading control), and membranes were stained with Sypro Ruby as an additional loading control (Figure 2-1B).

As expected, we observe a band at ~130 kDa using each OGA antibody that is not present in the OGT and OGA null MEFs (Figure 2-1B, blue star), suggesting that this band represents fOGA. OGA-A also detects strong signals at ~150 kDa and ~75 kDa in WT MEF lysates that are not reduced in the OGT and OGA nulls (Figure 2-1B). These data suggest that the only signal specific to OGA is that at ~130 kDa. OGA-B recognizes numerous bands, only one of which is significantly decreased by deletion of OGA and which migrates at ~130 kDa (fOGA). In U2OS cells, but not HEPG2 cells, OGA-B also

detects a doublet at ~130 kDa (Figure 2-1B). The presence of these additional bands likely underpins the application note from Bethyl Laboratories stating that this antibody does not perform satisfactorily for Western blots in crude lysates. Each of the non-commercial OGA antibodies (352, 345, 346) recognizes fOGA in the human and mouse samples tested, although cross-reactivity is observed (Figure 2-1B). OGA-352 and OGA-346 detect a strong signal at ~115 kDa, particularly in the MEFs (Figure 2-1B), and the identity of this protein is unknown. OGA-346 also reacts with a strong cross-reacting band just above 150 kDa similar to OGA-A and OGA-B (Figure 2-1B). OGA-345 demonstrates the least cross-reactivity (Figure 2-1B). Overall, all of the antibodies tested recognize fOGA in human and mouse cells, although cross-reacting bands warrant appropriate controls, such as deletion of OGA, to confirm specificity.

Enrichment of OGA by immunoprecipitation

We next assessed the utility of OGA-A and OGA-B for enriching fOGA from human and mouse lysates (Figure 2-2). These studies did not use the non-commercially available antibodies, as we have previously demonstrated that OGA-345 does not enrich fOGA to saturation and that there is significant background in the chicken immunoglobulin (Ig)Y isotype control immunoprecipitate (*data not shown*). Enriched OGA was detected by Western blot using OGA-A, OGA-B, and OGA-345. Western blotting using OGA-345 reveals a band at ~130 kDa in the inputs and immunoprecipitates (Figure 2-2, left panel) representing fOGA (blue star), which is nearly absent in the unbound fractions (Figure 2-2, right panel) of the OGA but not IgG immunoprecipitates. These data suggest that OGA-A (0.5 μg per 100 μg lysate) and OGA-B (0.75 μg per 100 μg lysate) enrich endogenous fOGA to near-saturation from MEFs and U2OS cells. Western blotting using OGA-A and

OGA-B demonstrated that these antibodies detect a cross-reacting band at ~150 kDa in the MEFs (Figure 2-2). Importantly, OGA-A does not enrich this band (Figure 2-2), suggesting that this antibody is suitable for immunoprecipitating fOGA from both human and mouse sources. However, the ~150 kDa protein is enriched to saturation by OGA-B in the mouse cell lysates (Figure 2-2). Finally, following immunoprecipitation, OGA-A detects a greater amount of overall non-specific staining compared to OGA-B.

Cross-reacting species detected by OGA-A, OGA-B, and OGA-346 near 150 kDa (Figure 2-1B) led us to initially consider the possibility of uncharacterized OGA isoforms. However, the presence of these signals in both the OGT and OGA null lysates does not support this hypothesis. Moreover, if the majority of the antibodies utilized in this study were detecting the same "uncharacterized isoform", we would expect OGA-A to also recognize the ~150 kDa protein in the OGA-B MEF immunoprecipitates. As shown in Figure 2-2, this is not the case and supports the notion that the additional signals are simply cross-reacting proteins.

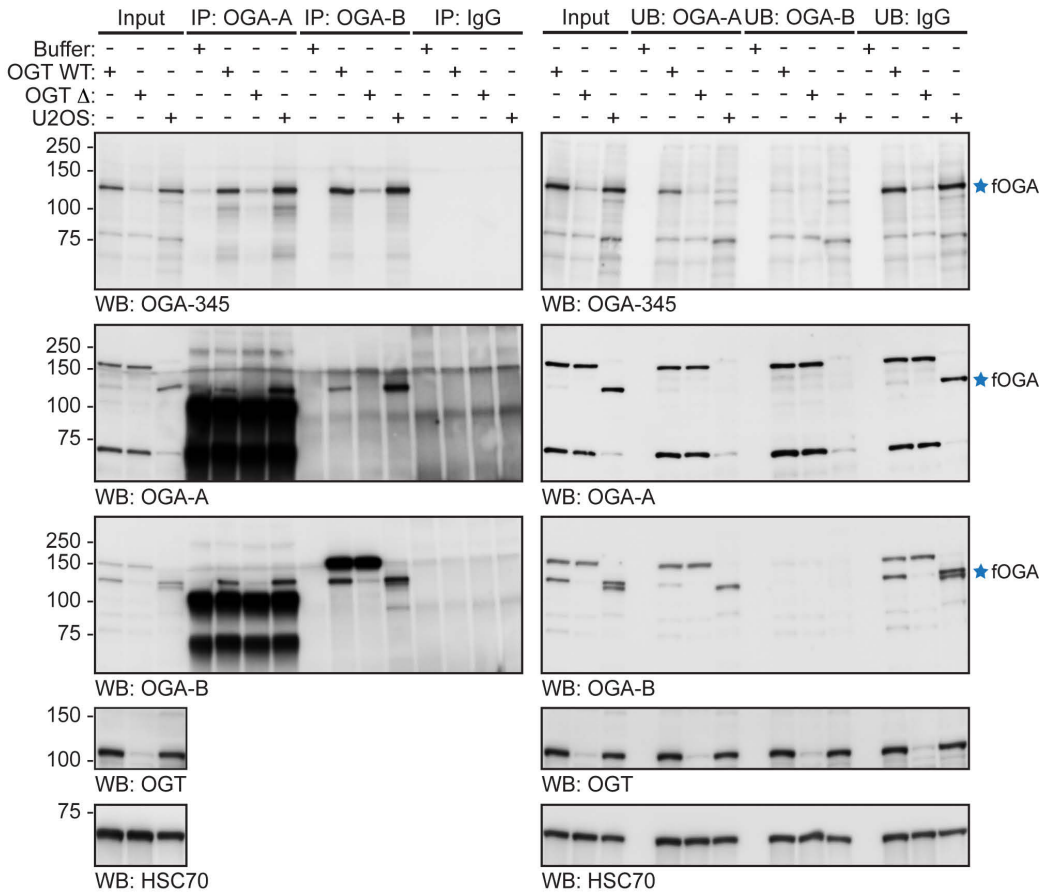

Figure 2-2: Enrichment of human and mouse OGA by immunoprecipitation. Anti-OGA antibodies from Abcam (OGA-A) and Bethyl Laboratories (OGA-B), or a rabbit isotype control IgG, were used to enrich endogenous OGA from U2OS, MEF OGT WT, and MEF OGT null (Δ) lysates (400 µg). Incubation of antibody in buffer was used as a control. The inputs (2.5%), immunoprecipitates (IP; 25%; left panel), and unbound fractions (UB; 2.5%; right panel) were analyzed by SDS-PAGE. Western blots (WB) were performed for OGA (OGA-345, OGA-A, OGA-B), OGT (positive control), and HSC70 (loading control).

Concluding remarks

The goal of this study was to identify commercial antibodies recognizing OGA that are useful for Western blotting and immunoprecipitation. Our studies highlight two commercially available antibodies (OGA-A, OGA-B) and three non-commercial antibodies (OGA-345, OGA-346, OGA-352) that recognize fOGA in both human and mouse lysates (Figure 2-1B). However, each antibody recognizes additional bands in the OGT and OGA null MEFs, indicating reactivity with proteins containing similar epitopes. Notably, these cross-reacting proteins often give a stronger signal than fOGA and are close in molecular weight to fOGA (Figure 2-1B, Figure 2-2). As such, use of ≤10% gels that provide adequate separation in this molecular weight range are ideal, as are controls in which OGA expression has been suppressed. Both OGA-A and OGA-B immunoprecipitate fOGA from human and mouse lysates to near-saturation, however, enrichment of a ~150 kDa protein by OGA-B limits the utility of this antibody in lysates of mouse origin. While not addressed in this study, cross-reacting proteins will likely impede the use of OGA antibodies for immunofluorescence unless antibody specificity is robustly demonstrated. Collectively, our data characterize useful antibodies for immunoprecipitation and Western blotting of OGA from mouse and human sources, and highlight technical challenges that can be overcome with appropriate controls.

Materials and methods

Antibodies

The following antibodies were purchased: anti-OGA-A (ab124807; Abcam); anti-OGA-B (A304-345A), anti-chicken IgY-horseradish peroxidase (HRP; A30-206P), rabbit isotype control IgG (P120-101; Bethyl Laboratories); anti-OGT (O6264), anti-mouse IgM-HRP (A8786; Sigma-Aldrich); anti-HSC70 (sc-7298; Santa Cruz Biotechnology); and anti-rabbit IgG-HRP (NA934V) and anti-mouse IgG-HRP (NA931V; GE Healthcare). The following previously characterized antigen-purified antibodies were gifts: anti-OGA-345, anti-OGA-346, anti-OGA-352, and anti-O-GlcNAc (CTD110.6) (Comer and Hart 2000; Butkinaree et al. 2008).

Cell and tissue preparation and extraction

Cells were cultured in DMEM (Corning) containing 4.5 g/L (U2OS, HEPG2; American Type Culture Collection) or 1 g/L (OGT WT/null MEFs) glucose, 10% (v/v) heat inactivated fetal bovine serum (Thermo Fisher Scientific), and 1% (v/v) penicillin/streptomycin (Corning) as previously described (Kazemi et al. 2010; Groves et al. 2017). Deletion of OGT was induced with 4-hydroxytamoxifen 4-OHT or vehicle control (100% ethanol) for 40-44 h as previously reported (Kazemi et al. 2010). OGA WT and null MEF pellets (Keembiyehetty et al. 2015; Olivier-Van Stichelen et al. 2017) were a kind gift from the laboratory of John Hanover, Ph.D (National Institutes of Health (NIH)).

Mouse care, procedures, and liver collections were performed as described (Groves et al. 2017). Cells and livers were lysed in NETN buffer and the protein concentrations were determined as reported (Groves et al. 2017).

Immunoprecipitation

Endogenous OGA was enriched by incubating cell lysates or buffer with OGA-A, OGA-B, or rabbit isotype control IgG (16-20 h, 4°C, with rotation). Antibody-protein complexes were captured using protein G or A/G magnetic beads pre-blocked with bovine serum albumin, washed with NETN buffer, and eluted in Laemmli sample buffer containing dithiothreitol as described (Groves et al. 2017).

Electrophoresis and Western blotting

These procedures have been reported (Groves et al. 2017). Briefly, sodium dodecyl sulfate (SDS)-polyacrylamide gel electrophoresis (PAGE) was performed using 7.5% or 10% Tris-Glycine eXtended polyacrylamide gels (Bio-Rad), and then proteins were electroblotted to nitrocellulose. Equal protein loading was assessed prior to blocking using the Sypro Ruby total protein membrane stain according to the manufacturer's instructions. Membranes were blocked in 3% (w/v) non-fat milk in Tris-buffered saline with 0.05% (v/v) TWEEN-20 (1 h, 25°C), and then incubated with primary (16-20 h, 4°C) and HRP-conjugated secondary (1 h, 25°C) antibodies. Western blots were developed using Immobilon Western Chemiluminescent Substrate (EMD Millipore) and captured on autoradiography film or the Amersham Imager 600 RGB (GE Healthcare). Membranes were stripped and re-probed as described (Groves et al. 2017).

Reproducibility

Four biological replicates were independently analyzed for Figure 2-1B, with the exception of OGA WT and null cells in which one biological replicate was used due to limited sample availability. For Figure 2-2, three biological replicates were independently analyzed.

Acknowledgements

Antibodies for OGA (345, 346, 352) (Butkinaree et al. 2008) and O-GlcNAc (CTD110.6) (Comer and Hart 2000) were a kind gift from the O-GlcNAc resources Core C4 (Gerald Hart, Ph.D. and Natasha Zachara, Ph.D., Department of Biological Chemistry, The Johns Hopkins University School of Medicine). OGA WT and null cell pellets were provided by John Hanover, Ph.D. and Michelle Bond, Ph.D. (NIH) (Keembiyehetty et al. 2015; Olivier-Van Stichelen et al. 2017), and OGT WT and null cell pellets were provided by Marissa Martinez, Ph.D. (Zachara laboratory, Department of Biological Chemistry, The Johns Hopkins University School of Medicine). This work was supported by grants from the NIH National Heart, Lung, and Blood Institute (P01HL107153 to NEZ) and the NIH National Institute on Aging (F31AG047724 to JAG).

Disclosures

The authors declare no conflicts of interest with the contents of this article.

References

1. Bond MR, Hanover JA (2015) A little sugar goes a long way: the cell biology of O-GlcNAc. J Cell Biol 208 (7):869–880
2. Butkinaree C, Cheung WD, Park S, Park K, Barber M, Hart GW (2008) Characterization of beta-N-acetylglucosaminidase cleavage by caspase-3 during apoptosis. J Biol Chem 283 (35):23557–23566
3. Comer FI, Hart GW (2000) O-Glycosylation of nuclear and cytosolic proteins. Dynamic interplay between O-GlcNAc and O-phosphate. J Biol Chem 275 (38):29179–29182
4. Comtesse N, Maldener E, Meese E (2001) Identification of a nuclear variant of MGEA5, a cytoplasmic hyaluronidase and a beta-N-acetylglucosaminidase. Biochem Biophys Res Commun 283 (3):634–640
5. Dong DL, Hart GW (1994) Purification and characterization of an O-GlcNAc selective N-acetyl-beta-D-glucosaminidase from rat spleen cytosol. J Biol Chem 269 (30):19321–19330
6. Gao Y, Wells L, Comer FI, Parker GJ, Hart GW (2001) Dynamic O-glycosylation of nuclear and cytosolic proteins: cloning and characterization of a neutral, cytosolic beta-N-acetylglucosaminidase from human brain. J Biol Chem 276 (13):9838–9845
7. Ghosh SK, Bond MR, Love DC, Ashwell GG, Krause MW, Hanover JA (2014) Disruption of O-GlcNAc Cycling in C. elegans Perturbs Nucleotide Sugar Pools and Complex Glycans. Front Endocrinol (Lausanne) 5197

8. Groves JA, Lee A, Yildirir G, Zachara NE (2013) Dynamic O-GlcNAcylation and its roles in the cellular stress response and homeostasis. Cell Stress Chaperones 18 (5):535–558

9. Groves JA, Maduka AO, O'Meally RN, Cole RN, Zachara NE (2017) Fatty acid synthase inhibits the O-GlcNAcase during oxidative stress. J Biol Chem 292 (16):6493–6511

10. Haltiwanger RS, Blomberg MA, Hart GW (1992) Glycosylation of nuclear and cytoplasmic proteins. Purification and characterization of a uridine diphospho-N-acetylglucosamine:polypeptide beta-N-acetylglucosaminyltransferase. J Biol Chem 267 (13):9005–9013

11. Hart GW, Slawson C, Ramirez-Correa G, Lagerlof O (2011) Cross talk between O-GlcNAcylation and phosphorylation: roles in signaling, transcription, and chronic disease. Annu Rev Biochem 80 (1):825–858

12. Heckel D, Comtesse N, Brass N, Blin N, Zang KD, Meese E (1998) Novel immunogenic antigen homologous to hyaluronidase in meningioma. Hum Mol Genet 7 (12):1859–1872

13. Kazemi Z, Chang H, Haserodt S, McKen C, Zachara NE (2010) O-linked beta-N-acetylglucosamine (O-GlcNAc) regulates stress-induced heat shock protein expression in a GSK-3beta-dependent manner. J Biol Chem 285 (50):39096–39107

14. Keembiyehetty C, Love DC, Harwood KR, Gavrilova O, Comly ME, Hanover JA (2015) Conditional knock-out reveals a requirement for O-linked N-Acetylglucosaminase (O-GlcNAcase) in metabolic homeostasis. J Biol Chem 290 (11):7097–7113

15. Keembiyehetty CN, Krzeslak A, Love DC, Hanover JA (2011) A lipid-droplet-targeted O-GlcNAcase isoform is a key regulator of the proteasome. J Cell Sci 124 (Pt 16):2851–2860

16. Kim EJ, Kang DO, Love DC, Hanover JA (2006) Enzymatic characterization of O-GlcNAcase isoforms using a fluorogenic GlcNAc substrate. Carbohydr Res 341 (8):971–982

17. Kreppel LK, Blomberg MA, Hart GW (1997) Dynamic glycosylation of nuclear and cytosolic proteins. Cloning and characterization of a unique O-GlcNAc transferase with multiple tetratricopeptide repeats. J Biol Chem 272 (14):9308–9315

18. Li J, Huang C-L, Zhang L-W, Lin L, Li Z-H, Zhang F-W, Wang P (2010) Isoforms of human O-GlcNAcase show distinct catalytic efficiencies. Biochemistry Mosc 75 (7):938–943

19. Lubas WA, Frank DW, Krause M, Hanover JA (1997) O-Linked GlcNAc transferase is a conserved nucleocytoplasmic protein containing tetratricopeptide repeats. J Biol Chem 272 (14):9316–9324

20. Martinez MR, Dias TB, Natov PS, Zachara NE (2017) Stress-induced O-GlcNAcylation: an adaptive process of injured cells. Biochem Soc Trans 45 (1):237–249

21. O'Donnell N, Zachara NE, Hart GW, Marth JD (2004) Ogt-dependent X-chromosome-linked protein glycosylation is a requisite modification in somatic cell function and embryo viability. Mol Cell Biol 24 (4):1680–1690

22. Olivier-Van Stichelen S, Wang P, Comly M, Love DC, Hanover JA (2017) Nutrient-driven O-linked N-acetylglucosamine (O-GlcNAc) cycling impacts neurodevelopmental timing and metabolism. J Biol Chem 292 (15):6076–6085

23. Rao FV, Schüttelkopf AW, Dorfmueller HC, Ferenbach AT, Navratilova I, van Aalten DMF (2013) Structure of a bacterial putative acetyltransferase defines the fold of the human O-GlcNAcase C-terminal domain. Open Biol 3 (10):130021–130021

24. Schultz J, Pils B (2002) Prediction of structure and functional residues for O-GlcNAcase, a divergent homologue of acetyltransferases. FEBS Lett 529 (2-3):179–182

25. Shafi R, Iyer SP, Ellies LG, O'Donnell N, Marek KW, Chui D, Hart GW, Marth JD (2000) The O-GlcNAc transferase gene resides on the X chromosome and is essential for embryonic stem cell viability and mouse ontogeny. Proc Natl Acad Sci USA 97 (11):5735–5739

26. Slawson C, Zachara NE, Vosseller K, Cheung WD, Lane MD, Hart GW (2005) Perturbations in O-linked beta-N-acetylglucosamine protein modification cause severe defects in mitotic progression and cytokinesis. J Biol Chem 280 (38):32944–32956

27. Toleman C, Paterson AJ, Whisenhunt TR, Kudlow JE (2004) Characterization of the histone acetyltransferase (HAT) domain of a bifunctional protein with activable O-GlcNAcase and HAT activities. J Biol Chem 279 (51):53665–53673

28. Wells L, Gao Y, Mahoney JA, Vosseller K, Chen C, Rosen A, Hart GW (2002) Dynamic O-glycosylation of nuclear and cytosolic proteins: further characterization

of the nucleocytoplasmic beta-N-acetylglucosaminidase, O-GlcNAcase. J Biol Chem 277 (3):1755–1761

29. Yang YR, Song M, Lee H, Jeon Y, Choi E-J, Jang H-J, Moon HY, Byun H-Y, Kim E-K, Kim DH, Lee MN, Koh A, Ghim J, Choi JH, Lee-Kwon W, Kim KT, Ryu SH, Suh P-G (2012) O-GlcNAcase is essential for embryonic development and maintenance of genomic stability. Aging Cell 11 (3):439–448

30. Zhang Z, Tan EP, VandenHull NJ, Peterson KR, Slawson C (2014) O-GlcNAcase Expression is Sensitive to Changes in O-GlcNAc Homeostasis. Front Endocrinol (Lausanne) 5 (5):206

Chapter 3

Fatty acid synthase inhibits the O-GlcNAcase during oxidative stress

Jennifer A. Groves, Austin O. Maduka, Robert N. O'Meally, Robert N. Cole, and Natasha E. Zachara

Originally published in *J Biol Chem*. 2017 Apr 21;292(16):6493-6511.

Format adapted for dissertation

Summary

The dynamic post-translational modification O-linked-β-N-acetylglucosamine (O-GlcNAc) regulates thousands of nuclear, cytoplasmic, and mitochondrial proteins. Cellular stress, including oxidative stress, results in increased O-GlcNAcylation of numerous proteins and this increase is thought to promote cell survival. The mechanisms by which the O-GlcNAc transferase (OGT) and the O-GlcNAcase (OGA), the enzymes that add and remove O-GlcNAc respectively, are regulated during oxidative stress to alter O-GlcNAcylation are not fully characterized. Here, we demonstrate that oxidative stress leads to elevated O-GlcNAc levels in U2OS cells, but has little impact on the activity of OGT. In contrast, the expression and activity of OGA are enhanced. We hypothesized that this seeming paradox could be explained by proteins that bind to and control the local activity or substrate targeting of OGA, thereby resulting in the observed stress-induced elevations of O-GlcNAc. To identify potential protein partners, we utilized BioID proximity biotinylation in combination with Stable Isotopic Labeling of Amino acids in Cell culture (SILAC). This analysis revealed 90 OGA-interacting partners, many of which exhibited increased binding to OGA upon stress. The associations of OGA with fatty acid synthase (FAS), filamin-A, heat shock cognate 70 kDa protein, and OGT were confirmed by co-immunoprecipitation. The pool of OGA bound to FAS demonstrated a substantial (~85%) reduction in specific activity, suggesting that FAS inhibits OGA. Consistent with this observation, FAS overexpression augmented stress-induced O-GlcNAcylation. While the mechanism by which FAS sequesters OGA remains unknown, these data suggest that FAS fine-tunes the cell's response to stress and injury by remodeling cellular O-GlcNAcylation.

Introduction

The modification of intracellular proteins by monosaccharides of O-linked β-N-acetylglucosamine (O-GlcNAc) has emerged as an essential and dynamic post-translational modification (PTM) of metazoans (Hart et al. 2011; Groves et al. 2013; Bond and Hanover 2015). O-GlcNAcylation is regulated by two enzymes, the O-GlcNAc transferase (OGT) (Kreppel et al. 1997; Lubas et al. 1997) and the O-GlcNAcase (OGA) (Gao et al. 2001; Wells et al. 2002), which catalyze the addition and removal of O-GlcNAc, respectively. OGT utilizes the nucleotide sugar uridine diphosphate (UDP)-GlcNAc (Haltiwanger et al. 1992; Bond and Hanover 2015), which is synthesized by the hexosamine biosynthetic pathway (HBP) (Hart et al. 2011; Groves et al. 2013; Bond and Hanover 2015). Highlighting the importance of O-GlcNAcylation in the maintenance of cellular homeostasis, *Ogt*, *Mgea5* (OGA), and *Pgm3*, a key enzyme in the HBP, are essential for the viability of cells, tissues, and organisms (Shafi et al. 2000; O'Donnell et al. 2004; Greig et al. 2007; Yang et al. 2012).

O-GlcNAcylation of cellular proteins is implicated in the regulation of diverse cellular pathways and processes such as development, aging, inflammation, cell cycle regulation, metabolic sensing, and the cellular stress response, the focus of this study (Zachara et al. 2004; Hart et al. 2011; Groves et al. 2013; Bond and Hanover 2015). O-GlcNAc levels are dynamically elevated in response to many forms of cellular stress (Zachara et al. 2004; Jones et al. 2008), including oxidative stress (Zachara et al. 2004; Jones et al. 2008) and ischemia reperfusion (I/R) injury (Liu et al. 2006; Fülöp et al. 2007; Champattanachai et al. 2008; Jones et al. 2008; Ngoh et al. 2011; Vibjerg Jensen et al. 2013). Elevating O-GlcNAc levels prior to (Zachara et al. 2004; Liu et al. 2006; Nagy et

al. 2006; Champattanachai et al. 2007; Fülöp et al. 2007; Champattanachai et al. 2008; Jones et al. 2008; Ngoh et al. 2008; 2009a; 2009b; Hwang et al. 2010; Laczy et al. 2010; Ngoh et al. 2011) or immediately after (Yang et al. 2006; Liu et al. 2007; Nöt et al. 2007; Zou et al. 2007; Nöt et al. 2010) injury significantly improves survival. In contrast, decreasing O-GlcNAc levels sensitizes cells and tissues to apoptosis and necrosis (Zachara et al. 2004; Ngoh et al. 2008; 2009a; 2009b; 2011). Together, these studies suggest that stress-induced changes in protein O-GlcNAcylation promote survival signaling.

Alterations in the expression, activity, localization, and targeting of OGT and OGA, as well as increased flux through the HBP, have been correlated with stress-induced changes in O-GlcNAcylation. For example, various cell culture models of stress result in enhanced O-GlcNAcylation that has been correlated with increases in the expression (Zachara et al. 2004; Cheung and Hart 2008), activity (Zachara et al. 2004; Ryu and Do 2011), and targeting (Cheung and Hart 2008) of OGT. In both *ex vivo* (Fülöp et al. 2007) and *in vivo* (Wang et al. 2014) rodent models of cardiac I/R injury, O-GlcNAc levels are elevated concomitant with UDP-GlcNAc levels. Furthermore, increased O-GlcNAc levels have been correlated with elevated OGT expression (Vibjerg Jensen et al. 2013) and activity (Jensen et al. 2013; Vibjerg Jensen et al. 2013), as well as decreased OGA activity (Jensen et al. 2013), in models of ischemic preconditioning. The mechanisms controlling the activity and substrate specificity of OGT and OGA in models of cellular injury remain unknown. However, it is generally accepted that these enzymes, like RNA polymerase II (Seither et al. 1998), exist as holoenzymes; that is, the proteins they interact with regulate their specificity and activity (Wells et al. 2003; Hart et al. 2011).

To identify protein candidates that regulate O-GlcNAc during oxidative stress, we have focused on the regulation of the full-length and predominant isoform of OGA (Comtesse et al. 2001; Gao et al. 2001; Wells et al. 2002; Hart et al. 2011; Groves et al. 2013; Bond and Hanover 2015). We have identified the basal and oxidative stress-dependent protein-protein interactions of OGA using proximity biotinylation (Roux et al. 2012) coupled with Stable Isotopic Labeling of Amino acids in Cell culture (SILAC)-based proteomics (Ong et al. 2002; Amanchy et al. 2005; Zachara et al. 2011). A total of 90 interaction partners of OGA were identified, many of which exhibit increased association with oxidative stress, including fatty acid synthase (FAS), filamin-A (FLNA), heat shock cognate 70 kDa protein (HSC70), and OGT. The pool of OGA bound to FAS exhibited a significant reduction (~85%) in catalytic activity. Consistent with the stress-induced inhibition of OGA by FAS, we observed elevated O-GlcNAcylation on a subset of proteins during oxidative stress in FAS-overexpressing cells. These results suggest a novel mechanism by which the components of two metabolic-sensing pathways, O-GlcNAc cycling and fatty acid biogenesis, are coordinated to respond to cellular injury and improve survival.

Results

Oxidative stress increases OGT and OGA expression, OGA activity, and O-GlcNAc levels

To characterize the mechanisms that cells use to modulate O-GlcNAc levels in response to oxidative stress, we first assessed the activity and expression of OGT and OGA in U2OS human osteosarcoma cells exposed to the oxidant hydrogen peroxide (H_2O_2; 2.5 mM, 1-3 h). Normalization was performed against the housekeeping protein actin, whose expression is not affected by H_2O_2 treatment (Figure 3-1A, B). Consistent with our previous data (Zachara et al. 2004; Jones et al. 2008), there is a time-dependent increase in O-GlcNAc levels upon the induction of oxidative stress that is significant at 3 h (Figure 3-1A, C; repeated measures one-way analysis of variance (RM-1ANOVA)/Dunnett's multiple comparison test (MCT), $p \leq 0.01$). The increase in O-GlcNAc levels is accompanied by an elevation in the expression of OGT at 3 h (Figure 3-1A, D; RM-1ANOVA/Dunnett's MCT, $p \leq 0.0001$). While we did not observe a statistically significant increase in OGT activity (Figure 3-1E), the fold change increase in OGT expression at 2 h and 3 h parallels that of OGT activity. Interestingly, we detected a modest but significant augmentation of OGA expression (Figure 3-1A, F; RM-1ANOVA/ Dunnett's MCT, $p \leq 0.01$) and activity (Figure 3-1G; RM-1ANOVA/Dunnett's MCT, $p \leq 0.05$ (2 h), $p \leq 0.0001$ (3 h)) after 2 h and 3 h of oxidative stress. These data suggest that increased O-GlcNAcylation during oxidative stress cannot be attributed solely to global changes in the expression and activity of OGT or OGA. Together, these findings suggest that the substrate specificity of OGA may be modulated during oxidative stress, likely resulting from changes in its targeting or local activity. As protein-protein interactions are integral to the

targeting of many enzymes including OGT (Cheung and Hart 2008; Cheung et al. 2008; Hart et al. 2011; Groves et al. 2013; Bond and Hanover 2015), we hypothesized that OGA may be regulated in a similar manner.

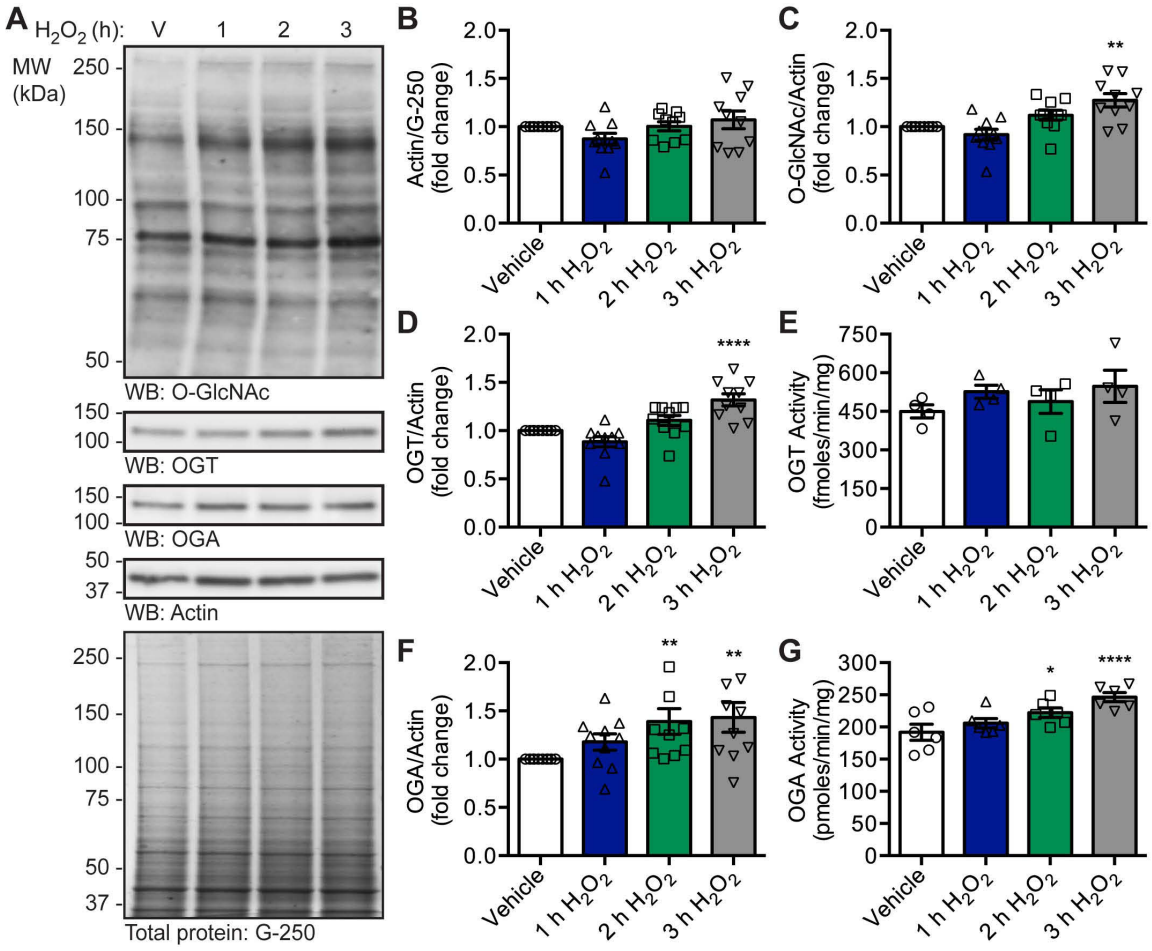

Figure 3-1: Oxidative stress increases OGT and OGA expression, OGA activity, and O-GlcNAc levels. U2OS cells were treated with vehicle (V) or H_2O_2 (2.5 mM, 1-3 h). N=10, unless otherwise indicated. (A) The expression of OGT, OGA, and actin, as well as O-GlcNAc levels, was assessed in NETN lysates (5 µg) by Western blot (WB). Protein load was assessed by total protein stain (colloidal Coomassie G-250) and by Western blot (actin). Molecular weight (MW) markers are indicated. (B) Quantitation of actin normalized to total protein (G-250). (C) Quantitation of O-GlcNAc levels normalized to actin. (D) Quantitation of OGT expression normalized to actin. (E) NETN lysates (5 µg) were assayed for OGT activity using ^{3}H-UDP-GlcNAc (0.5 µCi) and CKII acceptor peptide (1 mM). N=4, 3 technical replicates per assay. (F) Quantitation of OGA expression normalized to actin. (G) NETN lysates (5 µg) were assayed for OGA activity using 4MU-GlcNAc (1 mM). N=6, 2 technical replicates per assay. (B-G) Data are presented as the mean ± SEM. Significance was determined by RM-1ANOVA followed by Dunnett's multiple comparison test and differences were considered statistically significant at $p \leq 0.05$ (*), $p \leq 0.01$ (**), and $p \leq 0.0001$ (****).

The OGA-mBirA fusion proteins express, maintain catalytic activity, and biotinylate proteins *in vivo*

In order to identify the proteins that bind to and regulate OGA, we utilized the BioID proximity biotinylation methodology (Roux et al. 2012; 2013; Varnaitė and MacNeill 2016). This technique relies on the *Escherichia coli* biotin ligase BirA, which contains a single point mutation (R118G; herein referred to as mBirA) enabling it to release activated biotin and this results in the biotinylation of proteins within a ~10 nm radius (Kwon and Beckett 2000; Choi-Rhee et al. 2004; Cronan 2005; Kim et al. 2014; Varnaitė and MacNeill 2016). OGA is a large protein (916 amino acids) containing two domains, an N-terminal catalytic domain (β-N-acetylglucosaminidase; CD; amino acids 1-350) and a C-terminal histone acetyltransferase (HAT)-like domain (amino acids 583-916), which are separated by a linker (Figure 3-2A) (Gao et al. 2001; Schultz and Pils 2002; Wells et al. 2002). As such, full-length OGA was cloned in-frame on the N-terminus of mBirA-HA (OGA-mBirA-HA) or the C-terminus of Myc-mBirA (Myc-mBirA-OGA) to provide greater coverage of the OGA interactome (Figure 3-2A). The fusion constructs and a control vector (pcDNA3.1) were transiently transfected into U2OS cells and treated with or without biotin. Western blot analysis demonstrates that OGA-mBirA-HA and Myc-mBirA-OGA are overexpressed (Figure 3-2B). Of note, Myc-mBirA-OGA appears to be modestly stabilized by the addition of exogenous biotin, which is consistent with previous observations (Figure 3-2B; (Roux et al. 2012; Coyaud et al. 2015)). To determine if the fusion proteins maintain β-N-acetylglucosaminidase activity, desalted total cell lysates (TCL) were incubated with the small fluorescent small molecule substrate 4-methylumbelliferyl (4MU)-GlcNAc. Both fusion proteins maintain catalytic activity,

which is enhanced by the addition of exogenous biotin (Figure 3-2C). Interestingly, endogenous OGA activity is significantly elevated in pcDNA3.1-transfected cells treated with biotin (ratio-paired t-test (RPT), $p \leq 0.05$, N=3).

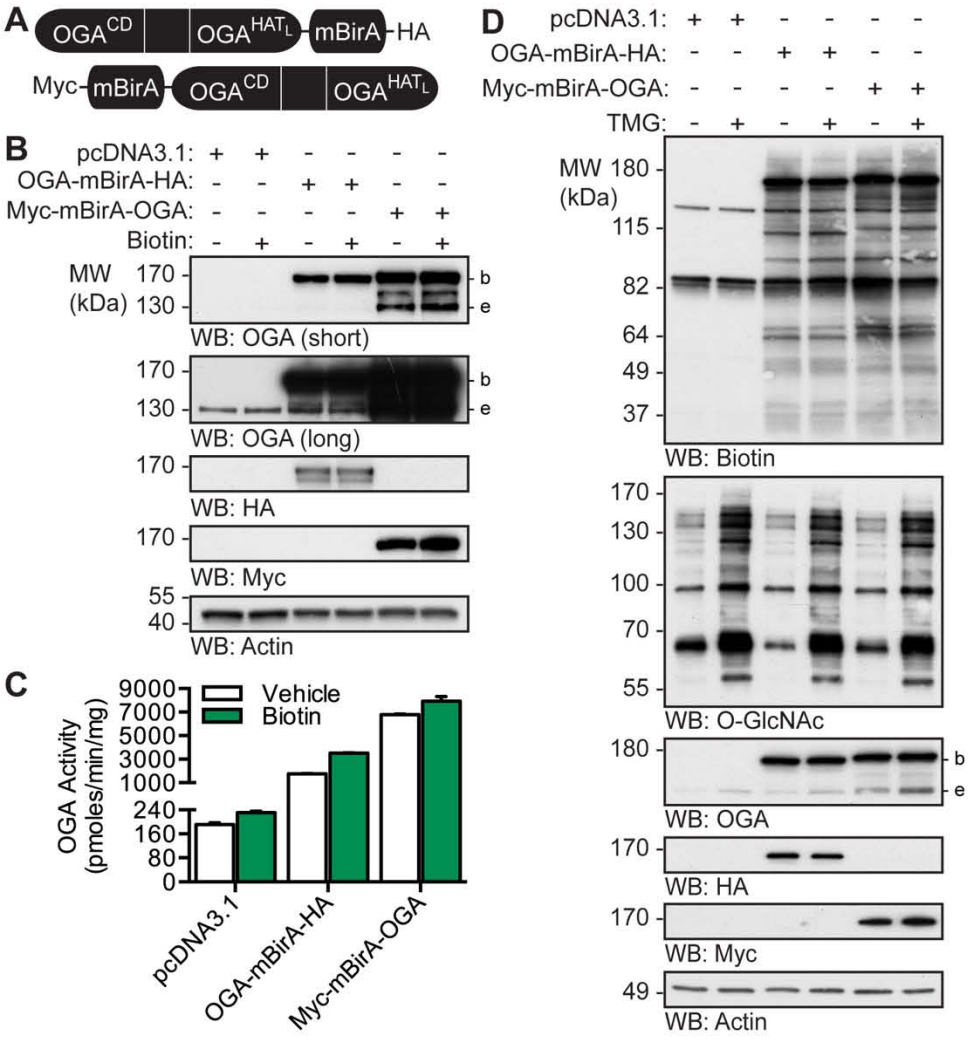

Figure 3-2: The OGA-mBirA fusion proteins express, maintain catalytic activity, and biotinylate proteins *in vivo*. (A) Schematic of the OGA-mBirA fusion proteins. CD and HAT_L represent the catalytic (β-N-acetylglucosaminidase) domain and histone acetyltransferase-like domain of OGA, respectively. (B-D) U2OS cells were transfected with pcDNA3.1, OGA-mBirA-HA, or Myc-mBirA-OGA, and treated with or without biotin (25 μM, 16 h) or TMG (100 nM, 20 h) as indicated. Proteins were extracted in TCL buffer. (B) Equal amounts of protein (10 μg) were separated by SDS-PAGE and the following were detected by Western blot (WB): OGA, HA, Myc, and actin. N=3. (C) Desalted lysates were assayed for OGA activity using 4MU-GlcNAc (1 mM). N=3, representative data from one experiment is shown. Error bars indicate the intra-assay standard deviation from two technical replicates. (D) Equal amounts of protein (4.5 μg) were separated by SDS-PAGE and the following were detected by Western blot: biotin, O-GlcNAc, OGA, HA, Myc, and actin. N=2. Migration of endogenous OGA (e), mBirA-tagged OGA (b), and the molecular weight (MW) markers are indicated.

To determine if the fusion proteins biotinylate proximal proteins *in vivo*, cell lysate was separated by sodium dodecyl sulfate (SDS)-polyacrylamide gel electrophoresis (PAGE) and biotinylated proteins were detected with NeutrAvidin-horseradish peroxidase (HRP). Of note, two signals were observed in the pcDNA3.1 transfected cells at ~130 kDa and ~80 kDa (Figure 3-2D). These molecular weights are consistent with the endogenously biotinylated mammalian carboxylases (acetyl-CoA carboxylase, pyruvate carboxylase, 3-methylcrotonyl-CoA carboxylase, propionyl-CoA carboxylase) (Moss and Lane 1971; Tong 2013) and have been previously reported (Roux et al. 2012; 2013). Overexpression of OGA-mBirA-HA and Myc-mBirA-OGA in the presence of exogenous biotin leads to the appearance of numerous biotinylated proteins (Figure 3-2D). The biotinylation patterns of OGA-mBirA-HA and Myc-mBirA-OGA are different, suggesting that our dual-tagging strategy provides greater coverage of the OGA interactome (Figure 3-2D). One potential control for our studies is overexpression of mBirA alone. However, mBirA-HA and Myc-mBirA biotinylate proteins in a promiscuous manner when compared to their OGA-mBirA counterparts (Figure 3-3). As such, mBirA was not used as a control for subsequent experiments and this is in accordance with previous BioID studies (Roux et al. 2012; 2013; Varnaitė and MacNeill 2016).

To determine whether interacting partners of OGA are predominantly substrates, cells were treated with the OGA inhibitor 2-ethylamino-3aR, 6S, 7R, 7aR-tetrahydro-5R-hydroxymethyl-5H-pyrano[3, 2-d]thiazole-6, 7-diol (Thiamet-G; TMG) (Yuzwa et al. 2008). Interestingly, there is not a dramatic change in the biotinylation pattern for either fusion protein with the addition of TMG. These data suggest that the biotinylated proteins are not predominantly substrates of OGA (Figure 3-2D).

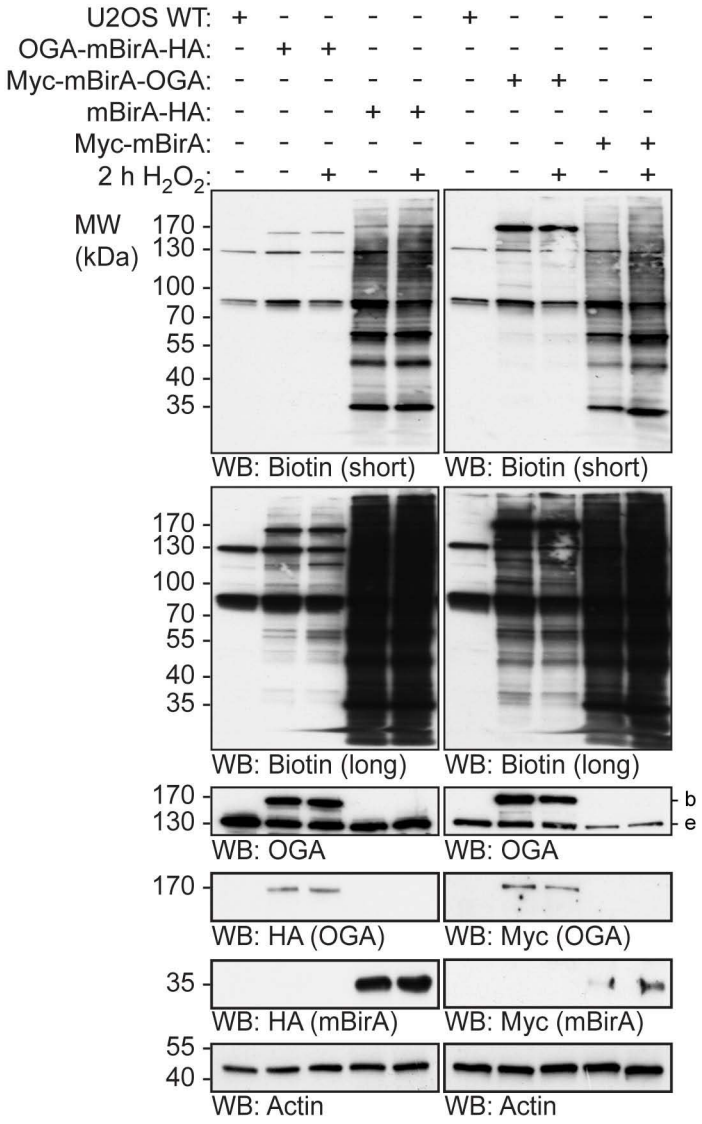

Figure 3-3: The biotinylation pattern produced by OGA-mBirA-HA and Myc-mBirA-OGA is different to that of mBirA alone. Cells were transfected with mBirA-HA, OGA-mBirA-HA, Myc-mBirA, or Myc-mBirA-OGA, and treated with or without H_2O_2 (2.5 mM, 2 h). Non-transfected wild type (WT) U2OS cells were treated with vehicle. All cells were treated with biotin (25 μM, 16 h). Equal amounts of protein (5 μg; TCL lysates) were separated by SDS-PAGE and the following were detected by Western blot (WB): biotin, OGA, HA, Myc, and actin. The migration of endogenous OGA (e), mBirA-tagged OGA (b), and the molecular weight markers (MW) are indicated.

The localization and *in vivo* biotinylation of the OGA-mBirA fusion proteins was confirmed by indirect immunofluorescence. As a control, we first determined the localization of endogenous OGA in U2OS cells. Our data demonstrate that OGA staining is detected in the nucleus and cytoplasm of U2OS cells under basal conditions (Figure 3-4), which is consistent with previous reports describing the subcellular localization of endogenous full-length OGA (Comtesse et al. 2001; Gao et al. 2001). OGA has recently been demonstrated to exist in mitochondria of neonatal rat cardiomyocytes (Banerjee et al. 2015), and the orange signal in the merged images (Figure 3-4; white triangles) may represent co-localization of OGA (green) and MitoTracker (red). Upon oxidative stress, we observe an increase in OGA staining that is consistent with the Western blot analysis (Figure 3-1A, F), but the overall pattern of localization remains unchanged.

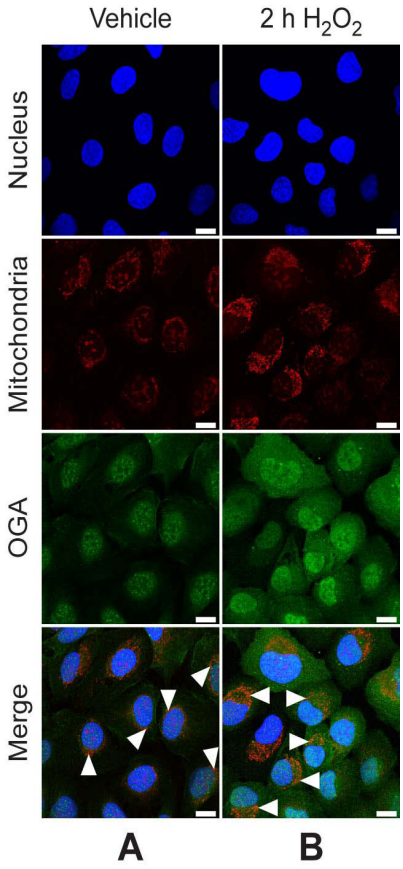

Figure 3-4: Endogenous OGA localizes to the nucleus, cytoplasm, and mitochondria of U2OS cells. U2OS cells were fixed, permeabilized, and stained for OGA. Nuclei and mitochondria were stained with Hoechst 33342 and MitoTracker Orange CMTMRos, respectively. White triangles indicate co-localization (orange) of MitoTracker and OGA. Images were acquired at 63x magnification on a Zeiss Axio Examiner 710NLO-Meta multiphoton microscope. N=3. The scale bar represents 15 μm. (A) Cells were treated with vehicle. (B) Cells were treated with H_2O_2 (2.5 mM, 2 h).

Like endogenous OGA, OGA-mBirA-HA (Figure 3-5B, C) and Myc-mBirA-OGA (Figure 3-5E, F) are present in the nucleus and cytoplasm. However, the overexpressed protein appears to have a more cytosolic distribution than the endogenous protein (Figure 3-4). Similar to the staining pattern of endogenous OGA, the orange signal in the merged images (Figure 3-5B, E; white triangles) may represent co-localization of the OGA-mBirA fusion proteins with MitoTracker. Biotinylation, which is stimulated by the addition of exogenous biotin, is observed in cells overexpressing OGA-mBirA-HA (Figure 3-5C) and Myc-mBirA-OGA (Figure 3-5F). Faint staining for biotin in control cells (pcDNA3.1;

Figure 3-5A) can be attributed to the endogenously biotinylated mammalian carboxylases described above. Finally, the localization and biotinylation of OGA-mBirA-HA (Figure 3-5D) and Myc-mBirA-OGA (Figure 3-5G) are not altered by oxidative stress.

OGA-mBirA-HA and Myc-mBirA-OGA biotinylate proximal proteins differentially in response to oxidative stress

To determine if oxidative stress alters the interactome of OGA, cells were transfected with the OGA-mBirA constructs and treated with biotin and H_2O_2 (2 h). Western blotting for biotin demonstrates that OGA-mBirA-HA and Myc-mBirA-OGA each exhibit a markedly altered biotinylation pattern in response to oxidative stress (Figure 3-6A). These data suggest that oxidative stress induces a change in the proteins associating with OGA, wherein some interactions appear to be augmented while others are decreased (Figure 3-6A). Similar to the results described above, OGA-mBirA-HA and Myc-mBirA-OGA have distinct biotinylation patterns. These results are further illustrated in the densitometric total lane profiling of the biotin signal (Figure 3-6B). Importantly, endogenous biotinylation and biotinylation by mBirA-HA and Myc-mBirA are not altered by oxidative stress (Figure 3-3). These data suggest that changes in the biotinylation pattern are not a result of changes in mBirA activity, but rather are due to specific changes in oxidative stress-dependent biotinylation by OGA-mBirA-HA and Myc-mBirA-OGA.

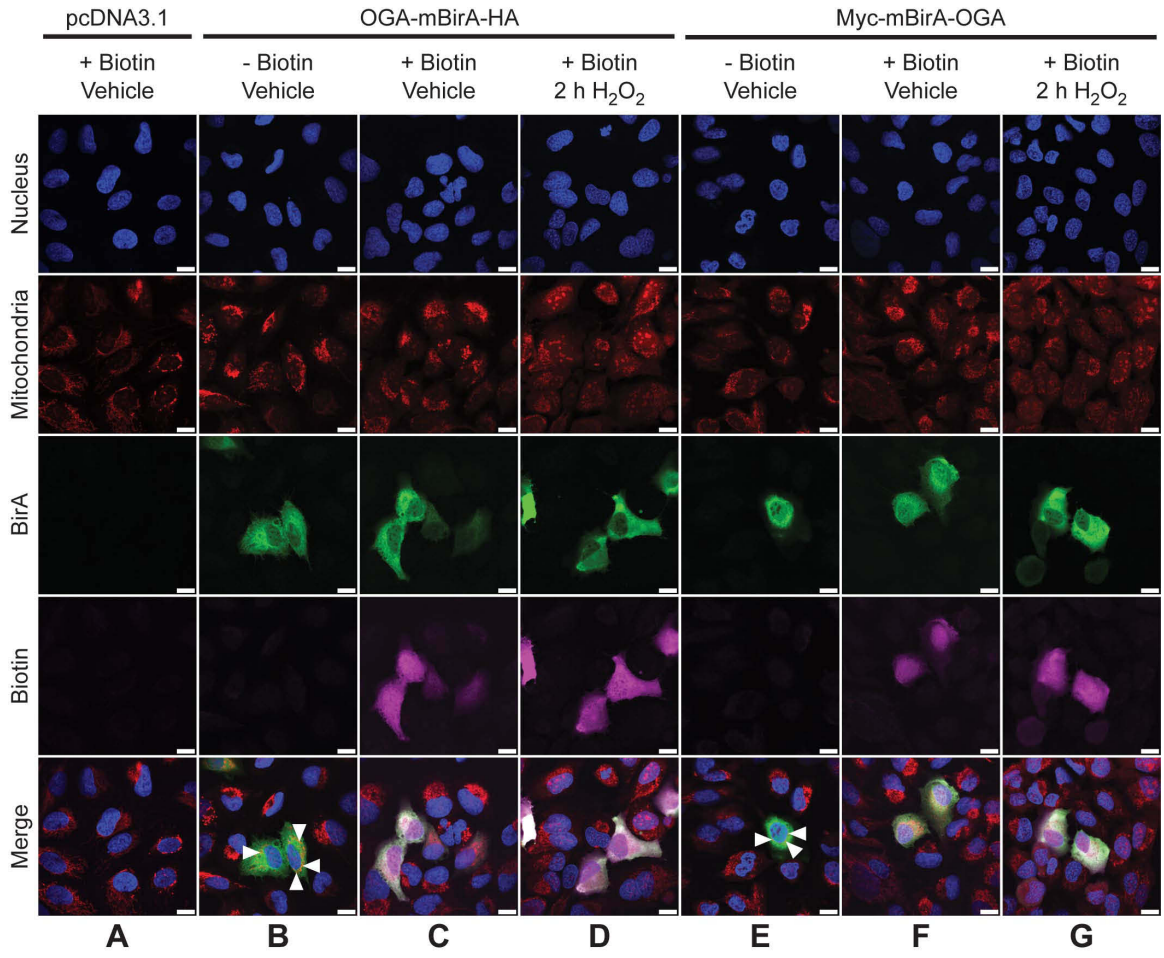

Figure 3-5: The OGA-mBirA fusion proteins localize to and biotinylate proteins in the nucleus, cytoplasm, and mitochondria of U2OS cells. U2OS cells were transfected with pcDNA3.1 (A), OGA-mBirA-HA (B-D), or Myc-mBirA-OGA (E-G), treated with (A, C, D, F, G) or without (B, E) biotin (25 µM, 16 h), and treated with (D, G) or without (A, B, C, E, F) H_2O_2 (2.5 mM, 2 h). Cells were fixed, permeabilized, and stained for BirA and biotin. Nuclei and mitochondria were stained with Hoechst 33342 and MitoTracker Orange CMTMRos, respectively. White triangles indicate co-localization (orange) of MitoTracker and OGA (B, E). Images were acquired at 63x magnification on a Zeiss Axio Examiner 710NLO-Meta multiphoton microscope. N=3. The scale bar represents 15 µm.

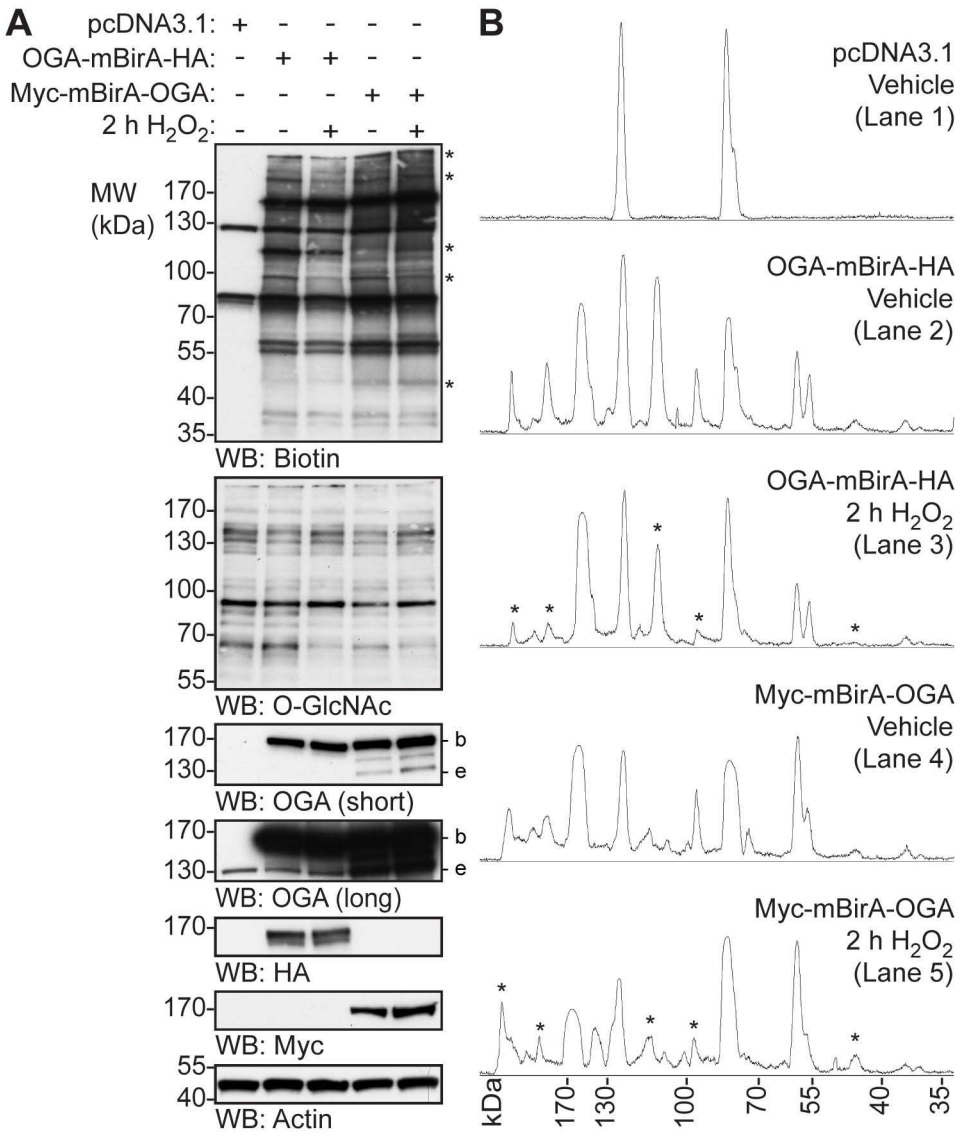

Figure 3-6: OGA-mBirA-HA and Myc-mBirA-OGA biotinylate proximal proteins differentially in response to oxidative stress. U2OS cells were transfected with pcDNA3.1, OGA-mBirA-HA, or Myc-mBirA-OGA and treated with biotin (25 μM, 16 h) in the presence or absence of H_2O_2 (2.5 mM, 2 h). (A) Equal amounts of protein (5 μg; denaturing TCL lysis) were separated by SDS-PAGE and the following were detected by Western blot (WB): biotin, O-GlcNAc, OGA, HA, Myc, and actin. N=4. (B) Densitometric total lane profiles for each lane from the biotin signal in (A). Asterisks are used to highlight a subset of the biotinylated signals that are altered by oxidative stress. Migration of endogenous OGA (e), mBirA-tagged OGA (b), and the molecular weight (MW) markers are indicated.

SILAC-BioID-MS/MS reveals numerous basal and stress-induced OGA-interacting proteins

To identify the proteins bound by OGA in basal and oxidatively stressed cells, we performed two SILAC-based proteomic experiments (Figure 3-7). In all cases, the heavy (H) SILAC-labeled cells were transfected with pcDNA3.1, and the light (L) and medium (M) labeled cells were transfected with OGA-mBirA-HA (Experiment 1) or Myc-mBirA-OGA (Experiment 2) (Figure 3-7A). Following transient transfection, biotinylation was stimulated and the cells were treated with vehicle (V; medium SILAC label) or 2 h H_2O_2 (light SILAC label) prior to harvesting (Figure 3-7A). SILAC-labeled proteins were extracted in denaturing TCL buffer and combined in equal amounts (Figure 3-7A, B). Biotinylated proteins in the 1:1:1 extract mixture were enriched using NeutrAvidin-agarose, eluted with SDS (95°C), and precipitated twice with acetone to remove free SDS. Peptides were generated by digestion with trypsin and LysC, and the resulting peptides were subjected to offline basic reversed phase (bRP) fractionation followed by reversed phase (RP) liquid chromatography (LC)-electrospray ionization (ESI)-tandem mass spectrometry (MS/MS) (Figure 3-7A). The mass spectrometry (MS) proteomics data have been deposited to the ProteomeXchange Consortium (http://proteomecentral.proteomexchange.org) via the PRIDE partner repository (Martens et al. 2005; Côté et al. 2012; Vizcaíno et al. 2014; Perez-Riverol et al. 2016; Vizcaíno et al. 2016) with the dataset identifier PXD005039.

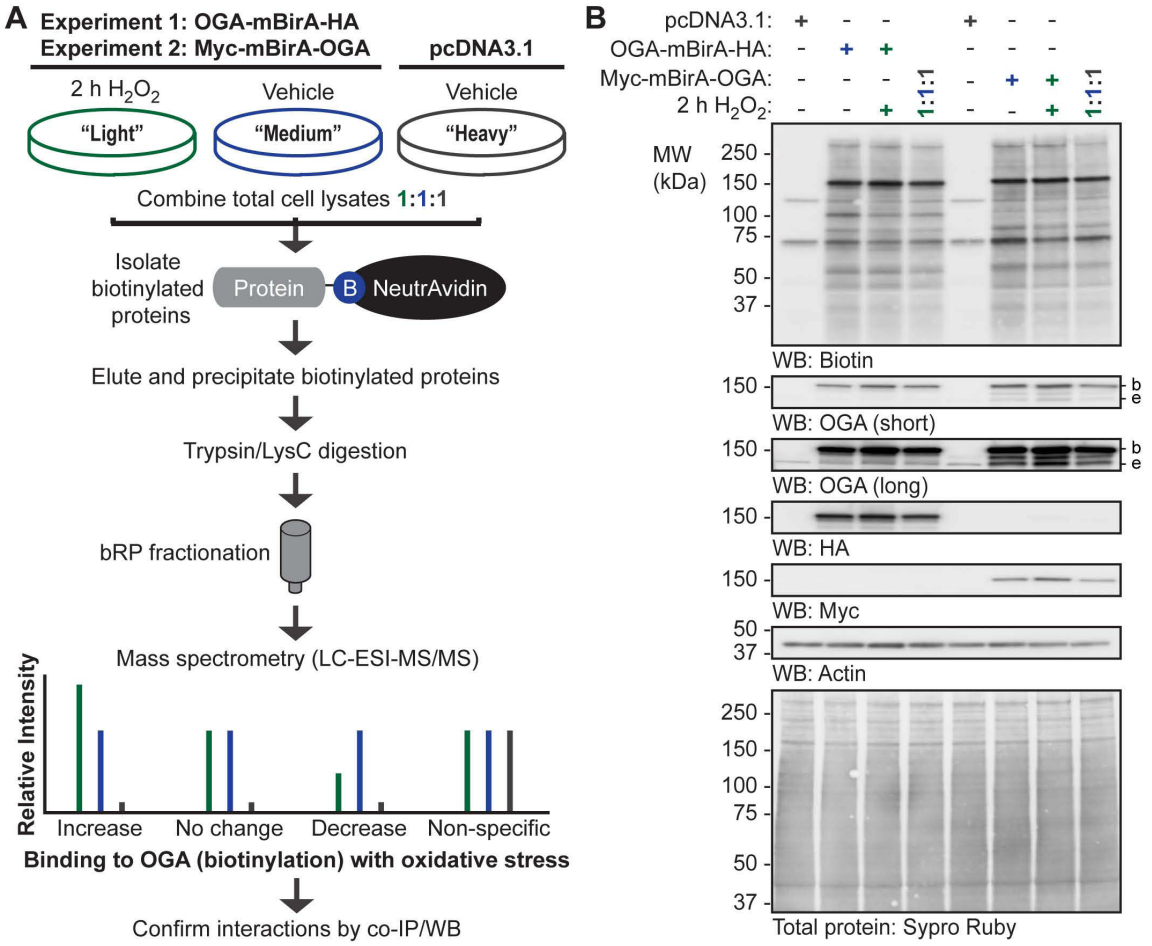

Figure 3-7: SILAC-BioID-MS/MS strategy used to identify the basal and oxidative stress-dependent interactome of OGA. (A) U2OS cells were labeled with light, medium, or heavy isotopes of arginine and lysine for 6 generations. In experiment 1, cells were transfected with pcDNA3.1 (heavy) or OGA-mBirA-HA (light, medium), treated with biotin (25 μM, 16 h), and treated with vehicle (medium, heavy) or H_2O_2 (light; 2.5 mM, 2 h, N=1). In experiment 2, Myc-mBirA-OGA was transfected in replacement of OGA-mBirA-HA. For each experiment, proteins were extracted in denaturing TCL buffer and combined in equal amounts. The biotinylated proteins were isolated on NeutrAvidin-agarose in denaturing conditions, eluted in 2% (w/v) SDS (95°C), and precipitated with acetone. Peptides were generated by trypsin and LysC digestion, separated by basic reversed phase (bRP) fractionation, and identified by liquid chromatography-tandem mass spectrometry (LC-ESI-MS/MS). Subsequently, protein-protein interactions were validated by co-immunoprecipitation (IP) and Western blot (WB). (B) For the SILAC experiments (N=1, each), equal amounts of protein (10 μg; denaturing TCL lysis) were separated by SDS-PAGE and the following were detected by Western blot: biotin, OGA, HA, Myc, and actin. Protein load was assessed by total protein stain (Sypro Ruby) and by Western blot (actin). Migration of endogenous OGA (e), mBirA-tagged OGA (b), and the molecular weight (MW) markers are indicated.

Raw MS protein and peptide identifications are reported in Supplemental Tables 3-1 through 3-6, and processing of the raw MS data, as described below, is outlined in Figure 3-8. LC-MS/MS identified 126 proteins in the OGA-mBirA-HA pulldown (Supplemental Table 3-7) and 157 proteins in the Myc-mBirA-OGA pulldown (Supplemental Table 3-8) after application of the following inclusion criteria in Proteome Discover 1.4: a peptide rank of 1 (filter 1), a 5% false discovery rate (FDR; filter 1), as well as >1 unique peptide, >2 total peptides, and >3 peptide spectral matches (PSMs) per identification (filter 2). Next, the variability in the endogenously biotinylated carboxylases was used to set a threshold for excluding non-specific interactors (Figure 3-8 (exclusion criteria 2), Figure 3-9; Supplemental Table 3-9), yielding 44 proteins and 41 proteins enriched above background for the HA (Figure 3-10A; Supplemental Table 3-10) and Myc (Figure 3-10B; Supplemental Table 3-11) screens, respectively. To determine the interactors that are induced upon oxidative stress, we set a threshold of a 25% increase in protein abundance in stressed cells compared to control cells (Supplemental Table 3-12). For the OGA-mBirA-HA pulldown, 48 proteins were identified as stress-induced interactors, of which 19 were present above background in only the stressed sample (Figure 3-10A; Supplemental Table 3-10). For the Myc-mBirA-OGA fusion protein, 28 proteins were identified as stress-induced interactors. Of these proteins, 12 were identified above background in only the stressed sample (Figure 3-10B; Supplemental Table 3-11). Highlighting the utility of our dual-tagging strategy for maximizing coverage of the OGA interactome, there were only 21 basal interactors (Figure 3-10C) and 15 stress-induced interactors (Figure 3-10D) that were present in both the HA and Myc datasets. MS protein identifications are summarized in Supplemental Table 3-13. In total, 90 proteins were

identified as potential OGA-interactors using SILAC-BioID-MS/MS (Table 3-1). Of these interactors, we identified 21 proteins above background in the basal and stressed samples (regardless of fold change upon stress) from both datasets (Figure 3-10E), and consider these proteins to be high-confidence binding partners of OGA (bold, Table 3-1). Finally, gene list analysis using the Protein Analysis Through Evolutionary Relationships (PANTHER) (Thomas et al. 2003; Mi et al. 2005) classification system revealed that the identified proteins have diverse functions, belonging to classes of chaperones, cytoskeletal proteins, nucleic acid binding proteins, and others (Figure 3-10F).

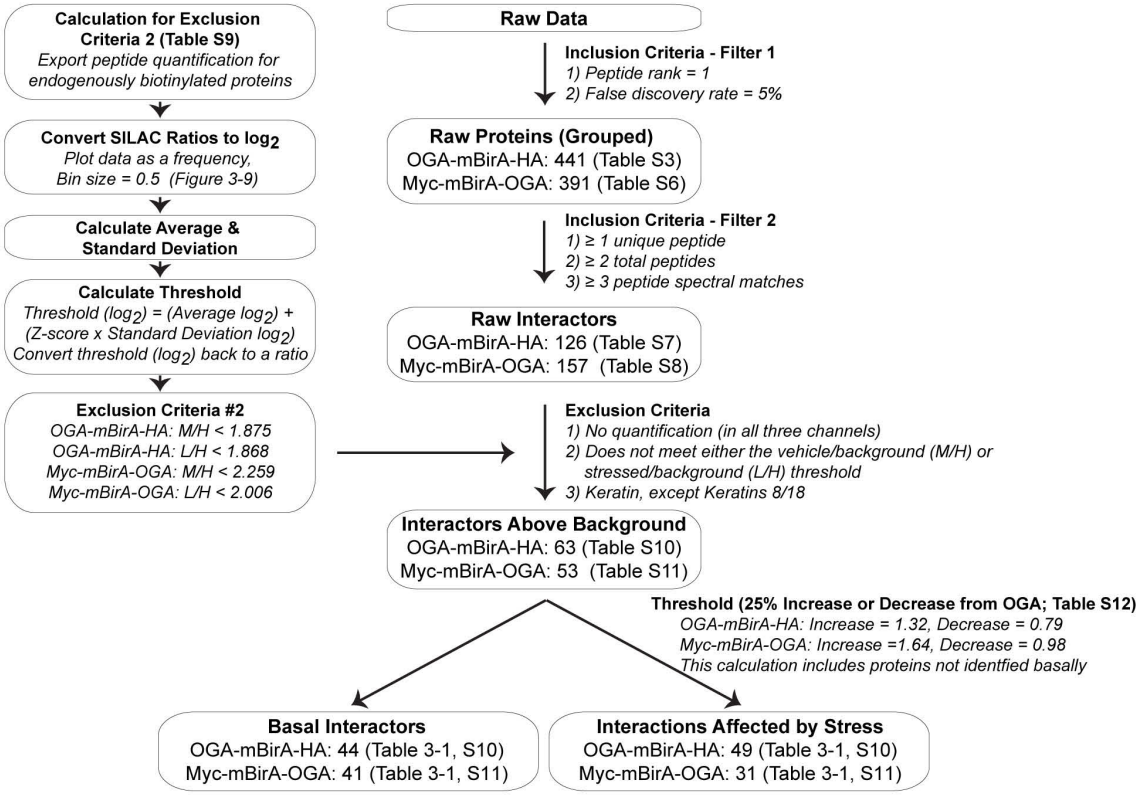

Figure 3-8: Flowchart for mass spectrometry dataset processing to generate the protein lists in the supplemental tables and table 3-1.

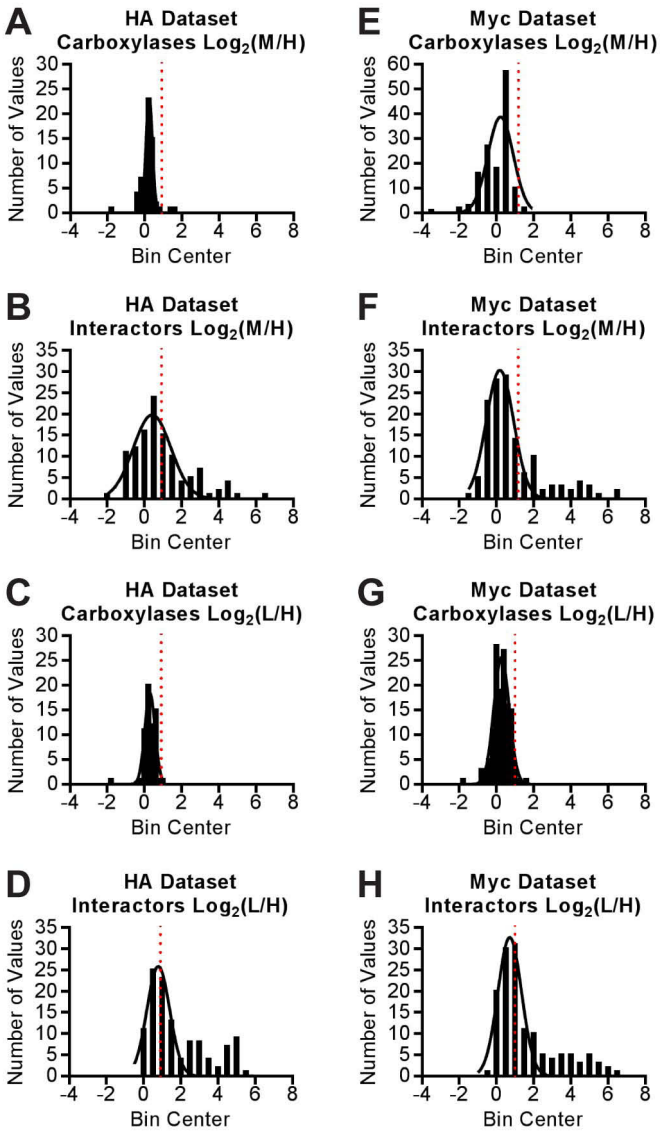

Figure 3-9: Determination of the threshold for non-specific interactors using Log_2 SILAC ratios and frequency histograms of the endogenously biotinylated carboxylases. Frequency histograms were generated from: (A) Log_2(M/H) SILAC ratios for the carboxylases (HA dataset; Supplemental Table 3-9); (B) Log_2(M/H) SILAC ratios for raw interactors (HA dataset; Supplemental Table 3-7); (C) Log_2(L/H) SILAC ratios for the carboxylases (HA dataset; Supplemental Table 3-9); (D) Log_2(L/H) SILAC ratios for raw interactors (HA dataset; Supplemental Table 3-7); (E) Log_2(M/H) SILAC ratios for the carboxylases (Myc dataset; Supplemental Table 3-9); (F) Log_2(M/H) SILAC ratios for raw interactors (Myc dataset; Supplemental Table 3-8); (G) Log_2(L/H) SILAC ratios for the carboxylases (Myc dataset; Supplemental Table 3-9); and (H) Log_2(L/H) SILAC ratios for raw interactors (Myc dataset; Supplemental Table 3-8). (A-H) Red dotted line represents the Log_2 threshold with a one-sided 95% confidence interval.

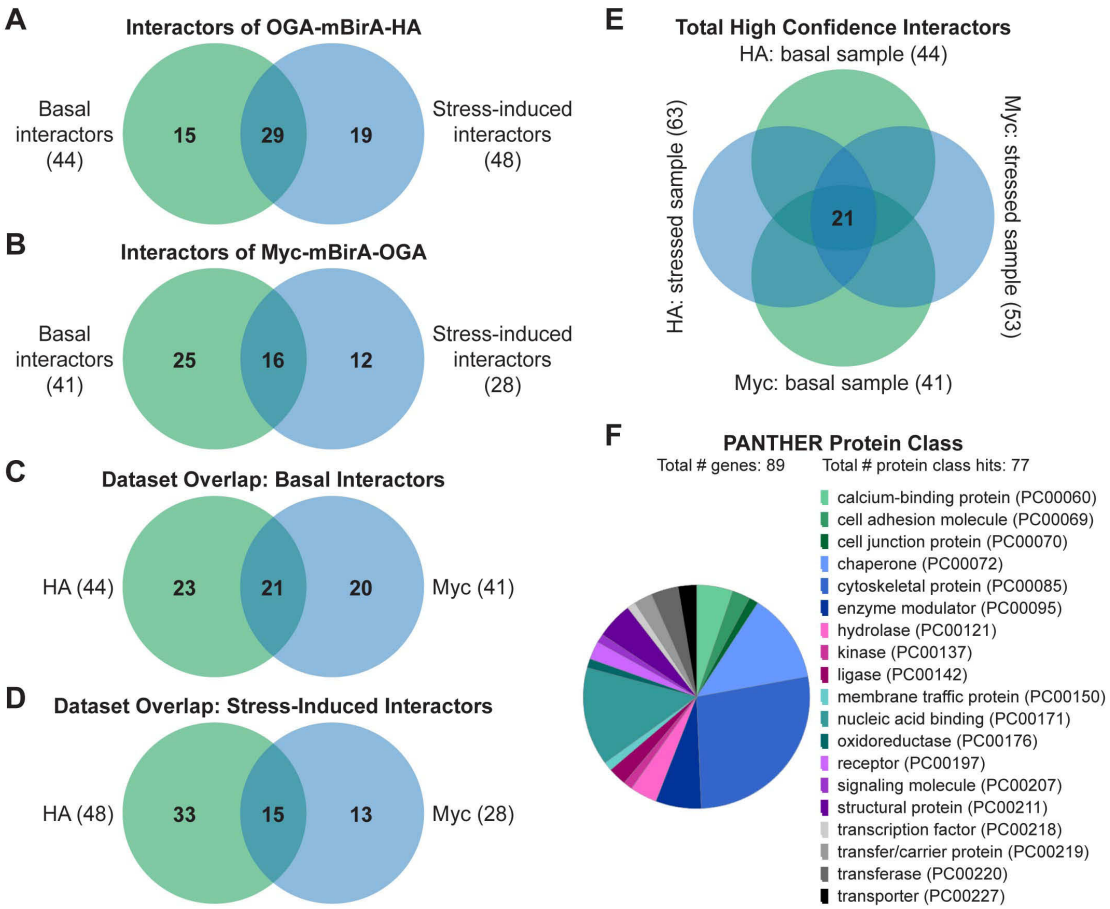

Figure 3-10: SILAC-BioID-MS/MS reveals numerous basal and stress-induced OGA-interacting proteins. Venn diagrams illustrate: (A) basal and stress-induced interactors identified in the OGA-mBirA-HA screen; (B) basal and stress-induced interactors identified in the Myc-mBirA-OGA screen; (C) basal interactors identified in the HA and Myc datasets; (D) stress-induced interactors identified in the HA and Myc datasets; and (E) interactors identified above background in the basal and stressed samples (regardless of fold change upon stress) in the HA and Myc datasets. (F) PANTHER gene list analysis indicating the protein classes represented in the OGA interactome.

Table 3-1: Interacting partners of OGA. Bold proteins are high confidence interactors that were identified in the basal and stressed samples in the HA and Myc datasets.

			HA Dataset			Myc Dataset		
Number	**Accession**	**Protein Description**	**Interacts Basally**	**Change with Stress**	**H_2O_2/ Vehicle**	**Interacts Basally**	**Change with Stress**	**H_2O_2/ Vehicle**
1	25777602	26S proteasome non-ATPase regulatory subunit 2 isoform 1				✓	↑	2.410
2	16507237	**78 kDa glucose-regulated protein precursor**	✓	↑	1.627	✓	↑	1.709
3	546231404	actin-binding protein anillin isoform 3	✓	↑	1.719			
4	156071459	ADP/ATP translocase 2	✓		1.042			
5	194097352	alpha-actinin-1 isoform c		↑	4.834		↑	6.123
6	224809474	ankycorbin isoform b	✓		1.310			
7	50845386	annexin A2 isoform 2		↑	2.000		↑	1.719
8	21264575	AT-rich interactive domain-containing protein 1A isoform b	✓		1.012			
9	528281421	**band 4.1-like protein 3 isoform 3**	✓		1.222	✓		1.389
10	62241042	**bifunctional glutamate/proline--tRNA ligase**	✓	↑	1.621	✓		1.328
11	11024698	**bifunctional protein NCOAT isoform a**	✓		1.057	✓		1.308
12	58218968	calmodulin					↑	2.772
13	24432106	cell cycle and apoptosis regulator protein 2	✓	↑	1.756			
14	5031635	cofilin-1					↑	2.083
15	65787364	**coronin-1B**	✓		0.934	✓	↓	0.791
16	451172106	coronin-1C isoform b				✓	↓	0.777
17	126032350	DNA-dependent protein kinase catalytic subunit isoform 2		↑	1.715			
18	4503471	elongation factor 1-alpha 1		↑	2.418			

			HA Dataset			Myc Dataset		
Number	**Accession**	**Protein Description**	**Interacts Basally**	**Change with Stress**	**H_2O_2/ Vehicle**	**Interacts Basally**	**Change with Stress**	**H_2O_2/ Vehicle**
19	4503483	elongation factor 2					↑	3.899
20	4758256	eukaryotic translation initiation factor 2 subunit 1	✓	↑	2.141			
21	302699239	eukaryotic translation initiation factor 4 gamma 1 isoform 4				✓		1.598
22	41872631	**fatty acid synthase**	✓	↑	1.357	✓		1.353
23	388490223	FERM domain-containing protein 6 isoform 3	✓		0.933			
24	116063573	**filamin-A isoform 1**	✓	↑	1.325	✓		1.335
25	256222415	**filamin-B isoform 4**	✓	↑	2.155	✓	↑	1.901
26	4504981	galectin-1		↑	1.714			
27	356461016	gem-associated protein 5 isoform 2				✓		1.572
28	66932975	gephyrin isoform 2	✓	↑	1.863			
29	194248072	heat shock 70 kDa protein 1A/1B	✓	↑	1.516			
30	34419635	heat shock 70 kDa protein 6				✓	↑	1.877
31	24234686	**heat shock cognate 71 kDa protein isoform 2**	✓	↑	1.689	✓	↑	2.019
32	4504517	heat shock protein beta-1		↑	12.816	✓	↑	7.830
33	154146191	heat shock protein HSP 90-alpha isoform 2	✓	↑	1.835			
34	431822406	heat shock protein HSP 90-beta isoform b	✓	↑	2.061			
35	431822408	heat shock protein HSP 90-beta isoform c					↑	2.152
36	10645195	histone H2A type 1-B/E		↑	3.832			
37	10800140	histone H2B type 1-B		↑	3.598			

			HA Dataset			Myc Dataset		
Number	**Accession**	**Protein Description**	**Interacts Basally**	**Change with Stress**	**H_2O_2/ Vehicle**	**Interacts Basally**	**Change with Stress**	**H_2O_2/ Vehicle**
38	4504301	histone H4		↑	3.731			
39	5032027	histone-binding protein RBBP4 isoform a				✓		1.616
40	98986457	host cell factor 1				✓		1.453
41	4557888	**keratin, type I cytoskeletal 18**	✓		1.240	✓		1.208
42	372466577	**keratin, type II cytoskeletal 8 isoform 2**	✓		1.204	✓		1.251
43	12383062	**kinesin light chain 2 isoform 1**	✓	↑	1.633	✓	↑	2.418
44	216548085	**leucine zipper protein 1**	✓	↑	2.504	✓	↑	2.497
45	41350320	melanoma-associated antigen D2	✓	↑	2.096		↑	2.407
46	262073007	monocarboxylate transporter 1		↑	1.325			
47	38176300	nestin	✓		0.880			
48	140972063	neurabin-2				✓	↑	1.638
49	114155142	nucleoprotein TPR				✓		1.162
50	170932516	paxillin isoform 1				✓	↑	3.692
51	196162711	PDZ and LIM domain protein 4 isoform 2				✓		1.397
52	33356174	pinin	✓		1.273			
53	41322910	plectin isoform 1d		↑	1.408		↑	1.657
54	601984520	**polyubiquitin-C**	✓	↑	3.919	✓	↑	2.781
55	530394628	PREDICTED: BAG family molecular chaperone regulator 3 isoform X1	✓	↑	2.677			

			HA Dataset			Myc Dataset		
Number	**Accession**	**Protein Description**	**Interacts Basally**	**Change with Stress**	**H_2O_2/ Vehicle**	**Interacts Basally**	**Change with Stress**	**H_2O_2/ Vehicle**
56	578812465	PREDICTED: band 4.1-like protein 2 isoform X12	✓	↑	1.881			
57	578812459	PREDICTED: band 4.1-like protein 2 isoform X9				✓		1.046
58	578822562	PREDICTED: chromodomain-helicase-DNA-binding protein 4 isoform X6	✓	↑	1.447			
59	578815876	PREDICTED: elongation factor 1-delta isoform X14				✓		1.353
60	530388831	PREDICTED: elongation factor 1-delta isoform X7				✓		1.411
61	578814066	**PREDICTED: filamin-C isoform X1**	✓	↑	3.169	✓	↑	2.390
62	530381927	**PREDICTED: heat shock 70 kDa protein 1-like isoform X4**	✓	↑	1.585	✓	↑	1.935
63	578824891	PREDICTED: LIM domain only protein 7 isoform X39					↑	2.027
64	530379305	**PREDICTED: microtubule-associated protein 1B isoform X1**	✓	↑	1.399	✓		1.359
65	530397279	**PREDICTED: neuroblast differentiation-associated protein AHNAK isoform X1**	✓		1.125	✓		1.288
66	578821456	PREDICTED: nuclear mitotic apparatus protein 1 isoform X9				✓	↓	0.799
67	530381066	PREDICTED: nucleophosmin isoform X2		↑	2.499			
68	578811124	PREDICTED: nucleophosmin isoform X3					↑	2.141
69	530403029	**PREDICTED: protein AHNAK2 isoform X1**	✓	↑	1.556	✓	↑	1.640
70	578805886	PREDICTED: raftlin isoform X7	✓	↓	0.772			
71	530407875	PREDICTED: RNA-binding protein FUS isoform X3	✓		0.857			
72	530411381	PREDICTED: septin-9 isoform X3				✓		1.278
73	530390127	PREDICTED: tropomyosin beta chain isoform X7		↑	2.926			

			HA Dataset			Myc Dataset		
Number	**Accession**	**Protein Description**	**Interacts Basally**	**Change with Stress**	**H_2O_2/ Vehicle**	**Interacts Basally**	**Change with Stress**	**H_2O_2/ Vehicle**
74	530383156	PREDICTED: unconventional myosin-VI isoform X8		↑	2.696			
75	578818565	**PREDICTED: vimentin isoform X1**	✓		1.162	✓		1.288
76	530365709	PREDICTED: zinc finger CCCH domain-containing protein 11A isoform X5	✓	↑	1.818			
77	5454064	RNA-binding protein 14 isoform 1					↑	2.047
78	55741709	RNA-binding protein 25	✓	↑	1.649			
79	148352331	septin-7 isoform 1				✓		1.392
80	112382252	spectrin beta chain, non-erythrocytic 1 isoform 2		↑	1.365			
81	24234688	stress-70 protein, mitochondrial precursor	✓	↑	1.578			
82	150417971	supervillin isoform 1		↑	2.454			
83	325651836	SWI/SNF-related matrix-associated actin-dependent regulator of chromatin subfamily A member 5		↑	1.553			
84	544711041	T-complex protein 1 subunit theta isoform 2				✓		1.329
85	116875765	tight junction protein ZO-1 isoform b	✓	↑	1.750			
86	98986464	transmembrane emp24 domain-containing protein 10 precursor					↑	2.674
87	393715095	tubulin alpha-1A chain isoform 2		↑	1.918			
88	29788785	tubulin beta chain isoform b		↑	3.379			
89	557129022	ubiquitin carboxyl-terminal hydrolase 7 isoform 3				✓	↑	2.354
90	296010977	**zinc finger protein 185 isoform 7**	✓	↑	2.983	✓	↑	2.027

Oxidative stress induces the association of OGA with FAS, FLNA, HSC70, and OGT

To validate a subset of the identified protein-protein interactions, endogenous OGA was enriched using the anti-OGA-Bethyl antibody from NETN U2OS cell lysates treated with H_2O_2 (1-3 h), and Western blots were performed for interacting partners-of-interest (Figure 3-11A). In addition to a subset of proteins identified in the screen, we also probed for OGT, a known binding partner of OGA (Whisenhunt et al. 2006). The interaction of OGA with FAS, FLNA, HSC70, and OGT is clearly induced in response to oxidative stress (Figure 3-11A). Actin is shown as both a loading and negative control.

Further validation of these protein-protein interactions was performed by immunoprecipitation (IP) of endogenous FAS and V5-tagged FAS using an anti-FAS antibody and an anti-V5 antibody, respectively. Endogenous FAS or transiently overexpressed pCMV-SPORT6 V5-FAS was enriched from NETN U2OS cell lysates treated with H_2O_2 (1-3 h), and Western blots were performed for interacting partners-of-interest (Figure 3-11B, C). Consistent with previous results (Figure 3-11A), the interaction between OGA and endogenous FAS is induced in response to oxidative stress (Figure 3-11B, C). Interestingly, we also observe that OGT and HSC70 exhibit increased binding to endogenous FAS and V5-FAS upon oxidative stress (Figure 3-11B, C).

To determine if these protein-protein interactions are conserved in other cell types in addition to U2OS cells, we enriched endogenous OGA and endogenous FAS from HEPG2 human hepatocellular carcinoma cells (Figure 3-12). We chose HEPG2 cells as a recent publication has indicated an interaction between OGT and FAS in the liver (Baldini et al. 2016). Western blots for the proteins-of-interest reveal that FAS and HSC70 co-IP

with OGA in HEPG2 cells under basal conditions (Figure 3-12A). We also observe that OGA and HSC70 co-IP with FAS basally in HEPG2 cells (Figure 3-12B). Unlike U2OS cells, the interactions in HEPG2 cells are not induced in response to oxidative stress (*data not shown*). Furthermore, we assessed these interactions in murine liver tissue by enriching endogenous OGA and endogenous FAS. We have demonstrated that HSC70 co-IPs with OGA (Figure 3-12C), and that OGA and HSC70 co-IP with FAS in normal liver tissue (Figure 3-12D). Overall, these data suggest that the aforementioned protein-protein interactions are not specific to only U2OS cells, but that the interactions also occur in normal tissue and that the pathways regulating OGT and OGA may be cell/tissue-type specific.

An immunoprecipitation with a rabbit isotype control immunoglobulin (Ig)G was used as an indicator of non-specific binding for the endogenous OGA and endogenous FAS IPs (Figure 3-11A, B; Figure 3-12), and pcDNA3.1-overexpressing cells were used to control for non-specific binding in the V5-FAS IPs (Figure 3-11C). Of note, a band at the apparent molecular weight of actin is observed in the control IgG IP (Figure 3-11B). Analysis of control IgG alone in buffer indicates that this signal arises from the anti-actin primary antibody (*data not shown*).

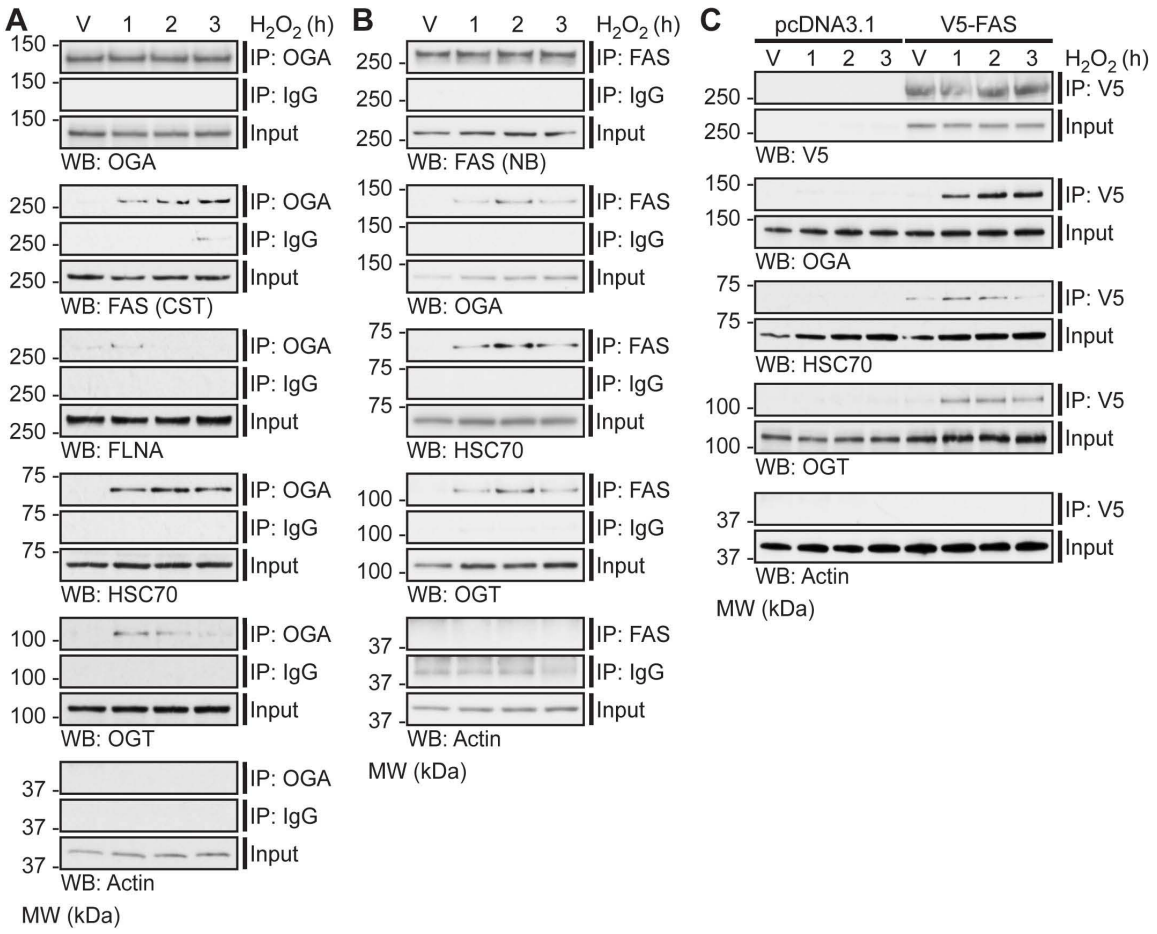

Figure 3-11: Oxidative stress induces the association of OGA with FAS, FLNA, HSC70, and OGT. U2OS cells were treated with vehicle (V) or H_2O_2 (2.5 mM, 1-3 h). N=3. (A) An anti-OGA antibody (IP: OGA; top panel) or a rabbit isotype control immunoglobulin (IP: IgG; middle panel) were used to enrich endogenous OGA from NETN cell lysates (500 µg), of which 1.5-2% (input) and 30-40% (immunoprecipitate) were analyzed by SDS-PAGE. OGA, FAS, FLNA, HSC70, OGT (positive control), and actin (loading/negative control) were detected by Western blot (WB). (B) An anti-FAS antibody (IP: FAS; top panel) or a rabbit isotype control immunoglobulin (IP: IgG; middle panel) were used to enrich endogenous FAS from NETN cell lysates (250 µg), of which 3% (input) and 60% (immunoprecipitate) were analyzed by SDS-PAGE. FAS, OGA, HSC70, OGT, and actin (loading/negative control) were detected by Western blot. (C) U2OS cells were transfected with pcDNA3.1 (control) or pCMV-SPORT6 V5-FAS (test). An anti-V5 antibody was used to enrich V5-FAS from control and test NETN cell lysates (300 µg), of which 1.7% (input) and 33.3% (immunoprecipitate) were analyzed by SDS-PAGE. V5, OGA, HSC70, OGT, and actin (loading/negative control) were detected by Western blot. (A-C) FAS (CST) and FAS (NB) represent anti-FAS antibody from Cell Signaling Technology and Novus Biologicals, respectively. To ensure that images were in the linear range, Western blot exposures from the input and immunoprecipitated fractions are often different. The exposure lengths for the test and control isotype antibody immunoprecipitates are always identical. The migration of molecular weight (MW) markers is indicated.

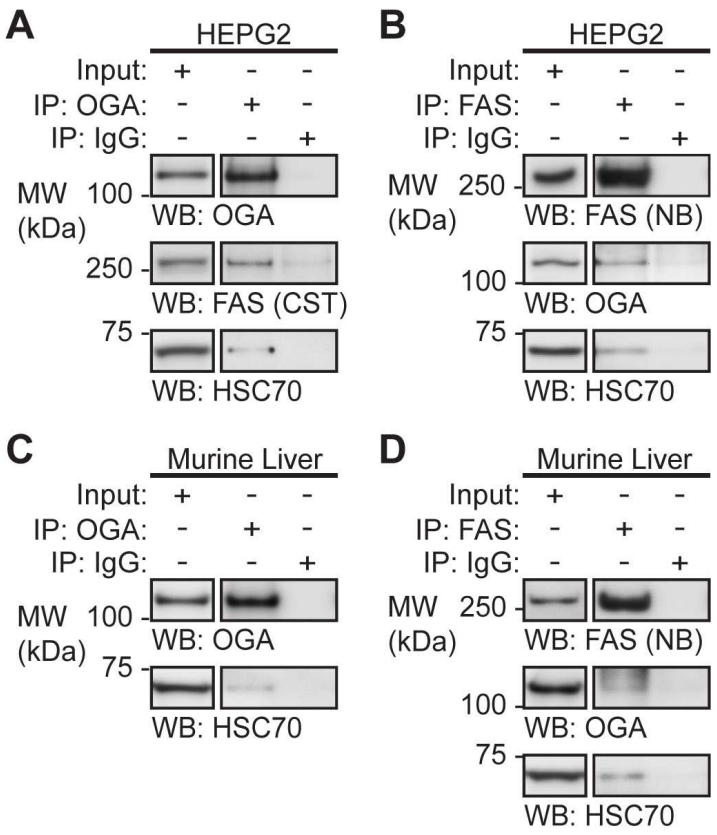

Figure 3-12: FAS, OGA, and HSC70 interact basally in human hepatocytes and murine liver tissue. Cells and tissue were lysed in NETN buffer and pre-cleared. Immunoprecipitations were performed with the anti-OGA-Bethyl antibody (IP: OGA; A, C), an anti-FAS antibody (IP: FAS; B, D), or a rabbit isotype control immunoglobulin (IP: IgG; A-D). (A) Endogenous OGA was enriched from HEPG2 cell lysate (500 µg), of which 2% (input) and 50% (immunoprecipitate) were analyzed by SDS-PAGE. OGA, FAS, and HSC70 were detected by Western blot (WB). N=4, except for WB: FAS (N=2). (B) Endogenous FAS was enriched from HEPG2 cell lysate (250-600 µg), of which 1.7-4% (input) and 33-80% (immunoprecipitate) were analyzed by SDS-PAGE. FAS, OGA, and HSC70 were detected by Western blot. N=4. (C) Endogenous OGA was enriched from normal murine liver tissue lysate (400 µg), of which 3.8% (input) and 63% (immunoprecipitate) were analyzed by SDS-PAGE. OGA and HSC70 were detected by Western blot. N=3. (D) Endogenous FAS was enriched from normal murine liver tissue lysate (400 µg), of which 3.8% (input) and 63% (immunoprecipitate) were analyzed by SDS-PAGE. FAS, OGA, and HSC70 were detected by Western blot. N=3. (A-D) FAS (CST) and FAS (NB) represent anti-FAS antibody from Cell Signaling Technology and Novus Biologicals, respectively. To ensure that images were in the linear range, Western blot exposures from the input and immunoprecipitated fractions are often different. The exposure lengths for the test and control isotype antibody immunoprecipitates are always identical. The migration of molecular weight (MW) markers is indicated.

OGA exhibits reduced catalytic activity when bound to FAS

Next, we sought to determine if FAS alters the catalytic activity of OGA. As the mechanism controlling the stress-induced association of OGA and FAS is currently unknown, we assessed the activity of OGA in cells stably overexpressing pcDNA3.1 or V5-FAS and treated with or without 2 h H_2O_2 (Figure 3-13). The immunoprecipitation technique utilized in Figure 3-11C was coupled with a downstream OGA activity assay. This allowed us to measure the activity of OGA in total cell lysates (Figure 3-13A, C) and the pool of OGA bound to FAS (Figure 3-13B, D). In total cell lysates (Figure 3-13A), overexpression of V5-FAS did not alter OGA activity (Figure 3-13C), and we attribute this observation to the small percentage of OGA that associates with FAS (<5%). To overcome the stoichiometry of this interaction, we enriched V5-FAS using an anti-V5 antibody and assessed the activity of OGA on the protein A/G magnetic beads (Figure 3-13B, D).

Consistent with previous results (Figure 3-11C), the interaction of V5-FAS with OGA was induced in response to oxidative stress (Figure 3-13B). To assess the specific activity of OGA bound to FAS (on-bead) and compare it to the specific activity of OGA in the unbound and input lysates, we determined the amount of OGA on the beads using Western blot quantitation of the bound fractions and a dilution series of the inputs. The fraction of OGA bound to V5-FAS during oxidative stress exhibited an ~85% reduction in specific activity (Figure 3-13D; RM-1ANOVA/Tukey's MCT, $p \leq 0.0001$) when compared to its activity in the unbound fraction. Importantly, we did not detect on-bead OGA activity above the baseline in the pcDNA3.1 controls or the vehicle-treated V5-FAS sample.

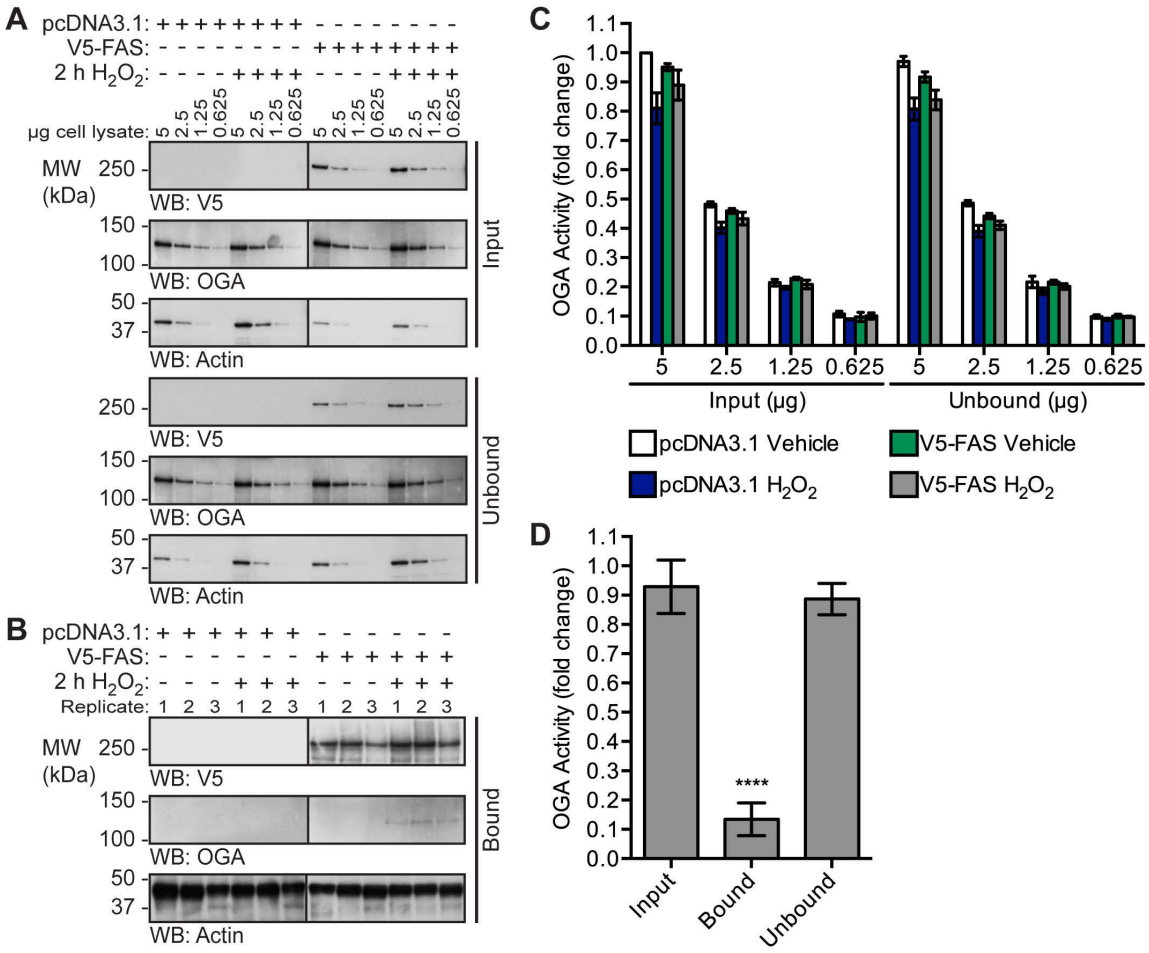

Figure 3-13: OGA exhibits reduced catalytic activity when bound to FAS. U2OS cells stably overexpressing pcDNA3.1 (control) or pcDNA3.1 V5-FAS (test) were treated with vehicle (V) or H_2O_2 (2.5 mM, 2 h). An anti-V5 antibody was used to enrich V5-FAS from control and test NETN cell lysates (1.6 mg). N=3. (A, B) V5, OGA, and actin (loading/negative control) were detected by Western blot (WB). Western blots for each antibody were exposed for equal lengths of time. (A) Analysis of the inputs and unbound fractions. (B) Analysis of the bound fractions (31.25%). (C) OGA activity was measured in the inputs and unbound fractions using 4MU-GlcNAc (1 mM). N=3, 2 technical replicates per assay. Fluorescence values were converted to pmoles/min and then normalized to the pcDNA3.1 vehicle-treated sample. (D) OGA activity was assessed in the input, bound (on-bead, 31.25%), and unbound fractions using 4MU-GlcNAc (1 mM). N=3, 2 technical replicates per assay. Fluorescence values were converted to pmoles/min/µg using densitometric analysis of OGA in the input serial dilutions and the bound fractions, and then normalized to the pcDNA3.1 vehicle-treated sample. Only the data from FAS-overexpressing cells treated with H_2O_2 are shown, as OGA protein and activity was absent in the bound fraction of the other samples. Data are presented as the mean ± SEM. Significance was determined by RM-1ANOVA followed by Tukey's multiple comparison test, and differences were considered statistically significant at $p \leq 0.0001$ (****). The migration of molecular weight (MW) markers is indicated.

FAS overexpression increases O-GlcNAcylation during oxidative stress

As the pool of OGA bound to FAS is inhibited, we hypothesized that overexpression of FAS would result in a stress-dependent increase in O-GlcNAcylation on a subset of proteins. To test this hypothesis, cells stably overexpressing pcDNA3.1 or V5-FAS were treated with vehicle or H_2O_2 (1-3 h). Proteins from NETN lysates were separated by SDS-PAGE and Western blots for OGT, OGA, and O-GlcNAc were performed. O-GlcNAc levels are significantly higher in FAS-overexpressing cells compared to control cells at 3 h H_2O_2 (Figure 3-14A, B; repeated measures two-way analysis of variance (RM-2ANOVA)/Sidak's MCT, $p \leq 0.01$). Of note, we observe variable changes in the expression of OGT and OGA basally upon V5-FAS overexpression that only reach statistical significance for OGT (Figure 3-14A, C, D; RM-2ANOVA/Sidak's MCT, $p \leq 0.001$). However, the expression of OGA and OGT remain unchanged in FAS-overexpressing cells during the hydrogen peroxide time course. Overall, these data suggest that FAS binds to and sequesters OGA preventing it from de-glycosylating a subset of proteins during oxidative stress, thereby augmenting cellular O-GlcNAcylation (Figure 3-15).

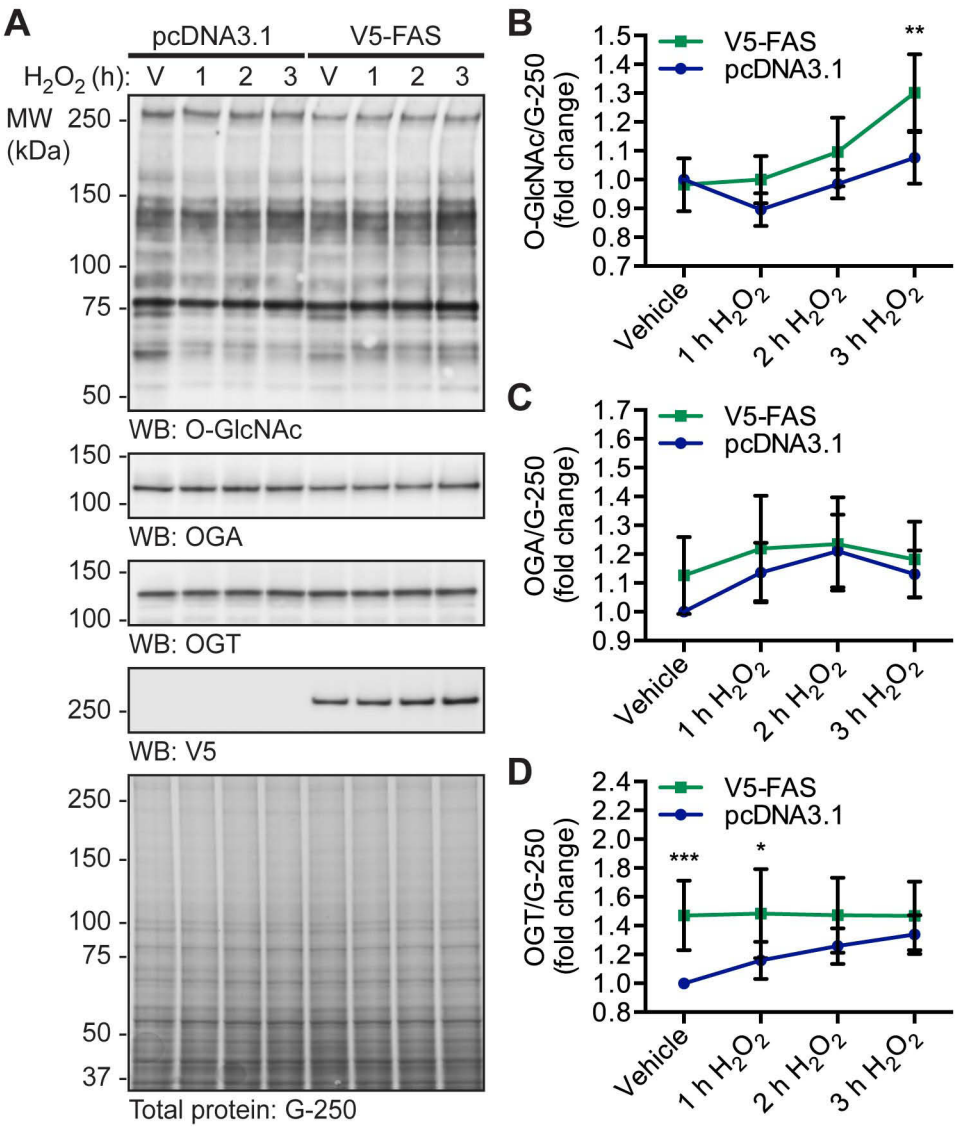

Figure 3-14: FAS overexpression increases O-GlcNAcylation during oxidative stress. U2OS cells stably overexpressing pcDNA3.1 or pcDNA3.1 V5-FAS were treated with vehicle (V) or H_2O_2 (2.5 mM, 1-3 h). N=5. (A) NETN lysates (~7.5 µg) were analyzed by SDS-PAGE. O-GlcNAc, OGA, OGT, V5, and actin were detected by Western blot (WB). Total protein stain (colloidal coomassie G-250) was used to assess protein load. The migration of molecular weight (MW) markers is indicated. (B) Quantitation of O-GlcNAc levels normalized to G-250. (C) Quantitation of OGA expression normalized to G-250. (D) Quantitation of OGT expression normalized to G-250. (B-D) Data are presented as the mean ± SEM. Significance was determined by RM-2ANOVA followed by Sidak's multiple comparison test, and differences were considered statistically significant at $p \leq 0.05$ (*), $p \leq 0.01$ (**), and $p \leq 0.001$ (***).

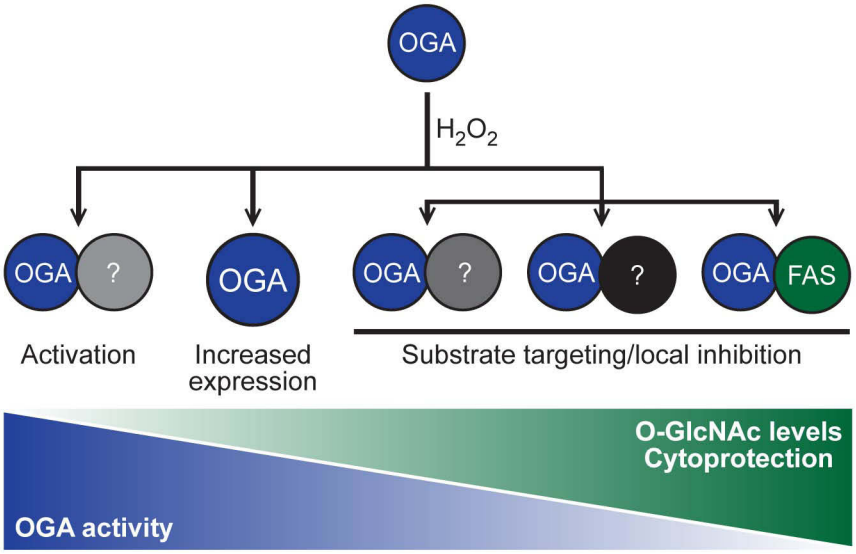

Figure 3-15: Proposed model for the regulation of OGA during oxidative stress resulting in elevated levels of O-GlcNAc. O-GlcNAc levels become elevated during oxidative stress, and this is associated with cytoprotection. Counterintuitively, in U2OS cells exposed to oxidative stress, OGT activity remains constant while OGA activity and expression are elevated. Our data supports a model in which OGA forms complexes with other proteins (?), such as FAS, that regulate its activity leading to a stress-induced elevation of O-GlcNAc.

Discussion

Dynamic O-GlcNAcylation is a critical regulator of many cellular processes including the cellular stress response and survival signaling (Zachara et al. 2004; Hart et al. 2011; Groves et al. 2013; Bond and Hanover 2015). The molecular mechanisms by which cells communicate with OGT and OGA to glycosylate and de-glycosylate the correct substrates in response to stimuli, including cell stress and injury, are not well understood. The goal of this study was to determine which mechanisms the cell utilizes to regulate O-GlcNAc levels during oxidative stress, and to provide insight into the proteins that interact with and regulate OGA. We have demonstrated that both OGA and OGT appear to be targeted during oxidative stress, resulting in an increase in the expression of both enzymes and elevated OGA activity (Figure 3-1). An increase in the expression and activity of OGA cannot be reconciled with the observed increase in O-GlcNAc (Figure 3-1), suggesting that OGA is targeted to substrates or that specific pools of OGA are inhibited. Several lines of evidence support this rationale. First, in glucose deprived Neuro2A cells, O-GlcNAc levels are robustly elevated. However, only modest changes in OGT expression, but not specific activity, are observed. Contrary to expectations, there is a decrease in UDP-GlcNAc levels and an increase in OGA activity (Cheung and Hart 2008). Second, OGT interacts with p38 mitogen-activated protein kinase during glucose starvation, resulting in the targeting of OGT to glycosylate substrates such as neurofilament H (Cheung and Hart 2008). Third, we have recently reported that a subset of proteins exhibit decreased O-GlcNAcylation during oxidative stress, even when global O-GlcNAc levels are elevated (Lee et al. 2016). To define the regulation of OGA during oxidative stress, we have identified a subset of its interaction partners and determined how these interactions change with oxidative stress.

Collectively, we have identified 90 binding partners and validated the interaction of OGA with FAS, FLNA, HSC70, and OGT. Notably, FAS was demonstrated to inhibit OGA activity, and consistent with this observation cellular O-GlcNAcylation was augmented in FAS-overexpressing cells upon oxidative stress.

In this study, we utilized BioID (Roux et al. 2012) to identify the interaction partners of OGA. BioID offers many advantages when compared to other methodologies (Roux et al. 2012; Mehta and Trinkle-Mulcahy 2016; Varnaitė and MacNeill 2016), such as identifying low affinity and transient interactors, as well as obviating the need for an antibody-based enrichment. One disadvantage of this technique, when combined with SILAC quantification, is that the fold change reported for signal-induced interactions can be diluted out by the long biotin-labeling step (16 h). This dilution effect is highlighted by our data, in which proteins such as FAS and FLNA demonstrate clear stress-induced associations with OGA by co-immunoprecipitation, but are only enriched ~25% over OGA in the BioID screen. We speculate that the interactions of OGA with FAS and FLNA exist with a low affinity basally, but are stabilized and enhanced during oxidative stress. In addition, BioID may be capturing stress-induced interactions between these proteins that occur as a result of natural fluctuations in reactive oxygen species levels that occur in growing cells. The recent development of spatially and temporally restricted enzymatic biotinylation has resolved this issue (Martell et al. 2012; Rhee et al. 2013). However, this second-generation approach relies on biotinylation that is activated by hydrogen peroxide (Martell et al. 2012; Rhee et al. 2013), a technique which is not compatible with our oxidative stress model. One additional caveat of the BioID approach is that the long biotin-labeling step reduces the chance of identifying interactions that dissociate upon stress. This

is further exacerbated by our analysis approach, which excluded proteins if mass spectrometric quantification was present in only one channel.

Our study, using SILAC-BioID-MS/MS, has discovered candidate regulatory proteins of OGA during injury through the global identification of OGA's binding partners. Collectively, our screen identified 90 interacting proteins of OGA, which fall into diverse groups but were enriched in chaperones, cytoskeletal proteins, and nucleic acid binding proteins (Figure 3-10F). Of these proteins, 21 were present in the basal and stressed samples from both datasets (bold, Table 3-1) suggesting that these proteins are robust, high confidence interactors of OGA. Of note, 6 proteins were identified to co-purify with OGA during its initial cloning and characterization (Gao et al. 2001), and one of these proteins (HSC70) was confirmed in our BioID screen. Recently, OGA was also identified to bind chromodomain helicase DNA-binding protein 4 (Mi2β), erythroid transcription factor (GATA-1), and Friend of GATA-1 at the Aγ-globin promoter using co-immunoprecipitation (Zhang et al. 2016), although none of these nuclear interactors were identified in our study. Interestingly, our BioID screen revealed mitochondrial OGA-interacting proteins such as adenosine disphosphate (ADP)/adenosine triphosphate (ATP) translocase 2, of which isoform 1 of this protein has previously been reported to be O-GlcNAcylated in cardiac mitochondria (Ma et al. 2015). While these results require further validation, our data are consistent with the co-localization of OGA(-mBirA) and MitoTracker in U2OS cells, as well as recent work demonstrating the mitochondrial localization of OGA (Banerjee et al. 2015).

As our goal is to understand the regulation of OGA during cellular injury, we focused our validation efforts on proteins whose association with OGA was augmented

during oxidative stress (61 total proteins; Figure 3-10D). A number of proteins were of particular interest including FAS, FLNA, and HSC70, as they are known to be involved in the cellular stress response. Furthermore, confirmation of FAS and FLNA allowed us to test the arbitrary threshold of 25% set for stress-induced interactions. FAS is most commonly known as the enzyme that performs de novo lipogenesis, synthesizing 16-carbon chain fatty acids (palmitate) from acetyl-CoA and malony-CoA (Semenkovich 1997). Recently, FAS has been implicated as a metabolic oncogene and a biomarker for cancer detection and prognosis (Kuhajda et al. 1994; Pizer et al. 1996; Hamada et al. 2014; Ito et al. 2014; Wakamiya et al. 2014; Mullen and Yet 2015). Suggesting that FAS is a pro-survival signaling molecule, its inhibition has been demonstrated to induce tumor cell apoptosis through various mechanisms including cell cycle arrest (Zhou et al. 2003), reduced cellular growth and proliferation (Kuhajda et al. 1994; Carvalho et al. 2008; Lee et al. 2009; Veigel et al. 2015; Ventura et al. 2015), decreased phospholipid biosynthesis (Ventura et al. 2015), disruption of lipid raft architecture (Ventura et al. 2015), and blockage of the β-catenin and phosphoinositide 3-kinase (PI3K)/Akt/mammalian target of rapamycin (mTOR) signal transduction pathways (Ventura et al. 2015). Importantly for our studies, FAS is also implicated in protecting the heart and has been demonstrated to be upregulated in cardiomyocytes during heart failure (van der Vusse et al. 1992; Abdalla et al. 2011; Razani et al. 2011). Interestingly, heart-specific FAS knockout mice exhibit upregulated calcium/calmodulin-dependent protein kinase (CaMK)II signaling upon an acute transaortic constriction mechanical stress, leading to rapid cardiac dysfunction and arrhythmias (Razani et al. 2011). Supporting this model, CaMKII is O-GlcNAc-modified at Ser279 during acute hyperglycemia, resulting in its activation and cardiac dysfunction

(Erickson et al. 2013). These data suggest that FAS induction in the stressed heart may be a protective compensatory response to pathological calcium flux (Razani et al. 2011), and may at least in part be under the control of O-GlcNAc cycling. In accordance with this hypothesis, we have demonstrated that FAS interacts with OGA in a stress-induced manner in U2OS cells (Figure 3-11), and that this results in the inhibition of OGA (Figure 3-13) and increased cellular O-GlcNAcylation (Figure 3-14). Collectively, these data lead to a novel and attractive model in which FAS binds to and inhibits OGA upon oxidative stress to promote cell survival (Figure 3-15).

In addition to FAS, we identified and validated the interactions of OGA with FLNA, HSC70, and OGT in U2OS cells (Figure 3-11A). While OGT and OGA have previously been reported to interact (Whisenhunt et al. 2006), the physiological significance of the stress-dependent association remains uncertain and suggests reciprocal regulation between the two enzymes. Interestingly, HSC70 and OGT were also demonstrated to interact with FAS in response to oxidative stress (Figure 3-11B, C), raising the possibility of a large stress-induced multi-protein complex containing FAS, OGT, OGA, and HSC70. These interactions are maintained basally in HEPG2 liver cancer cells and normal murine liver tissue (Figure 3-12), suggesting that the interactions are not specific to U2OS cells. These data are in concordance with a recent study by Baldini and colleagues demonstrating that FAS binds OGT in the liver of ob/ob mice (Baldini et al. 2016). Collectively, our data suggest that the cell/tissue type may regulate the interactions and thus the regulation of OGT and OGA.

Our study, utilizing proximity biotinylation and SILAC-based MS, has revealed a host of novel basal and oxidative stress-dependent binding partners of OGA (Figure 3-10;

Table 3-1). Our data provides evidence for a model in which the interactors of OGA, such as FAS, regulate its local activity in a manner consistent with cell survival (Figure 3-15). Such results will provide a framework for understanding the regulation of OGA during injury and in other models in which O-GlcNAc is misregulated, such as cancer, neurodegenerative disease, and metabolic syndrome.

Experimental procedures

Reagents

All chemicals and reagents were of the highest grade and supplied by Sigma-Aldrich (St. Louis, MO) or Thermo Fisher Scientific (Waltham, MA), unless otherwise indicated. TMG (Yuzwa et al. 2008) was synthesized by SD ChemMolecules LLC (Owings Mills, MD) to a purity of 99.1%, as determined by high-performance liquid chromatography. The chemical structure of TMG was verified by ^{1}H nuclear magnetic resonance and ESI-MS.

Antibodies

The following antibodies were used for Western blot analysis: anti-OGA (345), anti-O-GlcNAc (CTD110.6) (gift, The Johns Hopkins University School of Medicine (JHUSOM) Core C4); anti-FLNA (A301-135A; Bethyl Laboratories); anti-HA (H6908), anti-Actin (A5060), anti-OGT (DM17, O6264), anti-mouse IgM-HRP (A8786; Sigma-Aldrich); NeutrAvidin-HRP (31030), anti-V5 (461157; Thermo Fisher Scientific); anti-Myc (9E10, CRL-1729; American Type Culture Collection, Manassas, VA); anti-FAS (3180; Cell Signaling Technology, Danvers, MA); anti-FAS (H00002194-M01; Novus Biologicals, Littleton, CO); anti-HSC70 (sc-7298), anti-chicken IgY-HRP (sc-2428; Santa Cruz Biotechnology, Dallas, TX); anti-rabbit IgG-HRP (NA934V), anti-mouse IgG-HRP (NA931V; GE Healthcare, Pittsburgh, PA). The following antibodies were used for indirect immunofluorescence: anti-BirA (NB600-1098; Novus Biologicals); NeutrAvidin-DyLight 633 (22844; Thermo Fisher Scientific); anti-OGA (345), anti-chicken IgY-Alexa Fluor 488 (703-545-155; Jackson ImmunoResearch Laboratories, West Grove, PA). The

following antibodies were used for immunoprecipitation: rabbit isotype control IgG (P120-101), anti-OGA (A304-345A), anti-FAS (A301-324A; Bethyl Laboratories); anti-V5 (461157; Thermo Fisher Scientific).

Cloning

The following DNA constructs were gifts (Kyle Roux, Sanford Research; (Roux et al. 2012)): pcDNA3.1 Myc-mBirA-multiple cloning site (MCS; Plasmid #35700; Addgene, Cambridge, MA), pcDNA3.1 MCS-mBirA-HA (Plasmid #36047; Addgene). Myc-mBirA-OGA was generated by sub-cloning full-length human OGA (from pcDNA3.1 His_6-OGA; gift, JHUSOM Core C4; (Gao et al. 2001)) into the MCS of pcDNA3.1 Myc-mBirA-MCS using NotI and PmeI. OGA-mBirA-HA was generated as follows: 1) PCR insertion of a start codon upstream of mBirA in pcDNA3.1 MCS-mBirA-HA (Primers: BirAMetF, BirAMetR); 2) PCR deletion of 23 base pairs (bp) between the AgeI and BamHI restriction sites in pcDNA3.1 MCS-mBirA-HA (Primers: Del23bpF, Del23bpR); 3) PCR insertion of a NotI restriction site upstream of AgeI in pcDNA3.1 MCS-mBirA-HA (Primers: BirAHAinsNotIF, BirAHAinsNotIR); 4) PCR insertion of an AgeI restriction site 3' of full-length human OGA (from pcDNA3.1 His_6-OGA; gift, JHUSOM Core C4; Primers: OGAinsAgeIF, OGAinsAgeIR (Gao et al. 2001)); and 5) subcloning full-length OGA (from pcDNA3.1 His_6-OGA) into the MCS of pcDNA3.1 MCS-mBirA-HA using NotI and AgeI. All of the mutagenesis PCR reactions described above were performed with KOD polymerase (EMD Millipore, Billerica, MA). Full-length untagged human FAS in pCMV-SPORT6 was a gift (Michael Wolfgang, JHUSOM). pCMV-SPORT6 His_6-V5-TEV-FAS was generated by in-fusion using the SalI restriction site and **5' and 3' overhangs** for recombination (5'-**ATTCCCGGGATATC**GTCGACG

CCACCATGGGCCATCACCATCACCATCACGGCGGCGGTAAGCCTATCCCTAA CCCTCTCCTCGGTCTCGATTCTACGGAAAACCTGTATTTTCAGGGCGGTCGAC **CCACGCGTCCG**-3'). His_6-V5-TEV-FAS was sub-cloned into pcDNA3.1 using EcoRI and NotI. His_6-V5-TEV-FAS will be referred to as V5-FAS. All primer sequences for site-directed mutagenesis are listed in Appendix A. DNA constructs were verified by Sanger sequencing using an Applied Biosystems 3730xl DNA analyzer (Thermo Fisher Scientific; JHUSOM Synthesis and Sequencing Facility).

Cell culture

U2OS human osteosarcoma cells and HEPG2 human hepatocellular carcinoma cells (American Type Culture Collection) were cultured in high glucose (4.5 g/L) DMEM (Corning, Manassas, VA) supplemented with 10% (v/v) heat inactivated fetal bovine serum (Thermo Fisher Scientific) and 1% (v/v) penicillin/streptomycin (Corning) in a humidified water-jacketed CO2 (5%) incubator at 37°C. All experiments were performed in U2OS cells unless otherwise indicated (Figure 3-12 only).

All plasmid DNA transfections were performed in Opti-MEM (Thermo Fisher Scientific) using FuGENE 6 (Promega, Madison, WI). Cells were harvested 45-50 h post-transfection and 18-20 h post-feeding. Cell treatments included biotin (25 µM, 16 h; Sigma-Aldrich), H_2O_2 (2.5 mM, 1-3 h as indicated; Sigma-Aldrich), and TMG (100 nM, 20 h). Vehicle control was complete media (biotin, H_2O_2) or HEPES pH 7.8 (TMG).

For the SILAC experiment, U2OS cells were cultured in light (unlabeled arginine and lysine; Sigma-Aldrich), medium ($^{13}C^6$-arginine, lysine-D_4; Cambridge Isotopes, Tewksbury, MA), or heavy ($^{13}C_6{}^{15}N_4$-arginine, $^{13}C_6{}^{15}N_2$-lysine; Cambridge Isotopes) media (Ong et al. 2002; Amanchy et al. 2005). In all cases, low glucose (1 g/L) DMEM

(Athena Environmental Sciences, Baltimore, MD) was supplemented with unlabeled leucine (104.8 mg/L, Sigma-Aldrich) and methionine (30 mg/L, Sigma-Aldrich), 1 mM sodium pyruvate (Corning), 3.5 g/L glucose (Sigma-Aldrich), 10% (v/v) fetal bovine serum, and 1% (v/v) penicillin/streptomycin. Cells were passaged for 6 generations in SILAC media prior to transfection to ensure complete incorporation of the label (44, 45). Labeled cells were transfected with plasmid DNA encoding pcDNA3.1 (control vector), OGA-mBirA-HA, or Myc-mBirA-OGA, treated as indicated, and harvested 49 h post-transfection.

Generation of stable cell lines

Stable constitutive overexpression of V5-FAS in U2OS cells was carried out as follows. A pcDNA3.1 plasmid encoding V5-FAS (or empty vector as a control) was linearized with ScaI. The digested DNA was precipitated with ethanol prior to transfection with FuGENE 6. Stable cell selection was initiated ~48 hours post-transfection, and continued for 14 days in 750 μg/mL G418 (Sigma-Aldrich). Cells were maintained in 375 μg/mL G418.

Murine tissue

Male C57BL/6 mice (12-14 weeks of age) were obtained from Jackson Laboratories (Bar Harbor, ME). Animals were euthanized after anesthesia, and livers were rapidly removed, washed in ice cold phosphate-buffered saline (PBS), and snap frozen on liquid nitrogen. All animal procedures were performed in accordance with the National Institutes of Health (NIH) Guide for the Care and Use of Laboratory Animals and approved by the Institutional Laboratory Animal Care and Use Committee.

Preparation of cell and tissue lysates

The following lysis buffers were used in this study: TCL buffer (1% (v/v) Nonidet P-40, 2 mM ethylenediaminetetraacetic acid (EDTA) pH 8, 50 mM Tris pH 7.5, 150 mM sodium chloride (NaCl)); denaturing TCL buffer (1% (v/v) Nonidet P-40, 0.5 M urea, 2 mM EDTA pH 8, 50 mM Tris pH 7.5, 150 mM NaCl); and NETN buffer (0.5% (v/v) Nonidet P-40, 5 mM EDTA pH 8, 50 mM Tris pH 8, 250 mM NaCl). Unless indicated otherwise, lysis buffers were supplemented with the following inhibitors immediately prior to use: protease inhibitor cocktail sets II and III (EMD Millipore), 10 μM β-hexosaminidase inhibitor (376820; EMD Millipore); 0.5 μM TMG; 0.1 mM phenylmethylsulfonyl fluoride (PMSF), 10 mM sodium fluoride, 10 mM β-glycerophosphate, 3 μM trichostatin A1 (Sigma-Aldrich). Cells were extracted in the indicated lysis buffer for 30 min on ice with vortexing followed by sonication. Cell debris were pelleted at 17,111 x g (30 min, 4°C). Livers were extracted in NETN buffer for 10 min on ice followed by homogenization, sonication, and centrifugation (17,200 x g, 30 min, 4°C). Protein concentration was assessed using the 660 nm protein assay (Thermo Fisher Scientific).

Immunoprecipitation

For the SILAC study, cells were lysed in denaturing TCL buffer and equal amounts of protein from each sample (2.32 mg) were combined (6.96 mg total protein). Biotinylated proteins were isolated on high capacity NeutrAvidin-agarose (1.31 mL slurry, Thermo Fisher Scientific) with end-over-end rotation (2 h, 4°C). The beads were washed in TCL buffer supplemented with 2 M urea (3x) and subsequently in Tris-buffered saline (TBS) pH 7.5 (3x). Biotinylated proteins were eluted with 2% (w/v) SDS (1.5 mL, 5 min, 95°C, 10x). The elution fractions containing biotinylated protein (fractions 1-8, as identified by

electrophoresis) were combined and precipitated with acetone (65 h, -20°C). Protein was recovered by centrifugation (5,000 x g, 30 min, 4°C). Each pellet was re-suspended in 2% (w/v) SDS and combined, and then the proteins were re-precipitated with acetone (18 h, -20°C). The sample was centrifuged (25,000 x g, 30 min, 4°C), and the pellet was dried briefly under vacuum.

For co-immunoprecipitation studies, NETN lysate was incubated with antibody overnight (16-20 h, 4°C, with rotation). Endogenous OGA and FAS were enriched with an anti-OGA antibody and an anti-FAS antibody (Bethyl Laboratories), respectively. Samples were also incubated with rabbit isotype control IgG to indicate non-specific binding. V5-FAS was enriched with an anti-V5 antibody, and pcDNA3.1-overexpressing cells were used to control for non-specific binding. Antibody-protein complexes were captured using protein A/G magnetic beads (2 h, 4°C, with rotation; Thermo Fisher Scientific) pre-blocked with 1 mg/mL bovine serum albumin (BSA), washed extensively with NETN buffer, and then eluted and denatured in Laemmli sample buffer containing 25 mM dithiothreitol. For experiments in Figure 3-12, NETN lysate was pre-cleared with rabbit isotype control IgG and protein A/G magnetic beads (2-4 h, 4°C, with rotation) to reduce non-specific binding.

Electrophoresis and Western blotting

SDS-PAGE was performed using Tris-Glycine (TGX, Bio-Rad; Novex, Life Technologies) and Tris-Acetate (XT, Bio-Rad; Novex, Life Technologies) polyacrylamide gels. Equal sample volumes at equal concentration were loaded onto the gel, with the exception of immunoprecipitate fractions where the volume typically exceeded that of the input fractions. Proteins were electroblotted to nitrocellulose (0.45 μm; Bio-Rad). Membranes were blocked in 3% (w/v) non-fat milk in TBS with 0.05% (v/v) TWEEN-20

(1 h, 25°C), incubated with primary antibodies (16-20 h, 4°C), and then incubated with HRP-conjugated secondary antibodies (1 h, 25°C). Western blots were developed using Immobilon Western Chemiluminescent Substrate (EMD Millipore) and captured on autoradiography film or the Amersham Imager 600 RGB (GE Healthcare). Western blots were incubated with 0.1% (w/v) sodium azide in PBS (10 min, 25°C), stripped in 200 mM glycine pH 2.5 (1 h, 25°C), and then re-probed as described above. Stripped blots were re-probed for proteins that migrate at a different molecular weight than the original signal.

Protein load was assessed by Western blotting for a housekeeping protein (actin), total protein gel staining (colloidal Coomassie G-250), or total protein membrane staining (Sypro Ruby; Bio-Rad). Quantitation of Western blots and total protein stains was performed using ImageJ software (version 1.46; NIH, Bethesda, MD). Quantitation was performed on individual protein bands, except for O-GlcNAc Western blots and total protein stains where quantitation was performed on the entire lane signal.

Indirect immunofluorescence

U2OS cells were grown and transfected on glass cover slips. Mitochondria were stained *in vivo* with MitoTracker Orange CMTMRos (200 nM, 45 min, 37°C; Thermo Fisher Scientific). Cells were fixed in 4% (v/v) paraformaldehyde in PBS (15 min, on ice) and permeabilized with 0.5% (v/v) Triton X-100 in PBS (15 min, on ice). Slides were blocked in 3% (w/v) BSA in PBS (1-2 h, 25°C), incubated with primary antibodies in 3% (w/v) BSA-X (0.05% (v/v) Triton X-100; 16-20 h, 4°C), and then incubated with fluorophore-conjugated secondary antibodies in 3% (w/v) BSA-X (1 h, 25°C). Nuclei were stained with Hoechst 33342 (8 min, 25°C). Cover slips were mounted in VECTASHIELD Antifade Mounting Medium (Vector Laboratories, Burlingame, CA), sealed, and stored at

4°C. Images were captured at 25°C using an upright Zeiss (Carl Zeiss, Inc., Oberkochen, Germany) Axio Examiner 710NLO-Meta multiphoton and confocal laser-scanning microscope (C-Apochromat 63x/1.20 W Korr M27 water immersion objective) with spectral detection. Images were obtained on ZEN 2010 software (Carl Zeiss Inc.) and processed using Imaris software (version 7.6.5; Bitplane, Zurich, Switzerland). Image acquisition and processing was performed at the JHUSOM Microscope Facility.

OGA activity assays

Lysates for OGA assays were prepared as follows. For Figure 3-2C, lysates in TCL buffer at equal concentration (1 mg/mL) were desalted into desalting buffer (20 mM Tris pH 7.8, 20% (v/v) glycerol) using Zeba spin desalting columns (7,000 molecular weight cut off; Thermo Fisher Scientific), and then the protein concentration was re-assessed. For Figure 3-1G, 8C, and 8D, cells were lysed in NETN buffer without TMG. Lysates at equal concentration (1 mg/mL) were diluted 4-fold with ultrapure water (0.25x NETN), and assayed in a final concentration of 0.05x NETN.

The activity of OGA was assessed in duplicate with 1 mM 4MU-GlcNAc or 4MU-GalNAc (Sigma-Aldrich) fluorescent substrate, 100 mM GalNAc (Sigma-Aldrich), and OGA assay buffer (100 mM sodium cacodylate pH 6.4 (50 mM in Figure 3-2C), 0.3% (w/v) BSA) in a black flat/clear-bottomed 96-well plate as previously reported (Reeves et al. 2014). β-N-acetylhexosaminidase$_f$ (New England Biolabs, Ipswich, MA) diluted in desalting buffer or 0.25x NETN buffer was used as a positive control (5 units/well). Assays were quenched with glycine pH 10.75 (final concentration: 120 mM in 100 µL assays and 150 mM in 50 µL assays), and the fluorescence intensity was measured using the Synergy HT microplate reader (BioTek Instruments, Inc., Winooski, VT; excitation 360 nm,

emission 460 nm). OGA activity in cell lysates was normalized by subtracting the fluorescence signal resulting from lysosomal hexosaminidase contamination, which was assessed using 4MU-GalNAc (Reeves et al. 2014). Activity was converted to pmoles/min/mg using a standard curve of free 4MU.

To assay OGA on beads (Figure 3-13), U2OS cells stably overexpressing pcDNA3.1 or pcDNA3.1 V5-FAS were treated with vehicle or H_2O_2 (2.5 mM, 2 h). Cells were lysed in NETN buffer without TMG, and lysates were diluted to equal concentration (1 mg/mL). V5-FAS was enriched using an anti-V5 antibody (30 min, 4°C, with rotation) and captured using protein A/G magnetic beads (2 h, 4°C, with rotation) pre-blocked with BSA. Antibody-protein complexes were washed with 1x NETN buffer (5x) and subsequently with 0.25x NETN buffer (3x). OGA activity assays were performed on-bead (3 h, 37°C, with rotation) in duplicate (described above). The reaction product was transferred to a black flat/clear-bottomed 96-well plate for fluorescence measurements. Serial dilutions of lysates from the inputs and unbound fractions were prepared and processed in diluted NETN (described above). To assess the specific activity of OGA on-bead (bound to FAS) and compare it to the specific activity of OGA in the unbound and input lysates, the amount of OGA on the beads was determined by Western blot quantitation of the bound fractions and serial dilutions of the inputs. To ensure accurate quantitation of OGA, the bound fractions from the V5-FAS cells were electroblotted to the same membrane as the corresponding V5-FAS input serial dilutions. Western blots for each antibody were exposed for equal lengths of time. Fluorescence values were converted to pmoles/min (Figure 3-13C) or pmoles/min/μg (Figure 3-13D) using a standard curve of free 4MU and the densitometric analysis described above. Finally, the data were

normalized to the pcDNA3.1 vehicle-treated input sample to control for variable baseline OGA activity between biological replicates (reported as fold change).

OGT activity assays

Cells were lysed in NETN buffer without sodium fluoride and β-glycerophosphate (phosphatase inhibitors). Lysates at equal concentration (2 mg/mL) were diluted 8-fold with ultrapure water (0.125x NETN), and assayed in a final concentration of 0.05x NETN. In a clear round-bottomed 96-well plate, 5 µg cell lysate was incubated (1 h, 25°C) in triplicate with 0.5 µCi ^{3}H-UDP-GlcNAc (ART 0128; American Radiolabeled Chemicals, Saint Louis, MO; specific activity: 60 Ci/mmol), 1 mM casein kinase II (CKII) acceptor peptide (PGGSTPVSSANMM; JHUSOM Synthesis and Sequencing Facility), 2.5 units calf intestinal alkaline phosphatase (New England Biolabs), 0.25 mM 5' adenosine monophosphate (AMP; Sigma-Aldrich), and OGT assay buffer (100 mM sodium cacodylate pH 6.4, 0.3% (w/v) BSA). Recombinant His_6-OGT was purified in-house on Ni-NTA agarose (Qiagen, Venlo, The Netherlands), diluted in 0.125x NETN buffer, and used as a positive control (0.5 µg/well). Assays were quenched with 37.5 mM formate/750 mM NaCl (final concentration). Samples were loaded onto a Strata C_{18} 96-well plate (25 mg/well; 8E-S001-CGB; Phenomenex) activated with 100% methanol and equilibrated 50 mM formate/1 M NaCl (3x2 mL each). The C_{18} plate was subsequently washed with 50 mM formate/1 M NaCl, water, and 50 mM formate (2x2 mL each). The reaction product was eluted from the column with 100% methanol (2 mL), and the incorporation of radiolabeled GlcNAc was assessed by liquid scintillation counting (Beckman Coulter Inc., Indianapolis, IN). Activity was normalized by subtracting the counts arising from the average of triplicate samples incubated without CKII acceptor peptide. Counts per minute

were converted to disintegrations per minute using a standard curve of ^{3}H-UDP-GlcNAc, and then to fmoles/min/mg.

Mass spectrometry sample preparation and analysis

MS sample preparation and data acquisition was performed by the JHUSOM Mass Spectrometry and Proteomics Facility. Acetone protein pellets (described above) were resuspended in 100 µL of 100 mM ammonium bicarbonate (NH_4HCO_3) pH 7.8 and 1 µL of 1% Protease Max (Promega) and sonicated for 15 min. The sample was then reduced and alkylated with 10 mM dithiothreitol and 55 mM iodoacetamide, respectively, and digested with a Trypsin/LysC mixture (V5071; Promega). The resulting peptides were dried by vacuum centrifugation, and resuspended in 50 µL of 100 mM triethylammonium bicarbonate (TEAB). Subsequently, bRP micro-scale fractionation was performed using an Agilent 1200 capLC system with a multi-wavelength detector. Fractionation was performed at 5 µL/min on a 300 µm inner diameter fused silica column self-packed with Waters XBridge BEH130 C_{18} RP resin (3.5 µm, 130 Å; Milford, MA), and fractions were collected at 2 min intervals with a Probot (LC Packings) fraction collector (Dionex, Amsterdam, The Netherlands). After loading for 12 min onto the column, a gradient from 0-30% (v/v) mobile phase A (10 mM TEAB) to B (90% (v/v) acetonitrile, 10 mM TEAB) was performed over a 50 min time interval before ramping to 100% (v/v) B over 10 min, and then holding for an additional 10 min. Fractions were concatenated into 12 fractions for subsequent LC-MS/MS analysis. Peptide fractions from bRP chromatography were injected onto a 2 cm desalting trap column packed with YMC C_{18} material (75 µm inner diameter, 5–15 µm, 120 Å; Allentown, PA) at 5 µL/min for 6 min before being eluted onto an analytical column packed with Michrom Magic C_{18} (75 µm × 15 cm, 5 µm, 120 Å;

Bruker Daltonics, Billerica, MA) using a nanoAquity nanoLC system (Waters, MA) with a nanoflow solvent delivery of 300 nL/min. Each sample was separated on a 90 min gradient (5%–90% (v/v) acetonitrile, 0.1% (v/v) formate) with a flow rate of 300 nL/min. The peptides were eluted and ionized via emitter tip (10 μm; New Objective, Woburn, MA) and maintained at 2.2 kV electrospray voltage into a Q-Exactive mass spectrometer (Thermo Fisher Scientific). Precursor ions were selected for MS/MS fragmentation using a data-dependent "Top 15" method operating in a tandem Fourier transform (FT-FT) acquisition mode. Precursor ions were scanned between m/z (mass/charge) 350–1800 Da at 70,000 resolution with a target maximum of 3e6 ions. Fragment ions (MS/MS scans) were analyzed at 17,500 resolution with a target of 1e5 ions. Maximum injection times for the precursor and fragment ions were set to 100 and 250 milliseconds, respectively. The ion selection threshold for triggering MS/MS fragmentation was set to 2e4 counts. An isolation width and offset of 2.0 Da and 0.5 Da, respectively, were used to perform high-energy collision induced dissociation fragmentation with a normalized collision energy of 27. The polysiloxane background peak at 371.101230 m/z was used as a lock mass for each scan to maintain mass accuracy.

Search parameters and acceptance criteria

Peptide identifications were determined using a 30 parts per million precursor ion tolerance, a 0.05 Da MS/MS fragment ion tolerance, and a maximum of 2 missed cleavages. Methylthio modification of cysteine residues was considered a static modification, while oxidation of methionine, biotinylation of lysine, and deamidation of asparagine and glutamine were set as variable modifications. For the SILAC labeling, variable modifications included lysine ($^{2}H_4$ and $^{13}C_6{}^{15}N_2$) and arginine ($^{13}C_6$ and $^{13}C_6{}^{15}N_4$)

(Light: no labels; Medium: Arg6, Lys4; Heavy: Arg10, Lys8). Spectra files (*.RAW) were searched through Proteome Discoverer 1.4 (Thermo Fisher Scientific) using the Mascot algorithm (V2.1, Matrix Sciences, United Kingdom) against the RefSeq2014 human database. The data were processed through the Xtract and MS2 processor nodes together with an unaltered search, and the combined searches were processed through Percolator node (Department of Genome Sciences, University of Washington, Seattle, WA) for FDR estimation. Raw protein and peptide identifications were validated employing a q-value of 0.05 (5% FDR) and a peptide rank of 1 within Proteome Discoverer (Figure 3-8 (inclusion criteria, filter 1); Supplemental Tables 3-1 through 3-3 (HA dataset), 3-4 through 3-6 (Myc dataset)). The mass spectrometry proteomics data have been deposited to the ProteomeXchange Consortium (http://proteomecentral.proteomexchange.org) via the PRIDE partner repository (Martens et al. 2005; Côté et al. 2012; Vizcaíno et al. 2014; Perez-Riverol et al. 2016; Vizcaíno et al. 2016) with the dataset identifier PXD005039.

The ratio of L/H (H_2O_2/Background), M/H (Vehicle/Background), and L/M (H_2O_2/Vehicle) were generated in Proteome Discoverer. The following criteria were used to select proteins for further analysis (Figure 3-8): First, proteins considered for analysis have ≥1 unique peptide, ≥2 total peptides, and ≥3 PSMs per identification (Figure 3-8 (inclusion criteria, filter 2); Supplemental Tables 3-7 and 3-8). Second, the heavy sample represents background and is anticipated to contain the endogenously biotinylated proteins (carboxylases), proteins that associate with the carboxylases, and proteins that associate non-specifically with the NeutrAvidin resin used for biotin enrichment. To set a threshold at or below which proteins were considered background, the Log_2 of the SILAC ratios (L/H; M/H) for the endogenous carboxylases from the HA and Myc datasets (Supplemental

Table 3-9) were converted to frequencies and plotted as histograms (Figure 3-9) using GraphPad Prism (version 7; GraphPad Software Inc., La Jolla, CA). We then used the Z-score from a one–sided 95% confidence interval to calculate the Log_2 threshold for each ratio (L/H; M/H) in each dataset (HA; Myc), which was then converted back to a SILAC ratio (HA dataset: L/H >1.867, M/H >1.874; Myc dataset: L/H >2.005, M/H >2.258; Figure 3-8 (exclusion criteria 2), Figure 3-9; Supplemental Table 3-9). Proteins not meeting the background threshold were excluded (Supplemental Tables 3-10 and 3-11). Third, the majority of keratins were eliminated, as they are common environmental contaminants present in MS studies (Figure 3-8 (exclusion criteria 3); Supplemental Tables 3-10 and 3-11). Of note, keratin 8 and 18 were not excluded, as they are known to be O-GlcNAc-modified (Srikanth et al. 2010). Fourth, a variety of techniques have been used to set a threshold for signal-induced changes when using SILAC (Trinkle-Mulcahy et al. 2008; Boulon et al. 2010; Coombs et al. 2010; Neilson et al. 2013). As OGA is the "bait", we assessed the L/M SILAC ratio of OGA (NCOAT; accession 1102469) in each dataset: 1.057 and 1.308 for the HA and Myc datasets, respectively (Supplemental Tables 3-10 through 3-12). We set an arbitrary threshold of 25% above or below this number: 1.32125 and 0.79275, respectively, for the HA dataset; and 1.635 and 0.981, respectively, for the Myc dataset (Supplemental Tables 3-10 through 3-12). Our rationale for this threshold was as follows: as signal-induced changes are diluted out by the BioID labeling method, we set a lower threshold than we have used previously (30-50% change) (Zachara et al. 2011; Zhong et al. 2015; Lee et al. 2016). To validate this threshold, candidate proteins near the threshold (FAS, FLNA) were validated by co-IP. A summary of the protein identifications following each major exclusion criteria is in Supplemental Table 3-13.

Experimental design and statistical rationale

Graphs and statistical analyses were prepared using GraphPad Prism (version 6). Data are presented as the mean with errors bars representing the standard error of the mean (SEM) unless otherwise indicated. Unless otherwise noted, three biological replicates (N) were performed for each experiment and are indicated in the figure legends. For OGA activity assays, each biological replicate was assessed in duplicate. In Figure 3-2C the transfection efficiency, and thus corresponding OGA activity, varies for each biological replicate. As such, the OGA activity values cannot be averaged and one representative experiment is shown. In this case, the error bars represent the standard deviation of the two technical replicates. Data with at least three matched groups (Figure 3-1: V, 1-3 h H_2O_2; Figure 3-13D: input, bound, unbound) were analyzed by a parametric RM-1ANOVA. Dunnett's MCT was used to compare each H_2O_2-treated sample with the vehicle-treated control (Figure 3-1), and Tukey's MCT was used to compare OGA activity in the input, bound, and unbound fractions (Figure 3-13D). Matched two-sample data (Figure 3-2C; pcDNA3.1 ± biotin) were analyzed by a parametric RPT (two-tails, 95% confidence). Data with at least three matched groups (V, 1-3 h H_2O_2) in two matched samples (pcDNA3.1, V5-FAS) were analyzed by a parametric RM-2ANOVA (Figure 3-14). Sidak's MCT was used to compare differences between the two matched samples (pcDNA3.1, V5-FAS) at each H_2O_2 time point. For all statistical tests, differences were considered significant at $p \leq 0.05$ (*), $p \leq 0.01$ (**), $p \leq 0.001$ (***), and $p \leq 0.0001$ (****). SILAC-based MS analysis was performed once. Protein-protein interactions were validated by orthologous methods (IP/Western blotting) using three biological replicates.

Acknowledgements

Antibodies for OGA (345) and O-GlcNAc (CTD110.6), as well as pcDNA3.1 His_6-OGA, were a kind gift from the laboratory of Gerald Hart, Ph.D. (Department of Biological Chemistry, JHUSOM; JHUSOM Core C4, NIH P01HL107153). We would also like to thank Michael Wolfgang, Ph.D. (Department of Biological Chemistry, JHUSOM) for providing pCMV-SPORT6 FAS, and Kyle Roux, Ph.D. (Sanford Research) for providing pcDNA3.1 Myc-mBirA-MCS and pcDNA3.1 MCS-mBirA-HA via Addgene. Confocal microscopy was performed at the JHUSOM Microscope Facility (NIH Grant S10RR024550; Research Resources). Mass spectrometry sample preparation, data acquisition, and database searching was performed by the JHUSOM Mass Spectrometry and Proteomics Facility (NIH Grant P30CA006973; National Cancer Institute). This work was supported by grants from the NIH National Heart, Lung, and Blood Institute (P01HL107153), the NIH National Institute on Aging (F31AG047724), and the NIH National Institute of General Medical Sciences (MARC U-STAR; T34GM008663).

Disclosures

The authors declare that they have no conflicts of interest with the contents of this article. The content is solely the responsibility of the authors and does not necessarily represent the official views of the National Institutes of Health.

References

1. Abdalla S, Fu X, Elzahwy SS, Klaetschke K, Streichert T, Quitterer U (2011) Up-regulation of the cardiac lipid metabolism at the onset of heart failure. Cardiovasc Hematol Agents Med Chem 9 (3):190–206
2. Amanchy R, Kalume DE, Pandey A (2005) Stable isotope labeling with amino acids in cell culture (SILAC) for studying dynamics of protein abundance and posttranslational modifications. Sci STKE 2005 (267):pl2–pl2
3. Baldini SF, Wavelet C, Hainault I, Guinez C, Lefebvre T (2016) The Nutrient-Dependent O-GlcNAc Modification Controls the Expression of Liver Fatty Acid Synthase. J Mol Biol
4. Banerjee PS, Ma J, Hart GW (2015) Diabetes-associated dysregulation of O-GlcNAcylation in rat cardiac mitochondria. Proc Natl Acad Sci USA 112 (19):6050–6055
5. Bond MR, Hanover JA (2015) A little sugar goes a long way: the cell biology of O-GlcNAc. J Cell Biol 208 (7):869–880
6. Boulon S, Ahmad Y, Trinkle-Mulcahy L, Verheggen C, Cobley A, Gregor P, Bertrand E, Whitehorn M, Lamond AI (2010) Establishment of a protein frequency library and its application in the reliable identification of specific protein interaction partners. Mol Cell Proteomics 9 (5):861–879
7. Carvalho MA, Zecchin KG, Seguin F, Bastos DC, Agostini M, Rangel ALCA, Veiga SS, Raposo HF, Oliveira HCF, Loda M, Coletta RD, Graner E (2008) Fatty acid synthase inhibition with Orlistat promotes apoptosis and reduces cell growth and

lymph node metastasis in a mouse melanoma model. Int J Cancer 123 (11):2557–2565

8. Champattanachai V, Marchase RB, Chatham JC (2007) Glucosamine protects neonatal cardiomyocytes from ischemia-reperfusion injury via increased protein-associated O-GlcNAc. Am J Physiol, Cell Physiol 292 (1):C178–87
9. Champattanachai V, Marchase RB, Chatham JC (2008) Glucosamine protects neonatal cardiomyocytes from ischemia-reperfusion injury via increased protein O-GlcNAc and increased mitochondrial Bcl-2. Am J Physiol, Cell Physiol 294 (6):C1509–20
10. Cheung WD, Hart GW (2008) AMP-activated protein kinase and p38 MAPK activate O-GlcNAcylation of neuronal proteins during glucose deprivation. J Biol Chem 283 (19):13009–13020
11. Cheung WD, Sakabe K, Housley MP, Dias WB, Hart GW (2008) O-linked beta-N-acetylglucosaminyltransferase substrate specificity is regulated by myosin phosphatase targeting and other interacting proteins. J Biol Chem 283 (49):33935–33941
12. Choi-Rhee E, Schulman H, Cronan JE (2004) Promiscuous protein biotinylation by Escherichia coli biotin protein ligase. Protein Sci 13 (11):3043–3050
13. Comtesse N, Maldener E, Meese E (2001) Identification of a nuclear variant of MGEA5, a cytoplasmic hyaluronidase and a beta-N-acetylglucosaminidase. Biochem Biophys Res Commun 283 (3):634–640

14. Coombs KM, Berard A, Xu W, Krokhin O, Meng X, Cortens JP, Kobasa D, Wilkins J, Brown EG (2010) Quantitative proteomic analyses of influenza virus-infected cultured human lung cells. J Virol 84 (20):10888–10906

15. Coyaud E, Mis M, Laurent EMN, Dunham WH, Couzens AL, Robitaille M, Gingras A-C, Angers S, Raught B (2015) BioID-based Identification of Skp Cullin F-box (SCF)β-TrCP1/2 E3 Ligase Substrates. Mol Cell Proteomics 14 (7):1781–1795

16. Côté RG, Griss J, Dianes JA, Wang R, Wright JC, van den Toorn HWP, van Breukelen B, Heck AJR, Hulstaert N, Martens L, Reisinger F, Csordas A, Ovelleiro D, Perez-Rivevol Y, Barsnes H, Hermjakob H, Vizcaíno JA (2012) The PRoteomics IDEntification (PRIDE) Converter 2 framework: an improved suite of tools to facilitate data submission to the PRIDE database and the ProteomeXchange consortium. Mol Cell Proteomics 11 (12):1682–1689

17. Cronan JE (2005) Targeted and proximity-dependent promiscuous protein biotinylation by a mutant Escherichia coli biotin protein ligase. J Nutr Biochem 16 (7):416–418

18. Erickson JR, Pereira L, Wang L, Han G, Ferguson A, Dao K, Copeland RJ, Despa F, Hart GW, Ripplinger CM, Bers DM (2013) Diabetic hyperglycaemia activates CaMKII and arrhythmias by O-linked glycosylation. Nature 502 (7471):372–376

19. Fülöp N, Zhang Z, Marchase RB, Chatham JC (2007) Glucosamine cardioprotection in perfused rat hearts associated with increased O-linked N-acetylglucosamine protein modification and altered p38 activation. Am J Physiol Heart Circ Physiol 292 (5):H2227–36

20. Gao Y, Wells L, Comer FI, Parker GJ, Hart GW (2001) Dynamic O-glycosylation of nuclear and cytosolic proteins: cloning and characterization of a neutral, cytosolic beta-N-acetylglucosaminidase from human brain. J Biol Chem 276 (13):9838–9845

21. Greig KT, Antonchuk J, Metcalf D, Morgan PO, Krebs DL, Zhang J-G, Hacking DF, Bode L, Robb L, Kranz C, de Graaf C, Bahlo M, Nicola NA, Nutt SL, Freeze HH, Alexander WS, Hilton DJ, Kile BT (2007) Agm1/Pgm3-mediated sugar nucleotide synthesis is essential for hematopoiesis and development. Mol Cell Biol 27 (16):5849–5859

22. Groves JA, Lee A, Yildirir G, Zachara NE (2013) Dynamic O-GlcNAcylation and its roles in the cellular stress response and homeostasis. Cell Stress Chaperones 18 (5):535–558

23. Haltiwanger RS, Blomberg MA, Hart GW (1992) Glycosylation of nuclear and cytoplasmic proteins. Purification and characterization of a uridine diphospho-N-acetylglucosamine:polypeptide beta-N-acetylglucosaminyltransferase. J Biol Chem 267 (13):9005–9013

24. Hamada S, Horiguchi A, Asano T, Kuroda K, Asakuma J, Ito K, Asano T, Miyai K, Iwaya K (2014) Prognostic impact of fatty acid synthase expression in upper urinary tract urothelial carcinoma. Jpn J Clin Oncol 44 (5):486–492

25. Hart GW, Slawson C, Ramirez-Correa G, Lagerlof O (2011) Cross talk between O-GlcNAcylation and phosphorylation: roles in signaling, transcription, and chronic disease. Annu Rev Biochem 80 (1):825–858

26. Hwang S-Y, Shin J-H, Hwang J-S, Kim S-Y, Shin J-A, Oh E-S, Oh S, Kim J-B, Lee J-K, Han I-O (2010) Glucosamine exerts a neuroprotective effect via suppression of inflammation in rat brain ischemia/reperfusion injury. Glia 58 (15):1881–1892

27. Ito T, Sato K, Maekawa H, Sakurada M, Orita H, Shimada K, Daida H, Wada R, Abe M, Hino O, Kajiyama Y (2014) Elevated levels of serum fatty acid synthase in patients with gastric carcinoma. Oncol Lett 7 (3):616–620

28. Jensen RV, Zachara NE, Nielsen PH, Kimose HH, Kristiansen SB, Bøtker HE (2013) Impact of O-GlcNAc on cardioprotection by remote ischaemic preconditioning in non-diabetic and diabetic patients. Cardiovasc Res 97 (2):369–378

29. Jones SP, Zachara NE, Ngoh GA, Hill BG, Teshima Y, Bhatnagar A, Hart GW, Marbán E (2008) Cardioprotection by N-acetylglucosamine linkage to cellular proteins. Circulation 117 (9):1172–1182

30. Kim DI, Birendra KC, Zhu W, Motamedchaboki K, Doye V, Roux KJ (2014) Probing nuclear pore complex architecture with proximity-dependent biotinylation. Proc Natl Acad Sci USA 111 (24):E2453–61

31. Kreppel LK, Blomberg MA, Hart GW (1997) Dynamic glycosylation of nuclear and cytosolic proteins. Cloning and characterization of a unique O-GlcNAc transferase with multiple tetratricopeptide repeats. J Biol Chem 272 (14):9308–9315

32. Kuhajda FP, Jenner K, Wood FD, Hennigar RA, Jacobs LB, Dick JD, Pasternack GR (1994) Fatty acid synthesis: a potential selective target for antineoplastic therapy. Proc Natl Acad Sci USA 91 (14):6379–6383

33. Kwon K, Beckett D (2000) Function of a conserved sequence motif in biotin holoenzyme synthetases. Protein Sci 9 (8):1530–1539

34. Laczy B, Marsh SA, Brocks CA, Wittmann I, Chatham JC (2010) Inhibition of O-GlcNAcase in perfused rat hearts by NAG-thiazolines at the time of reperfusion is cardioprotective in an O-GlcNAc-dependent manner. Am J Physiol Heart Circ Physiol 299 (5):H1715–27

35. Lee A, Miller D, Henry R, Paruchuri VDP, O'Meally RN, Boronina T, Cole RN, Zachara NE (2016) Combined Antibody/Lectin Enrichment Identifies Extensive Changes in the O-GlcNAc Sub-proteome upon Oxidative Stress. J Proteome Res 15 (12):4318–4336

36. Lee JS, Lee MS, Oh WK, Sul JY (2009) Fatty acid synthase inhibition by amentoflavone induces apoptosis and antiproliferation in human breast cancer cells. Biol Pharm Bull 32 (8):1427–1432

37. Liu J, Marchase RB, Chatham JC (2007) Increased O-GlcNAc levels during reperfusion lead to improved functional recovery and reduced calpain proteolysis. Am J Physiol Heart Circ Physiol 293 (3):H1391–9

38. Liu J, Pang Y, Chang T, Bounelis P, Chatham JC, Marchase RB (2006) Increased hexosamine biosynthesis and protein O-GlcNAc levels associated with myocardial protection against calcium paradox and ischemia. J Mol Cell Cardiol 40 (2):303–312

39. Lubas WA, Frank DW, Krause M, Hanover JA (1997) O-Linked GlcNAc transferase is a conserved nucleocytoplasmic protein containing tetratricopeptide repeats. J Biol Chem 272 (14):9316–9324

40. Ma J, Liu T, Wei A-C, Banerjee P, O'Rourke B, Hart GW (2015) O-GlcNAcomic Profiling Identifies Widespread O-GlcNAcylation in Oxidative Phosphorylation System Regulating Cardiac Mitochondrial Function. J Biol Chem jbc.M115.691741

41. Martell JD, Deerinck TJ, Sancak Y, Poulos TL, Mootha VK, Sosinsky GE, Ellisman MH, Ting AY (2012) Engineered ascorbate peroxidase as a genetically encoded reporter for electron microscopy. Nat Biotechnol 30 (11):1143–1148

42. Martens L, Hermjakob H, Jones P, Adamski M, Taylor C, States D, Gevaert K, Vandekerckhove J, Apweiler R (2005) PRIDE: the proteomics identifications database. Proteomics 5 (13):3537–3545

43. Mehta V, Trinkle-Mulcahy L (2016) Recent advances in large-scale protein interactome mapping. F1000Res 5782

44. Mi H, Lazareva-Ulitsky B, Loo R, Kejariwal A, Vandergriff J, Rabkin S, Guo N, Muruganujan A, Doremieux O, Campbell MJ, Kitano H, Thomas PD (2005) The PANTHER database of protein families, subfamilies, functions and pathways. Nucleic Acids Res 33 (Database issue):D284–8

45. Moss J, Lane MD (1971) The biotin-dependent enzymes. Adv Enzymol Relat Areas Mol Biol 35321–442

46. Mullen GE, Yet L (2015) Progress in the development of fatty acid synthase inhibitors as anticancer targets. Bioorg Med Chem Lett 25 (20):4363–4369

47. Nagy T, Champattanachai V, Marchase RB, Chatham JC (2006) Glucosamine inhibits angiotensin II-induced cytoplasmic Ca2+ elevation in neonatal cardiomyocytes via protein-associated O-linked N-acetylglucosamine. Am J Physiol, Cell Physiol 290 (1):C57–65

48. Neilson KA, Keighley T, Pascovici D, Cooke B, Haynes PA (2013) Label-free quantitative shotgun proteomics using normalized spectral abundance factors. Methods Mol Biol 1002 (Chapter 17):205–222

49. Ngoh GA, Facundo HT, Hamid T, Dillmann W, Zachara NE, Jones SP (2009a) Unique hexosaminidase reduces metabolic survival signal and sensitizes cardiac myocytes to hypoxia/reoxygenation injury. Circ Res 104 (1):41–49

50. Ngoh GA, Hamid T, Prabhu SD, Jones SP (2009b) O-GlcNAc signaling attenuates ER stress-induced cardiomyocyte death. Am J Physiol Heart Circ Physiol 297 (5):H1711–9

51. Ngoh GA, Watson LJ, Facundo HT, Dillmann W, Jones SP (2008) Non-canonical glycosyltransferase modulates post-hypoxic cardiac myocyte death and mitochondrial permeability transition. J Mol Cell Cardiol 45 (2):313–325

52. Ngoh GA, Watson LJ, Facundo HT, Jones SP (2011) Augmented O-GlcNAc signaling attenuates oxidative stress and calcium overload in cardiomyocytes. Amino Acids 40 (3):895–911

53. Nöt LG, Brocks CA, Vámhidy L, Marchase RB, Chatham JC (2010) Increased O-linked beta-N-acetylglucosamine levels on proteins improves survival, reduces inflammation and organ damage 24 hours after trauma-hemorrhage in rats. Crit Care Med 38 (2):562–571

54. Nöt LG, Marchase RB, Fülöp N, Brocks CA, Chatham JC (2007) Glucosamine administration improves survival rate after severe hemorrhagic shock combined with trauma in rats. Shock 28 (3):345–352

55. O'Donnell N, Zachara NE, Hart GW, Marth JD (2004) Ogt-dependent X-chromosome-linked protein glycosylation is a requisite modification in somatic cell function and embryo viability. Mol Cell Biol 24 (4):1680–1690

56. Ong S-E, Blagoev B, Kratchmarova I, Kristensen DB, Steen H, Pandey A, Mann M (2002) Stable isotope labeling by amino acids in cell culture, SILAC, as a simple and accurate approach to expression proteomics. Mol Cell Proteomics 1 (5):376–386

57. Perez-Riverol Y, Xu Q-W, Wang R, Uszkoreit J, Griss J, Sanchez A, Reisinger F, Csordas A, Ternent T, del-Toro N, Dianes JA, Eisenacher M, Hermjakob H, Vizcaíno JA (2016) PRIDE Inspector Toolsuite: Moving Toward a Universal Visualization Tool for Proteomics Data Standard Formats and Quality Assessment of ProteomeXchange Datasets. Mol Cell Proteomics 15 (1):305–317

58. Pizer ES, Wood FD, Heine HS, Romantsev FE, Pasternack GR, Kuhajda FP (1996) Inhibition of fatty acid synthesis delays disease progression in a xenograft model of ovarian cancer. Cancer Res 56 (6):1189–1193

59. Razani B, Zhang H, Schulze PC, Schilling JD, Verbsky J, Lodhi IJ, Topkara VK, Feng C, Coleman T, Kovacs A, Kelly DP, Saffitz JE, Dorn GW, Nichols CG, Semenkovich CF (2011) Fatty acid synthase modulates homeostatic responses to myocardial stress. J Biol Chem 286 (35):30949–30961

60. Reeves RA, Lee A, Henry R, Zachara NE (2014) Characterization of the specificity of O-GlcNAc reactive antibodies under conditions of starvation and stress. Anal Biochem 457:8–18

61. Rhee H-W, Zou P, Udeshi ND, Martell JD, Mootha VK, Carr SA, Ting AY (2013) Proteomic mapping of mitochondria in living cells via spatially restricted enzymatic tagging. Science 339 (6125):1328–1331

62. Roux KJ, Kim DI, Burke B (2013) BioID: a screen for protein-protein interactions. Curr Protoc Protein Sci 74:19.23.1–19.23.14.

63. Roux KJ, Kim DI, Raida M, Burke B (2012) A promiscuous biotin ligase fusion protein identifies proximal and interacting proteins in mammalian cells. J Cell Biol 196 (6):801–810

64. Ryu I-H, Do S-I (2011) Denitrosylation of S-nitrosylated OGT is triggered in LPS-stimulated innate immune response. Biochem Biophys Res Commun 408 (1):52–57

65. Schultz J, Pils B (2002) Prediction of structure and functional residues for O-GlcNAcase, a divergent homologue of acetyltransferases. FEBS Lett 529 (2-3):179–182

66. Seither P, Iben S, Grummt I (1998) Mammalian RNA polymerase I exists as a holoenzyme with associated basal transcription factors. J Mol Biol 275 (1):43–53

67. Semenkovich CF (1997) Regulation of fatty acid synthase (FAS). Prog Lipid Res 36 (1):43–53

68. Shafi R, Iyer SP, Ellies LG, O'Donnell N, Marek KW, Chui D, Hart GW, Marth JD (2000) The O-GlcNAc transferase gene resides on the X chromosome and is essential for embryonic stem cell viability and mouse ontogeny. Proc Natl Acad Sci USA 97 (11):5735–5739

69. Srikanth B, Vaidya MM, Kalraiya RD (2010) O-GlcNAcylation determines the solubility, filament organization, and stability of keratins 8 and 18. J Biol Chem 285 (44):34062–34071

70. Thomas PD, Campbell MJ, Kejariwal A, Mi H, Karlak B, Daverman R, Diemer K, Muruganujan A, Narechania A (2003) PANTHER: a library of protein families and subfamilies indexed by function. Genome Res 13 (9):2129–2141

71. Tong L (2013) Structure and function of biotin-dependent carboxylases. Cell Mol Life Sci 70 (5):863–891

72. Trinkle-Mulcahy L, Boulon S, Lam YW, Urcia R, Boisvert F-M, Vandermoere F, Morrice NA, Swift S, Rothbauer U, Leonhardt H, Lamond A (2008) Identifying specific protein interaction partners using quantitative mass spectrometry and bead proteomes. J Cell Biol 183 (2):223–239

73. van der Vusse GJ, Glatz JF, Stam HC, Reneman RS (1992) Fatty acid homeostasis in the normoxic and ischemic heart. Physiol Rev 72 (4):881–940

74. Varnaitė R, MacNeill SA (2016) Meet the neighbours: mapping local protein interactomes by proximity-dependent labelling with BioID. Proteomics

75. Veigel D, Wagner R, Stübiger G, Wuczkowski M, Filipits M, Horvat R, Benhamú B, López-Rodríguez ML, Leisser A, Valent P, Grusch M, Hegardt FG, García J, Serra D, Auersperg N, Colomer R, Grunt TW (2015) Fatty acid synthase is a metabolic marker of cell proliferation rather than malignancy in ovarian cancer and its precursor cells. Int J Cancer 136 (9):2078–2090

76. Ventura R, Mordec K, Waszczuk J, Wang Z, Lai J, Fridlib M, Buckley D, Kemble G, Heuer TS (2015) Inhibition of de novo Palmitate Synthesis by Fatty Acid Synthase Induces Apoptosis in Tumor Cells by Remodeling Cell Membranes, Inhibiting Signaling Pathways, and Reprogramming Gene Expression. EBioMedicine 2 (8):806–822

77. Vibjerg Jensen R, Johnsen J, Buus Kristiansen S, Zachara NE, Bøtker HE (2013) Ischemic preconditioning increases myocardial O-GlcNAc glycosylation. Scand Cardiovasc J 47 (3):168–174

78. Vizcaíno JA, Csordas A, del-Toro N, Dianes JA, Griss J, Lavidas I, Mayer G, Perez-Riverol Y, Reisinger F, Ternent T, Xu Q-W, Wang R, Hermjakob H (2016) 2016 update of the PRIDE database and its related tools. Nucleic Acids Res 44 (D1):D447–56

79. Vizcaíno JA, Deutsch EW, Wang R, Csordas A, Reisinger F, Ríos D, Dianes JA, Sun Z, Farrah T, Bandeira N, Binz P-A, Xenarios I, Eisenacher M, Mayer G, Gatto L, Campos A, Chalkley RJ, Kraus H-J, Albar JP, Martinez-Bartolomé S, Apweiler R, Omenn GS, Martens L, Jones AR, Hermjakob H (2014) ProteomeXchange provides globally coordinated proteomics data submission and dissemination. Nat Biotechnol 32 (3):223–226

80. Wakamiya T, Suzuki SO, Hamasaki H, Honda H, Mizoguchi M, Yoshimoto K, Iwaki T (2014) Elevated expression of fatty acid synthase and nuclear localization of carnitine palmitoyltransferase 1C are common among human gliomas. Neuropathology 34 (5):465–474

81. Wang ZV, Deng Y, Gao N, Pedrozo Z, Li DL, Morales CR, Criollo A, Luo X, Tan W, Jiang N, Lehrman MA, Rothermel BA, Lee A-H, Lavandero S, Mammen PPA, Ferdous A, Gillette TG, Scherer PE, Hill JA (2014) Spliced X-box binding protein 1 couples the unfolded protein response to hexosamine biosynthetic pathway. Cell 156 (6):1179–1192

82. Wells L, Gao Y, Mahoney JA, Vosseller K, Chen C, Rosen A, Hart GW (2002) Dynamic O-glycosylation of nuclear and cytosolic proteins: further characterization of the nucleocytoplasmic beta-N-acetylglucosaminidase, O-GlcNAcase. J Biol Chem 277 (3):1755–1761

83. Wells L, Whelan SA, Hart GW (2003) O-GlcNAc: a regulatory post-translational modification. Biochem Biophys Res Commun 302 (3):435–441

84. Whisenhunt TR, Yang X, Bowe DB, Paterson AJ, Van Tine BA, Kudlow JE (2006) Disrupting the enzyme complex regulating O-GlcNAcylation blocks signaling and development. Glycobiology 16 (6):551–563

85. Yang S, Zou L-Y, Bounelis P, Chaudry I, Chatham JC, Marchase RB (2006) Glucosamine administration during resuscitation improves organ function after trauma hemorrhage. Shock 25 (6):600–607

86. Yang YR, Song M, Lee H, Jeon Y, Choi E-J, Jang H-J, Moon HY, Byun H-Y, Kim E-K, Kim DH, Lee MN, Koh A, Ghim J, Choi JH, Lee-Kwon W, Kim KT, Ryu SH, Suh P-G (2012) O-GlcNAcase is essential for embryonic development and maintenance of genomic stability. Aging Cell 11 (3):439–448

87. Yuzwa SA, Macauley MS, Heinonen JE, Shan X, Dennis RJ, He Y, Whitworth GE, Stubbs KA, McEachern EJ, Davies GJ, Vocadlo DJ (2008) A potent mechanism-inspired O-GlcNAcase inhibitor that blocks phosphorylation of tau *in vivo*. Nat Chem Biol 4 (8):483–490

88. Zachara NE, Molina H, Wong KY, Pandey A, Hart GW (2011) The dynamic stress-induced "O-GlcNAc-ome" highlights functions for O-GlcNAc in regulating DNA damage/repair and other cellular pathways. Amino Acids 40 (3):793–808

89. Zachara NE, O'Donnell N, Cheung WD, Mercer JJ, Marth JD, Hart GW (2004) Dynamic O-GlcNAc modification of nucleocytoplasmic proteins in response to stress. A survival response of mammalian cells. J Biol Chem 279 (29):30133–30142

90. Zhang Z, Costa FC, Tan EP, Bushue N, DiTacchio L, Costello CE, McComb ME, Whelan SA, Peterson KR, Slawson C (2016) O-GlcNAc transferase and O-GlcNAcase interact with Mi2β at the Aγ-globin promoter. J Biol Chem jbc.M116.721928

91. Zhong J, Martinez M, Sengupta S, Lee A, Wu X, Chaerkady R, Chatterjee A, O'Meally RN, Cole RN, Pandey A, Zachara NE (2015) Quantitative phosphoproteomics reveals crosstalk between phosphorylation and O-GlcNAc in the DNA damage response pathway. Proteomics 15 (2-3):591–607

92. Zhou W, Simpson PJ, McFadden JM, Townsend CA, Medghalchi SM, Vadlamudi A, Pinn ML, Ronnett GV, Kuhajda FP (2003) Fatty acid synthase inhibition triggers apoptosis during S phase in human cancer cells. Cancer Res 63 (21):7330–7337

93. Zou L, Yang S, Hu S, Chaudry IH, Marchase RB, Chatham JC (2007) The protective effects of PUGNAc on cardiac function after trauma-hemorrhage are mediated via increased protein O-GlcNAc levels. Shock 27 (4):402–408

Appendix A: Polymerase Chain Reaction Primers for Site-Directed Mutagenesis

Primer Name	Primer Sequence (5'→3')
BirAMetF	GATTCGAATTCGGATCCATGAAGGACAACACCGTGCC
BirAMetR	GGCACGGTGTTGTCCTTCATGGATCCGAATTCGAATC
Del23bpF	TAAGGCCTGTTAACCGGTGGATCCAAGGACAAC
Del23bpR	GTTGTCCTTGGATCCACCGGTTAACAGGCCTTA
BirAHAinsNotIF	TATAGGGAGACCCAAGCGGCCGCTGGCTAGCGCTTAAG
BirAHAinsNotIR	CTTAAGCGCTAGCCAGCGGCCGCTTGGGTCTCCCTATA
OGAinsAgeIF	TACTTGGTCGGAGCCTGACCGGTTGACATTTGTTGACACT
OGAinsAgeIR	AGTGTCAACAAATGTCAACCGGTCAGGCTCCGACCAAGT A

CURRICULUM VITAE FOR Ph.D. CANDIDATES

The Johns Hopkins University School of Medicine

Jennifer A. Groves Born 08/13/1989 (Seattle, WA) 08/19/2017

Educational History:

Ph.D. expected	2017	Biological Chemistry Mentor: Natasha E. Zachara, Ph.D.	Johns Hopkins School of Medicine
B.S.	2011	Chemistry	Central Washington University
B.A.	2011	Biology	Central Washington University
B.A.	2011	Spanish	Central Washington University

Other Professional Experience:

Cardio PEG Trainee	2011-2017	Program for Excellence in Glycosciences Johns Hopkins School of Medicine
Textbook Reviewer	2016	Essentials of Glycobiology, 3rd edition, chapters on microbial lectins and parasitic infections
Discussion Leader	2015-2016	Led cell physiology discussion group for first year medical students
Specialty Course	2014	Biol/Chem Threat Response and Forensics The Johns Hopkins University
Specialty Course	2014	Science, Medicine, and Policy in Biodefense The Johns Hopkins University
Research Assistant	2009-2011	Lab of Todd T. Kroll, Ph.D. Central Washington University (Chemistry)
Research Assistant	2009	Lab of Lucinda Carnell, Ph.D. Central Washington University (Biology)
Research Assistant	2008	Lab of Michael Jackson, Ph.D. Central Washington University (Physics)

Fellowships/External Funding:

Ruth L. Kirschstein National Research Service Award Individual Pre-doctoral Fellowship (F31AG047724); NIH National Institute on Aging, 2014-2017

Academic Honors and Awards:

2016	Travel Award	Society for Glycobiology Annual Meeting
2014	Poster Award	VIIth International Symposium on Heat Shock Proteins in Biology and Medicine
2014	Travel Award	American Society for Biochemistry and Molecular Biology (ASBMB) Annual Meeting
2013	Honorable Mention	NSF Graduate Research Fellowship Program

Peer-Reviewed Publications:

Groves JA, Zachara NE (2017) Characterization of tools to detect and enrich human and mouse O-GlcNAcase. Glycobiology. doi: 10.1093/glycob/cwx051 (Epub).

Groves JA, Maduka AO, O'Meally RN, Cole RN, Zachara NE (2017) Fatty acid synthase inhibits the O-GlcNAcase during oxidative stress. J Biol Chem. 292(16):6493-6511.

Groves JA, Lee A, Yildirir G, Zachara NE (2013) Dynamic O-GlcNAcylation and its roles in the cellular stress response and homeostasis. Cell Stress Chaperones. 18(5):535-58.

Abstracts, Posters, and Oral Presentations:

Groves JA, Maduka AO, O'Meally RN, Cole RN, Zachara NE (2017) Proteomics reveals fatty acid synthase as a novel oxidative stress-induced inhibitor of the O-GlcNAcase. Inter-Programs of Excellence in Glycosciences Annual Meeting, Bethesda, MD, April 13, 2017.

Groves JA, Maduka AO, O'Meally RN, Cole RN, Zachara NE (2016) Proteomics reveals fatty acid synthase as a novel oxidative stress-induced inhibitor of the O-GlcNAcase. Society for Glycobiology Annual Meeting, New Orleans, LA, November 21, 2016.

Groves JA, Maduka AO, O'Meally RN, Cole RN, Zachara NE (2016) Proteomics reveals fatty acid synthase as a novel oxidative stress-induced inhibitor of the O-GlcNAcase. Glycoconjugates and Cardiovascular Disease Program of Excellence in Glycosciences Monthly Meeting, Baltimore, MD, November 9, 2016.

Groves JA, Maduka AO, O'Meally RN, Cole RN, Zachara NE (2016) Proteomics reveals fatty acid synthase as a novel oxidative stress-induced inhibitor of the O-GlcNAcase. Department of Biological Chemistry Retreat, Baltimore, MD, October 14, 2016.

Groves JA, Maduka AO, O'Meally RN, Cole RN, Zachara NE (2016) Proteomics reveals fatty acid synthase as a novel oxidative stress-induced inhibitor of the O-GlcNAcase. Glycoconjugates and Cardiovascular Disease Program of Excellence in Glycosciences Annual Retreat, Baltimore, MD, July 15, 2016.

Groves JA, Maduka AO, O'Meally RN, Cole RN, Zachara NE (2016) Proteomics reveals fatty acid synthase as a novel oxidative stress-induced inhibitor of the O-GlcNAcase. Baltimore-Washington Area Glycobiology Interest Group, Baltimore, MD, May 10, 2016.

Maduka AO, Fahie KF, **Groves JA**, Zachara NE (2016) Assessing the Stress-Dependent role of AMPK on OGT and OGA Activity and Localization. Undergraduate Research and Creative Achievement Day at the University of Maryland, Baltimore County, Baltimore, MD, April 27, 2016.

Groves JA, Maduka AO, O'Meally RN, Cole RN, Zachara NE (2016) Proteomics reveals fatty acid synthase as a novel oxidative stress-induced inhibitor of the O-GlcNAcase. Inter-Programs of Excellence in Glycosciences Annual Meeting, Bethesda, MD, April 20, 2016.

Taparra K, Wang H, Nugent K, Malek R, **Groves JA**, Yildirir G, Simons B, Felsher D, Zachara N, Tran P (2016) SNAI1 regulates the hexosamine biosynthetic pathway to promote tumorigenesis and oncogene-induced senescence escape in lung cancer. American Association for Cancer Research Annual Meeting, New Orleans, LA, April 18, 2016.

Groves JA, Maduka AO, O'Meally RN, Cole RN, Zachara NE (2016) The stress-dependent interactome of the O-GlcNAcase. Biological Chemistry Student Seminar Series, Baltimore, MD, January 29, 2016.

Groves JA, Maduka AO, O'Meally RN, Cole RN, Zachara NE (2016) The stress-dependent interactome of the O-GlcNAcase. Glycoconjugates and Cardiovascular Disease Program of Excellence in Glycosciences Monthly Meeting, Baltimore, MD, January 15, 2016.

Groves JA, Maduka AO, O'Meally RN, Cole RN, Zachara NE (2015) Understanding the mechanisms that lead to dynamic stress-induced O-GlcNAcylation; identification of the stress-dependent interactome of the O-GlcNAcase. Glycoconjugates and Cardiovascular Disease Program of Excellence in Glycosciences Annual Retreat, Baltimore, MD, July 24, 2015.

Groves JA, Maduka AO, O'Meally RN, Cole RN, Zachara NE (2015) Understanding the mechanisms that lead to dynamic stress-induced O-GlcNAcylation; identification of the stress-dependent interactome of the O-GlcNAcase. Baltimore-Washington Area Glycobiology Interest Group, Baltimore, MD, May 14, 2015.

Groves JA, Maduka AO, O'Meally RN, Cole RN, Zachara NE (2015) The stress-dependent interactome of the O-GlcNAcase. Department of Biological Chemistry Retreat, Baltimore, MD, May 8, 2015.

Maduka AO, **Groves JA**, Zachara NE (2015) Generation and characterization of a stable inducible O-GlcNAcase cell line. 19th Annual Undergraduate Research and Creative Achievement Day at the University of Maryland, Baltimore County, Baltimore, MD, April 22, 2015.

Groves JA, Maduka AO, O'Meally RN, Cole RN, Zachara NE (2015) Understanding the mechanisms that lead to dynamic stress-induced O-GlcNAcylation; identification of the stress-dependent interactome of the O-GlcNAcase. Inter-Programs of Excellence in Glycosciences Annual Meeting, Bethesda, MD, April 16, 2015.

Maduka AO, **Groves JA**, Zachara NE (2015) Generation and characterization of a stable inducible O-GlcNAcase cell line. The American Society for Biochemistry and Molecular

Biology Annual Meeting in Conjunction with the Experimental Biology Annual Meeting, Boston, MA, March 30, 2015.

Groves JA, Maduka AO, O'Meally RN, Cole RN, Zachara NE (2015) Understanding the mechanisms that lead to dynamic stress-induced O-GlcNAcylation; identification of the stress-dependent interactome of the O-GlcNAcase. The American Society for Biochemistry and Molecular Biology Annual Meeting in Conjunction with the Experimental Biology Annual Meeting, Boston, MA, March 29, 2015.

Groves JA, Maduka AO, O'Meally RN, Cole RN, Zachara NE (2015) The stress-dependent interactome of the O-GlcNAcase. Glycoconjugates and Cardiovascular Disease Program of Excellence in Glycosciences Monthly Meeting, Baltimore, MD, March 19, 2015.

Groves JA, Maduka AO, O'Meally RN, Cole RN, Zachara NE (2015) The stress-dependent interactome of the O-GlcNAcase. Biological Chemistry Student Seminar Series, Baltimore, MD, March 12, 2015.

Groves JA, Maduka AO, O'Meally RN, Cole RN, Zachara NE (2015) The stress-dependent interactome of the O-GlcNAcase. Department of Biological Chemistry Thursday Evening Dinner Discussion, Baltimore, MD, February 12, 2015.

Maduka AO, **Groves JA**, Zachara NE (2014) Identification of the stress-dependent interactome of O-GlcNAcase. Annual Biomedical Research Conference for Minority Students, San Antonio, TX, November 15, 2014.

Groves JA, Zachara NE (2014) Understanding the molecular basis by which O-GlcNAc regulates the cellular stress response; characterization of the putative O-GlcNAc-binding protein p32. VIIth International Symposium on Heat Shock Proteins in Biology & Medicine, Alexandria, VA, November 2, 2014.

Maduka AO, **Groves JA**, Zachara NE (2014) Identification of the stress-dependent interactome of O-GlcNAcase. 17th Annual Undergraduate Research Symposium in the Chemical and Biological Sciences at the University of Maryland, Baltimore County, Baltimore, MD, October 25, 2014.

Maduka AO, **Groves JA**, Zachara NE (2014) Identification of the stress-dependent interactome of O-GlcNAcase. The Johns Hopkins University Summer Internship Program Poster Session, Baltimore, MD, July 30, 2014.

Maduka AO, **Groves JA**, Zachara NE (2014) Identification of the stress-dependent interactome of O-GlcNAcase. The Leadership Alliance National Symposium, Stamford, CT, July 26, 2014.

Groves JA, Maduka AO, Zachara NE (2014) Understanding the molecular basis by which O-GlcNAc regulates the cellular stress response; identification of the stress-dependent interactome of O-GlcNAcase. Glycoconjugates and Cardiovascular Disease Program of Excellence in Glycosciences Annual Retreat, Baltimore, MD, July 25, 2014.

Groves JA, Maduka AO, Zachara NE (2014) Understanding the molecular basis by which O-GlcNAc regulates the cellular stress response; identification of the stress-dependent interactome of O-GlcNAcase. Glycoconjugates and Cardiovascular Disease Program of Excellence in Glycosciences Monthly Meeting, Baltimore, MD, July 02, 2014.

Groves JA, Zachara NE (2014) Characterization of an O-GlcNAc-binding protein. Baltimore-Washington Area Glycobiology Interest Group, Baltimore, MD, May 15, 2014.

Groves JA, Zachara NE (2014) Characterization of an O-GlcNAc-binding protein. The American Society for Biochemistry and Molecular Biology Annual Meeting in Conjunction with the Experimental Biology Annual Meeting, San Diego, CA, April 29, 2014.

Groves JA, Zachara NE (2014) Understanding the molecular basis by which O-GlcNAc regulates the cellular stress response; characterization of the putative O-GlcNAc-binding protein p32. Inter-Programs of Excellence in Glycosciences Annual Meeting, Bethesda, MD, March 27, 2014.

Groves JA, Zachara NE (2014) Understanding the molecular basis by which O-GlcNAc regulates the cellular stress response. Biological Chemistry Student Seminar Series, Baltimore, MD, March 13, 2014.

Groves JA, Zachara NE (2013) Characterization of the O-GlcNAc-binding protein p32. The Johns Hopkins University School of Medicine HUb Club, Baltimore, MD, September 4, 2013.

Groves JA, Zachara NE (2013) Identification and characterization of an O-GlcNAc-binding protein. Baltimore-Washington Area Glycobiology Interest Group, Baltimore, MD, May 14, 2013.

Groves JA, Zachara NE (2013) Identification and characterization of an O-GlcNAc-binding protein. Biological Chemistry Student Seminar Series, Baltimore, MD, May 9, 2013.

Groves JA, Zachara NE (2013) Identification and characterization of an O-GlcNAc-binding protein. Inter-Programs of Excellence in Glycosciences Annual Meeting, Cleveland, OH, April 11, 2013.

Groves JA, Zachara NE (2013) Identification and characterization of an O-GlcNAc-binding protein. Department of Biological Chemistry Thursday Evening Dinner Discussion, Baltimore, MD, March 21, 2013.

Groves JA, Zachara NE (2013) Defining the role of O-GlcNAc-binding proteins in survival signaling. Glycoconjugates and Cardiovascular Disease Program of Excellence in Glycosciences Annual Retreat, Baltimore, MD, January 23, 2013.

Groves JA, Yu SH, Hart GW, Kohler JJ, Zachara NE (2012) Defining the role of O-GlcNAc-binding proteins in survival signaling. Baltimore-Washington Area Glycobiology Interest Group, Baltimore, MD, May 8, 2012.

Service and Leadership:

2015-present	Clinical Trial Volunteer	Volunteer for experimental Zika virus and malaria vaccines at the University of Maryland Center for Vaccine Development

2017	Poster Judge	Evaluated Stevenson University undergraduate's research posters
2016	Science Fest Volunteer	Promoted STEM careers to students at the USA Science and Engineering Festival
2014-2016	Mentor	Mentored an undergraduate student and graduate rotation student in the Zachara laboratory
2013-2015	Coordinator	Managed logistics for the Biological Chemistry Student Seminar Series
2015	Science Fest Volunteer	Oversaw middle/high school students and lab events at the Maryland Science Olympiad
2014	Science Advocate	Advocated for biomedical funding with U.S. Congressional Representatives